Technische Universität München
Lehrstuhl für Technische Chemie II

# Novel Heterogeneous Catalysts for Intermolecular Hydroamination Reactions

Oriol Jiménez Silva

Vollständiger Abdruck der von der Fakultät für Chemie der Technischen Universität München zur Erlangung des akademischen Grades eines

**Doktors der Naturwissenschaften**

genehmigten Dissertation.

Vorsitzender: Univ. –Prof. Dr. Klaus Köhler

Prüfer der Dissertation:

1. Univ. –Prof. Dr. Johannes A. Lercher
2. Univ. –Prof. Dr. Peter Härter

Die Dissertation wurde am 08.09.2006 bei der Technischen Universität München eingericht und durch die Fakultät für Chemie am 25.09.2006 angenommen.

With true love to
Mariela and German Dario

# Acknowledgements

First and foremost, I would like to express my deep gratitude to **Prof. Dr. Johannes Lercher**, as supervisor, teacher and friend. Thank you for your constant guidance, motivation, suggestions and discussions throughout this work. Your patience, ability and frank attitude to explain any situation has made this time very stimulating. I also thank you for the care towards my family during my stay in Germany. You were very nice with them, which made our stay in Munich unforgettable.

I am most grateful to my co-supervisor PD Thomas Müller, who generously shared his knowledge and skills and patiently introduced me into the field of hydroamination. He provided support whenever needed.

I am grateful for the financial support provided by Max-Buchner Forschungstiftung. Thanks to Helen, Frau Hermann and Frau Schüler for taking care of my financial situation.

I would also like to thank you Xaver, Martin and Andreas for your help with measurements and troubleshooting

Thanks to Alex, Bertha, Florencia and Iker, my spanish speaker friends you have made my life in Munich easier.

It is my pleasure to thank all those who assisted me in any way during my PhD, at the TC2 or elsewhere at the TUM. Special thanks are due to my friends and colleagues of the JAL group – Andreas S, Phillip, Xuebing, Wolfgang, Felix, Rino, Krishna, Andreas F, Lay Hwa, Aon, Hendrik, Adam, Carsten, Maria, Olga, Christian, Hitri, Peter, Qinq, Manuel, Virginia, Elvira, Benjamin, Roberta and every one else not mentioned here in person - for providing a stimulating atmosphere in the lab, for many engaging discussions on chemical and not-so chemical topics and for the good time we had in and out of the labs.

Last but not least, I would like to thank to my family (Mariela and German Dario), por la paciencia, el amor y la ayuda, demostrados en toda ocasión.

# TABLE OF CONTENTS

**I. Abstract** ..... **1**

**II. Zusammenfassung** ..... **3**

**Chapter 1**
**Introduction**

1 General Introduction ..... 6

2 Homogeneous Catalysis ..... 8

2.1 Palladium catalysts for hydroamination reactions ..... 9

3 Two-phase Catalysis ..... 10

3.1 Ionic liquids. ..... 11

3.1.1 Ionic liquids for hydroamination reactions ..... 13

4 Heterogeneous Catalysis ..... 13

4.1 Zeolites ..... 14

4.1.1 Ion exchanged zeolites for hydroamination reactions ..... 16

4.2 Supported ionic liquids ..... 17

5 Scope of the thesis ..... 18

6 References ..... 19

**Chapter 2**
**Hydroamination of 1,3-cyclohexadiene with aryl amines catalyzed with acidic form zeolites**

1 Introduction ..... 24

2 Experimental ..... 25

2.1 General ..... 25

2.2 Physical and analytical methods ..... 26

3 Results and Discussion ..... 27

3.1 Catalyst characterization ..... 27

3.2 Catalytic measurements ..... 32

3.3 Mechanism proposed ..... 40

3.4 Influence of the amine basicity ..... 41

4 Conclusions ..... 43
5 References ..... 44

**Chapter 3**
**Formation of solvent cages around organometallic complexes in thin films of supported ionic liquid**

1 Introduction ..... 47
2 Experimental ..... 48
2.1 Catalysts preparation ..... 48
2.2 Catalysts characterization ..... 48
3 Results and discussion ..... 49
3.1 Catalysts characterization ..... 49
4 Conclusions ..... 55
5 References ..... 56

**Chapter 4**
**Markownikoff and *anti*-Markownikoff hydroamination with palladium catalysts immobilized in thin films of silica supported ionic liquids**

1 Introduction ..... 58
2 Experimental ..... 59
2.1 Catalysts preparation ..... 59
2.2 Determination of the absorption constants of aniline and vinylbenzene ..... 60
2.3 Catalytic testing in batch mode ..... 60
2.4 Catalytic testing in fixed bed reactor ..... 60
3 Results and Discussion ..... 60
4 Conclusions ..... 64
5 References ..... 65

**Chapter 5**
**Palladium complexes immobilized in thin films of supported ionic liquids for the direct addition of aniline to vinyl-benzene**

1 Introduction ..... 68
2 Experimental ..... 70
2.1 General ..... 70

2.2 Physical and analytical methods ..... 70
2.3 Preparation of the supported catalysts ..... 71
2.4 Catalysis ..... 72
2.4.1 Testing in batch mode ..... 72
2.4.2 Test on leaching of palladium complex ..... 73
2.4.3 Catalytic testing in fixed bed reactor ..... 73
2.4.4 Determination of the absorption constants for aniline and styrene ..... 73
3 Results and Discussion ..... 73
3.1 Preparation of the supported catalysts ..... 73
3.2 Characterization of the supported catalysts ..... 76
3.3 Catalytic activity of the supported catalysts ..... 82
4 Conclusions ..... 88
5 References ..... 89

**Chapter 6**
**General conclusions**

General conclusions ..... 92

# I. Abstract

The hydroamination of alkenes is a synthetically highly attractive transformation, for which up to now no general and efficient solution exists. In this thesis, intermolecular hydroamination reactions were studied on a new type of heterogeneous catalysts in both a slurry reactor and a fixed bed reactor. For industrial applications solid catalysts are generally preferred as they often provide high stability and can be used in fixed catalyst beds or are readily separated from the reaction mixture in case that a suspended catalyst is used.

In the first part of the thesis, catalysts (acidic or zinc ion exchanged zeolites) with a high concentration of strong Brønsted acid sites and a high ratio of Brønsted to Lewis acid sites exhibited an especially high catalytic activitity for the addition of aniline to 1,3-cyclohexadiene. The results suggest that the hydroamination reaction can be catalyzed most efficiently in the pores of a zeolite with 12 membered ring openings, such H-BEA zeolite, and that subtle shape selective effects determine reactivity and selectivity. Mechanistically, the key step seems to be the adsorption of 1,3-cyclohexadiene at the Brønsted acid sites and protonation to the corresponding allyl- or enyl- cation.

In the second part, palladium complexes immobilized in a thin film of supported ionic liquid were used to catalyze the addition of aniline to vinyl-benzene providing the Markownikoff product N-(1-phenylethyl)aniline under kinetic control and the anti-Markownikoff product N-(2-phenylethyl)aniline under thermodynamic control. As expected, the catalytic activity increased linearly with the palladium loading. Particularly noteworthy is that the initial catalytic activity was strongly dependent on the choice of the ionic liquid. The differences between the catalysts can be explained by significant variations in the adsorption properties of the ionic liquids towards reactants (highly soluble in the IL phase) and products (hardly soluble in the IL phase). The catalytic activity of the immobilized catalysts also exceeded the activity of the corresponding homogeneous catalysts. Ionic liquids are particularly favourable as their appropriate selection allows to influence adsorption properties and, in consequence, catalytic activity, selectivity and chemical equilibrium.

Detailed characterization of the catalysts, showed that the imidazolium cations of the ionic liquids decrease in mobility forming solvent cages around the palladium complex. The first experimental evidence for the formation of ordered three-dimensional supramolecular structures in thin films of supported ionic liquid is reported.

# II. Zusammenfassung

Die Hydroaminierung von Alkenen ist eine synthetisch sehr attraktive chemische Transformation, für die bisher keine effizienten und allgemein anwendbaren Katalysatoren existieren. In dieser Doktorarbeit werden intermolekulare Hydroaminierungen mit einem neuartigen heterogenen Katalysator in einem Slurry-Reaktor, sowie in einem Festbettreaktor untersucht. Für industrielle Anwendungen werden feste Katalysatoren bevorzugt, da diese in der Regel verhältnismäβig stabil sind und in Festbettreaktoren eingesetzt werden können. Die einfache Abtrennung von den Reaktionsprodukten ist von Vorteil, wenn der Katalysator in der Reaktionsmischung suspendiert eingesetzt wurde.

Im ersten Teil dieser Arbeit kommen (saure oder mit Zink-Ionen angereicherte Zeolith) Katalysatoren zum Einsatz, die über eine hohe Konzentration an stark Brønsted-sauren Funktionalitäten sowie über ein großes Verhältnis von Brønsted- zu Lewis-sauren gruppen, verfügen. Diese zeigen eine besonders hohe katalytische Aktivität bei der Addition von Anilin an 1,3-Cyclohexadien. Die Resultate legen nahe, dass die Hydroaminierungsreaktion am effektivsten in den Poren von Zeolithen katalysiert werden, die über eine 12-teilige Porenöffnung (wie z. B. Zeolith H-BEA) verfügen, und dass formselektive Effekte die Reaktivität und Selektivität bestimmen. Mechanistisch gesehen scheint der Schlüsselschritt die Adsorption von 1,3-Cyclohexadien an die Brønsted-saure Funktionalität und Protonierung zum entsprechenden Allyl- oder Enyl-Kation zu sein.

Im zweiten Teil werden in einem dünnen Film einer geträgerten ionischen Flüssigkeit (IL) immobilisierte Palladium-Komplexe genutzt, um die Addition von Anilin an Vinylbenzol zu Katalysieren. Diese Umsetzung liefert kinetisch kontrolliert das Markownikoff-Produkt (N-(1-phenylethyl)anilin), und unter thermodynamischer Kontrolle das anti-Markownikoff-Produkt (N-(2-phenylethyl)anilin). Wie erwartet steigt die katalytische Aktivität linear mit der eingesetzten Menge Palladium an. Besonders erwähnenswert ist, dass die katalytische Aktivität zu Beginn der Reaktion stark von der Wahl der ionischen Flüssigkeit abhängt. Die Unterschiede zwischen den Katalysatoren können mit einer signifikanten Änderung der Adsorptionseigenschaften der ionischen Flüssigkeiten in Bezug auf die eingesetzten Reaktanden (sehr gut löslich

in der IL-Phase) und Produkte (wenig löslich in der IL-Phase) erklärt werden. Die katalytische Aktivität der immobilisierten Katalysatoren übertraf die Aktivität der entsprechenden homogenen Katalysatoren. Der Einsatz von ionischen Flüssigkeiten ist besonders Vorteilhaft, da man durch die Wahl der geeigneten IL einen Einfluss auf die Adsorptionseigenschaften und daher auf die katalytische Aktivität und Selektivität ausüben kann.

Detaillierte Charakterisierung der Katalysatoren zeigte, dass die Imidazolium-Kationen der ionischen Flüssigkeiten die Mobilität der Palladium-Komplexe verringern, indem sie einen Lösemittel-Käfig aufbauen. In dieser Arbeit wird über den ersten experimentellen Beweis für die Bildung solcher geordneter, dreidimensionaler Strukturen in Filmen geträgerter ionischen Flüssigkeiten berichtet.

# *Chapter 1*

## *Introduction*

This chapter features a general introduction into the subject highlighting the importance of hydroamination reactions. Catalytic routes to secondary and tertiary amines are presented and the different catalytic systems for the addition of amines to alkenes discussed in detail. In order to better understand the structure and the theme of this thesis, we present here the general ideas that are the starting points for developing the topics in the following chapters and highlight the motivation for the research conducted.

## 1.1. General introduction

Amines are a highly valuable and relevant class of compounds, both as final products and as versatile intermediates in many processes [1]. Their use ranges from products such as corrosion inhibitors, wetting and surface-active agents, dyes, dispersing agents, emulsifiers, or petroleum additives to highly value-added intermediates for drugs and crop protection agents. The most widely employed routes [2-3] for the synthesis of amines on an industrial scale are (i) the reaction of alcohols with ammonia or amines over a solid-state catalyst (metal oxides, transition metals, zeolites) and the reductive amination of aldehydes or ketones by reaction with ammonia or amines and (ii) hydrogen in the presence of a heterogeneous transition-metal catalyst. In both cases, the starting materials (alcohols or carbonyl compounds, respectively) are refined intermediates. They are typically obtained by hydration or hydroformylation of inexpensive and readily available alkenes, respectively.

The synthesis of amines could, thus, be considerably improved and simplified by a direct process converting alkenes and alkynes into amines. Depending on the nature of the substrates and the catalysts either Markovnikov or anti-Markovnikov products are obtained (Eq. 1) [4].

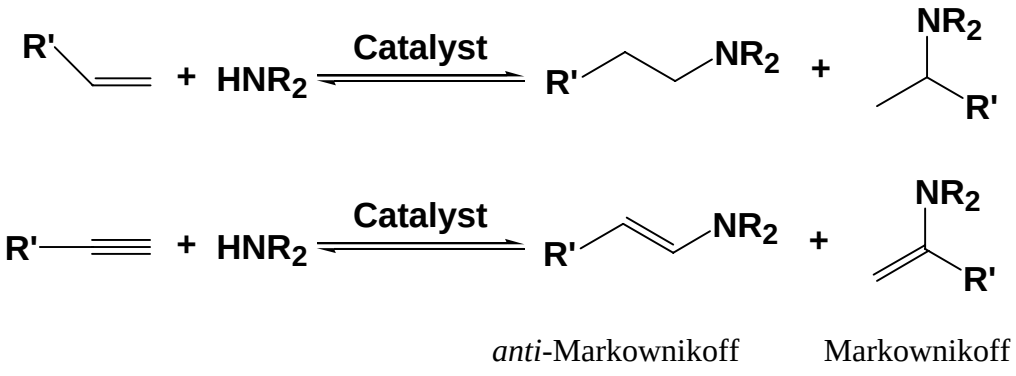


**Scheme 1**. Hydroamination of alkenes and alkynes.

The formal addition of the N-H bond of an amine across a carbon-carbon double or triple bond yields substituted amines in a direct, 100 % atom-economic [2] process, that is, each atom of the starting materials is present in the product and no by-products

are formed. From a thermodynamic standpoint, the hydroamination reaction is feasible (Table 1). It is slightly exergonic and exothermic under standard conditions.

However, the direct addition of an amine to an alkene has a high activation barrier due to the repulsive electrostatic interaction between the lone pair of the amine and the π system of the alkene. The entropy of reaction being negative, performing the reaction at elevated temperature to overcome this barrier is precluded as the equilibrium is shifted to the reactants with increasing temperature. Catalysis is obligatory for this conversion and hence the functionalization of olefins with anti-Markownikoff regioselectivity is viewed as one of the major challenges of catalysis [5].

| Reaction | $\Delta_R G^0$ (kJ.mol$^{-1}$) | $\Delta_R H^0$ (kJ.mol$^{-1}$) | $\Delta_R S^0$ (J.(mol.K)$^{-1}$) |
|---|---|---|---|
| $C_2H_4 + NH_3 \rightleftharpoons EtNH_2$ | -14.7 | -52.7 | -127.3 |
| $C_2H_4 + EtNH_2 \rightleftharpoons Et_2NH$ | -33.4 | -78.7 | -152.2 |
| $C_2H_4 + Et_2NH \rightleftharpoons Et_3NH$ | -30.0 | -79.5 | -166.3 |

**Table 1.** Thermodynamic data for the stepwise reaction of ethylene with ammonia [5]

Active research work in this field for the past years shows several possibilities for developing catalytic routes for this transformation [5]. The two principal mechanistic pathways conceivable for hydroamination involve either activation of the alkene (C=C activation) or of the amine (N-H activation) (Scheme 2).

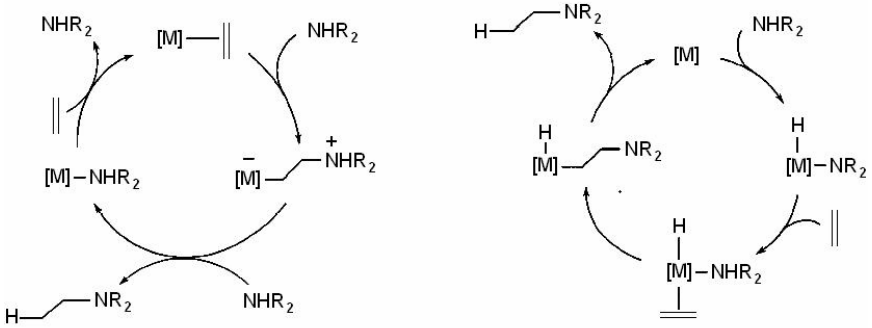


**Scheme 2**. Alternative mechanism for hydroamination reactions, C=C activation (left) and N-H activation (right) [6, 7].

In the alkene-activation mechanism, the C=C double bond is activated by coordination to a metal, and the C-N bond is formed by nucleophilic attack of the amine on the coordinated alkene. To liberate the product, the metal-carbon bond in the

resulting 2-ammonioalkyl complex needs to be cleaved. This can be brought about either direct protonolysis or by protonation of the metal centre, affording a hydrido complex, and subsequent C-H reductive elimination. The resulting amine complex finally undergoes ligand exchange with a new alkene, regenerating the starting complex [6].

The amine-activation mechanism proceeds via oxidative addition of the amine N-H bond to the coordinatively unsaturated metal centre to form an amido hydrido complex, followed by alkene coordination, insertion of the alkene into the metal-nitrogen bond, and finally C-H reductive elimination, liberating the product and closing the catalytic cycle [7].

Developing a highly active and selective catalytic system for hydroamination is a very important academic challenge. Also from an industrial point of view the catalytic hydroamination reaction is very attractive as a variety of secondary and tertiary amines are used as precursors to drugs, agro chemicals and many other compounds [1-3].

## 2. Homogeneous catalysis

One application of organometallic chemistry is the development of new catalysts for the synthesis of organic compounds. Recently, attention moved from the well-known formation of C-C or C-H bonds to the most suitable formation of C-N, C-O or C-X functional groups, as they are e. g. contained in a large number of biologically active species. Hydroamination is one of these atom economical, industrially very interesting processes to build – with as little side products as possible – higher amines starting from olefins and either ammonia, primary or secondary amines [8].

A range of catalysts [9], from early transition metals (Ti, Zr) [10, 11], over lanthanides [12] and actinides [13], to late transition metals (Ru, Rh, Ir, Pd, Pt, Cu, and Zn) [14-20] have been reported to catalyze the addition of amines to alkenes or alkynes under various conditions. There are also base catalyzed systems [21-22]. The most efficient systems were developed with lanthanide catalysts for the intramolecular hydroamination and with iridium and palladium systems for the intermolecular reaction. However, no catalyst is active enough for industrial applications where turnover frequencies in the range TOF = 100 – 10000 $h^{-1}$ are required [23].

## 2.1. Palladium catalysts for hydroamination reactions

Cationic palladium(II) complexes can be employed as homogeneous catalysts for both intramolecular [24] and intermolecular [25] hydroamination reactions. Palladium complexes have been shown to catalyze the addition of arylamines to cyclohexadiene [26]. Using colorimetric assay to detect primary amines, it was possible to identify the *in situ* combination of $[Pd(\pi\text{-allyl})Cl]_2$ and $PPh_3$ (1:2 or 1:4) as suitable catalysts for the reaction between aniline derivatives and cyclohexadiene [27]. All reactions gave high yields (78 – 98% of the isolated products). Also the addition of arylamines to dienes, such as cycloheptadiene or acyclic dienes, works with good yield, but is rather slow.

Hartwig et al. developed one of the most efficient systems for catalysis of hydroamination reactions [28]. The addition of aromatic amines to vinylarenes yielded sec-phenethylamine with good to high yield (64-99%, TOF up to 8.3 $h^{-1}$ at 100 °C, $[Pd(dppf)(OTf)_2]$ as catalyst). A variety of aromatic amines from the electron rich anisidine (93% yield after 12 h) to the electron poor 4-trifluoromethylaniline (64% yield after 12 h) could be reacted under these conditions. Aliphatic amines gave only low turnover numbers.

Li and coworkers have also reported the addition of arylamine to α,β-unsaturated oxazolidinones as the olefinic substrate [29], and the addition of arylamines to styrene derivatives catalyzed by Pd-complexes [30]. Aryl amines containing both electron donating and electron withdrawing substituents readily react with styrene, in the presence of the dicationic Pd catalyst. Interestingly, in the chiral variant the electronic effect of the amine influences the enantioselectivity: electron poor amines provided high enantioselectivity, while electron rich amines gave lower enantioselectivity.

Yamamoto and coworkers recently reported the asymmetric intermolecular hydroamination of alkynes catalyzed by Pd complexes [31]. Various optically active nitrogen heterocycles were prepared in good yields using Pd((R,R)-Renorphos) complexes (Scheme 3.)

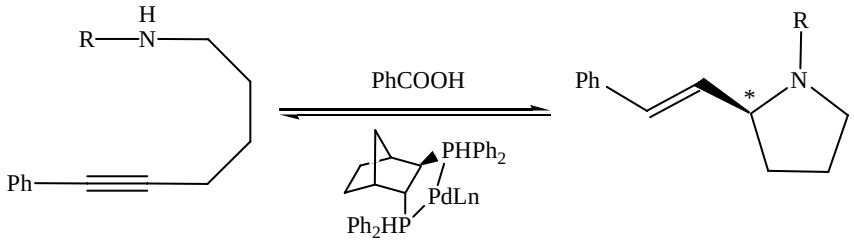


[Pd((R,R)-Renorphos)]

**Scheme 3**. Palladium catalyzed assymetric intramolecular hydroamination of alkynes.

Homogeneous catalysis has provided a lot of progress for hydroamination reactions. However, separating the product phase from a therein soluble molecular catalyst is often a major challenge. Thermal separation rarely leads to quantitative recovery of the catalyst and normally induces thermal stress. Therefore, other catalytic systems for hydroamination are needed as e.g. heterogeneous or two phase catalysis.

## 3. Two-phase catalysis

Homogeneous and heterogeneous catalysts enjoy advantages of their own. An alternative is biphasic catalysis in a liquid-liquid system, which is an ideal approach to combine the advantages of both homogeneous and heterogeneous catalysis. The reaction mixture consists of two immiscible solvents. Only one phase contains the catalyst, allowing easy separation by simple decantation. The catalyst phase can be recycled without any further treatment. However, the right combination of catalyst, solvent for the catalyst and solvent for the product is crucial for the success of biphasic catalysis [32].

Biphasic catalysis relies on the transfer of organic substrates into the catalyst phase or on catalysis at the phase boundary. Frequenty, organic substrates do not have sufficient solubility in the catalyst phase to give practical reaction rates in catalytic applications. The addition of co-solvents to the aqueous phase has been investigated extensively as a means to improve the solubility of higher olefinic substrates in the catalyst-containing phase. Other studies have focused on improving the catalytic activity of the biphasic systems by immobilizing the catalyst on a support [33]. Although these techniques can change the solubility of organic substrates in the aqueous phase or favor the accumulation of the active center at the interface, they can also cause leaching of the catalyst into the organic phase.

The major advantage of two-phase catalysis is the easy separation of the catalyst and product phases. However, the co-miscibility of the product and catalyst phases can be problematic. An example is given by the biphasic aqueous hydroformylation of ethene to propanal [34]. Firstly, the propanal formed contains water, which has to be removed by distillation. Later is difficult as azeotropic mixtures are formed. Secondly, a significant proportion of the rhodium catalyst is extracted with the products from the catalyst phase, which prevents its efficient recovery. Nevertheless, the reaction of ethene in the water-based Rh-TPPTS (trisulfonated-triphenyl-phosphine) system is fast. It is the high solubility of water in the propanal that prevents the application of the aqueous biphasic process. A new class of solvents, which might be particularly suitable for two-phase catalysis are ionic liquids (IL).

### 3.1. Ionic liquids

Ionic liquids (IL) are salts that are liquid at low temperature (< 100 $^{o}$C). The development of ionic liquids goes back to 1914, where first research efforts dealt with the synthesis of ethylammonium nitrate [35]. The use of ionic liquids as solvents for homogenous transition metal catalysts was pioneered in 1990 by Chauvin et al. [36] and by Wilkes et al [37]. Ionic liquids form biphasic systems with many organic product mixtures. This gives rise to the possibility of a variety of multiphase reaction procedures.

Ionic liquids have often been discussed as promising solvents for “clean processes” and “green chemistry” [38]. These two concepts represent current efforts to drastically reduce the amounts of side and coupling products and also the solvent and catalyst consumption in chemical processes. Room-temperature ionic liquids have been developed over the past decade as green solvents for industrial applications [39], ranging from the petrochemical industry, to heavy chemicals, fine chemicals, agrochemicals, and pharmaceuticals [40], and to the nuclear industry [41]. Recent independent reports [42], and many reviews [43], have highlighted ionic liquids as representing a state-of-the-art, innovative approach to green chemistry. The potential of ionic liquids to act as solvents for a broad spectrum of chemical processes currently attracts increasing attention from industry as they promise significant environmental and economics benefits [39].

In contrast to volatile organic solvents and extraction media, ionic liquids have no measureable vapor pressure. Therefore, there is no loss of solvent through evaporation. With respect to efforts to decrease catalyst consumption, two aspects arise with the use of ionic liquids. First, the special characteristics of an ionic reaction medium enable a biphasic reaction procedure in many cases. Exploitation of the miscibility gap between the ionic catalyst phase and the products allows, in this case, the catalyst to be isolated effectively from the product and reused many times. Here, the possibility to adjust solubility properties by different anion and cation combinations allows systematic optimization of the biphasic reaction. Second, the non-volatile nature of ionic liquids enables effective product isolation by distillation.

In addition, ionic liquids are able to dissolve organometallic compounds and are therefore suitable solvents for reactions with homogenous catalysts. Depending on the coordinative properties of the anion, the ionic liquid can be regarded as an “innocent” solvent or a co-catalyst. In many cases, ionic liquids are a superior solvent for transition metal catalysts compared to organic solvents and water, especially when ionic complexes are used as catalyst. The use of ionic liquids as solvents for transition metal catalysis opens up a wide field for future investigations.

In general, ionic liquids exhibit many properties that make them potentially attractive media for homogeneous catalysis [44].

- They have essentially no vapor pressure.
- They generally have a reasonable thermal stability.
- They are able to dissolve a wide range of organic, inorganic and organometallic compounds.
- The solubility of gases is generally good, which makes them attractive solvents for gas-liquid two phase reactions.
- They are immiscible with many organic solvents and hence, can be used in liquid-liquid two-phase systems.
- Polarity and hydrophilicity / lipophilicity can be readily adjusted by a suitable choice of the cation-anion combination.
- They can be synthesized with weakly coordinating anions and, hence, have the potential to be highly polar yet non-coordinating solvents.

Incorporation of an active transition metal catalyst into an ionic liquid appears to be an attractive method for applications, in which a high catalyst concentration is

needed. Beside the advantages of ionic liquids listed above, it could be anticipated that the anion could play a beneficial role (e.g. as proton shuttle), depending on the strength of its interaction with transition metal species.

### 3.1.1. Ionic liquids for hydroamination reactions

There are only few examples of addition of amines to alkenes or alkynes in ionic liquids. Brunet and co-workers have shown that ionic solvents could increase rates and overall turnover number of Rh(III) catalysts for the hydroamination of norbornene with aniline [45]. The nature of the anion seems to be the important key to increased activity. This was be explained by the stabilization of the cationic catalyst in the polar ionic liquid.

Recently, Müller et al., described the cyclization of 1-amino-6-hexyne catalyzed by Lewis acids [46]. Reaction and selectivity are improved when the reacion is carried out in ionic liquids.

Recently, zinc catalysts in a biphasic system comprising ionic liquid and heptane were used for the intermolecular addition of arylamines to cyclohexadiene or for the addition of phenylacetylene to different primary amines [32]. The results have shown that with ionic liquids the catalyst activity in hydroamination reactions can be increased.

## 4. Heterogeneous catalysis

In spite of the fact that various homogeneous catalysts are known for hydroamination reactions, only few examples of heterogeneous catalysts have been reported [47]. The BASF process for tert-butylamine production from isobutene and ammonia takes places over a modified beta zeolite with more than 90 % selectivity [48, 49]. Solid acids were found to be good catalysts for the reaction between ammonia and alkenes. The key step in the reaction sequence is the protonation of the alkene to the corresponding carbenium ion [1]. Secondary alkenes show a higher tendency to form carbenium ions than primary alkenes and are generally more reactive. Once formed, a tertiary carbenium ion is more stable and provides a longer present reactive site. One essential function of the solid acid is the stabilization of the carbenium ion as alkoxy group (e.g. in zeolites) or ester group (e.g. when sulphonated polymers are used). The carbenium ion easily reacts with amine nucleophiles to form

the alkyl ammonium salt, which in turn can be deprotonated to the alkylamine. The most common solid acids used for the direct amination of alkenes with ammonia are zeolites in the proton form [50]. Reaction conditions play a major role. When using a solid acid to protonate the alkene, the more basic ammonia is also protonated to the ammonium salt. The product alkylamine is also a base and, therefore, needs to be efficiently removed from the reaction mixture. In this respect, it was shown that rate and conversion increase with increasing temperature. However at higher temperatures, the conversion decreases due to a negative reaction enthalpy, which leads to a shift in the thermodynamic equilibrium towards the starting material.

### 4.1. Zeolites

Zeolites are crystalline silicates and aluminosilicates linked through oxygen atoms, which are shaped into a three-dimensional network containing channels and cavities of molecular dimensions. Crystalline structures of the zeolite type containing mainly Si, and Al atoms are synthesized. Other structures containing different metals such as B, Ga, Fe, Cr, Ge, Ti, V, Mn, Co, Zn, Be, Cu, etc. can also by synthesized, and they are referred by the generic name of zeotypes; they include, among others, ALPO4, SAPO, MeAPO, and MeAPSO molecular sieves [51]. Such tri-dimensional networks of well-defined micropores can act as reaction channels whose activity and selectivity will be determined by introduced active sites. The presence of strong electric fields and controllable adsorption properties within the pores produce a unique type of catalyst, which by itself can be considered as a catalytic microreactor. Summarizing, zeolites in the proton form are solid catalysts with the following properties:

- High surface area.
- Molecular dimensions of the pores.
- High adsorption capacity.
- Partitioning of reactant/products.
- Possibility of modulating the electronic properties of the active sites.
- Possibility for preactivating the molecules when in the pores by strong electric fields and molecular confinement.

Analogously to enzymes, zeolites with their regular well defined pore dimensions are able to discriminate [52] reactants and products by size and shape, when they

present significant differences in diffusivity through a given pore channel system. A particular relevant example of this type is the selective cracking of n-paraffins and n-olefins with respect to their branched isomers using medium-pore-size zeolites with pore diameters in the range 0.45–0.56 nm. This effect is based on zeolite shape selectivity by mass transport discrimination, when the diffusion coefficients for branched and linear hydrocarbons within the pores are at least one order of magnitude different. Researchers from Mobil pioneered extensive research effort on the synthesis of new zeolites and their geometrical implications for reactivity [53] that culminated in a series of industrial processes.

The Brønsted acidity of zeolites is generally ascribed to their bridging [Si–(OH)–Al] hydroxyl groups. Therefore, the concentration of Brønsted sites is directly related to the number of framework Al atoms per unit cell, hence, decreases with treatments used for dealumination: steaming, treatments with acids or with silicon compounds, such as silicon tetrachloride or ammonium hexafluorosilicate. However with certain zeolites, part of the Brønsted acidity is not due to the bridging hydroxyl groups but to hydroxyl groups associated with silica alumina debris [54].

Lewis sites can be related to aluminum species either in extraframework positions or partly linked to the framework and their concentration decreases on acid leaching [55], but increases on calcination [56] and steaming [57]. The existence of Brønsted sites, different by their strength, has been demonstrated [58]. The strongest Brønsted sites are located in well crystallized areas, whereas the weakest are found in areas of lower crystallinity [59]. The presence of very strong Brønsted sites has also been noticed in several works [57-59].

Catalytic, sorptive, and ion-exchange properties of zeolites as well as their chemical and thermal stability are strongly dependent on the amount of tetrahedrally co-ordinated aluminum in the framework. Thus, the ability to vary the Si/Al ratio of the parent zeolite, while maintaining its topology and crystallinity is of great importance.

Zeolite Beta, a 12-ring aperture threedimensional high-silica zeolite, currently receives much attention as a potential catalyst in numerous reactions [60]. In addition to its Brønsted acidic properties it displays Lewis acidity as well. Interestingly, this Lewis acidity is believed not to be solely generated by extraframework aluminum (EF-Al) species, as is known for ultra stable Y (USY) samples [61], but can also be

displayed by framework aluminum atoms in a non-tetrahedral environment. The structure of zeolite Beta (BEA) is shown in Fig. 1.

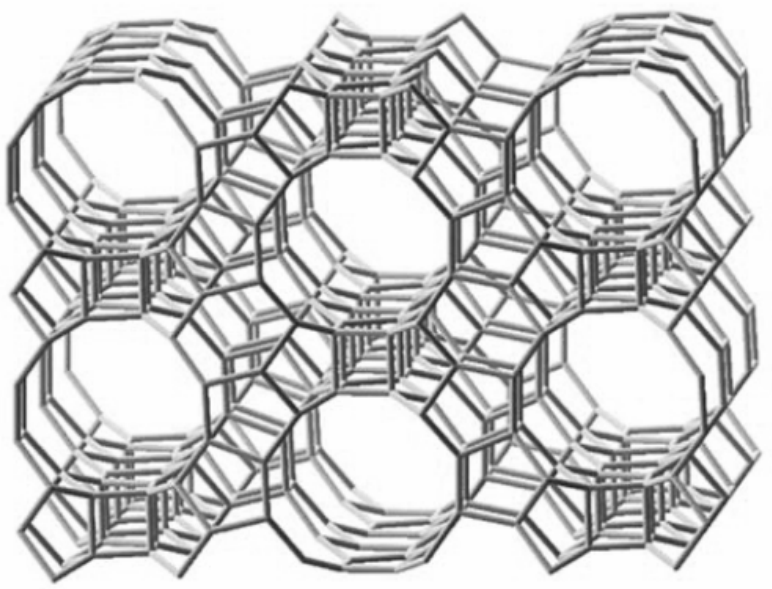

**Figure 1.** Zeolite type BEA [62] viewed along the [100] direction.

4.1.1. Ion exchanged zeolites for hydroamination reactions

Zeolites ion exchanged with late transition metal cations, such as $Rh^{+}$, $Cu^{+}$ and $Zn^{2+}$ provide an especially high catalytic activity in the addition of amines to alkynes [20]. The initial rate of reaction increases with the cation concentration in the material. However, at a certain concentration a maximum in the intrinsic activity per metal cation is achieved. It was postulated that co-catalysis between Lewis acidic metal centers ($M^{n+}$) and Brønsted acid sites ($H^{+}$) can explain these observations. The mechanism is probably similar to that using homogeneous catalysts based on late transition metals [19, 20]. The protons might be involved in three elementary steps, suggesting that Brønsted and Lewis acidic centers might be necessary in the ideal catalyst.

- As amine is the strongest base in the reaction mixture, added acids will protonate it *in situ* to the ammonium salt that has a much lower tendency to coordinate to the metal center. Thus, the probability of coordination of the alkyne group to the metal center is increased in acidic reaction media.
- The protolytic cleavage of the metal-carbon bond in an intermediate ammonium alkenyl complex is facilitated in acidic conditions.

- Enamines are coordinated more strongly to the late transition metal centers than the corresponding imines [19].

The concept of supported ionic liquids offers a new alternative for hydroamination reactions using heterogeneous catalysts.

## 4.2. Supported ionic liquids

Catalytic properties of homogeneous catalysts, in particular of transition metal complexes can be transferred onto solid supports using the concept of supported ionic liquids (Fig. 2). Preparation of well-tailored catalysts using immobilizing techniques is advantageous due to the easily tunable polarity of ionic liquids. Hydrophilicity or hydrophobicity of the liquid film can be modified by changing the length of side chains of the inorganic cation. A practical aspect is that immobilization of ionic liquids facilitates recovery of the catalyst [63].

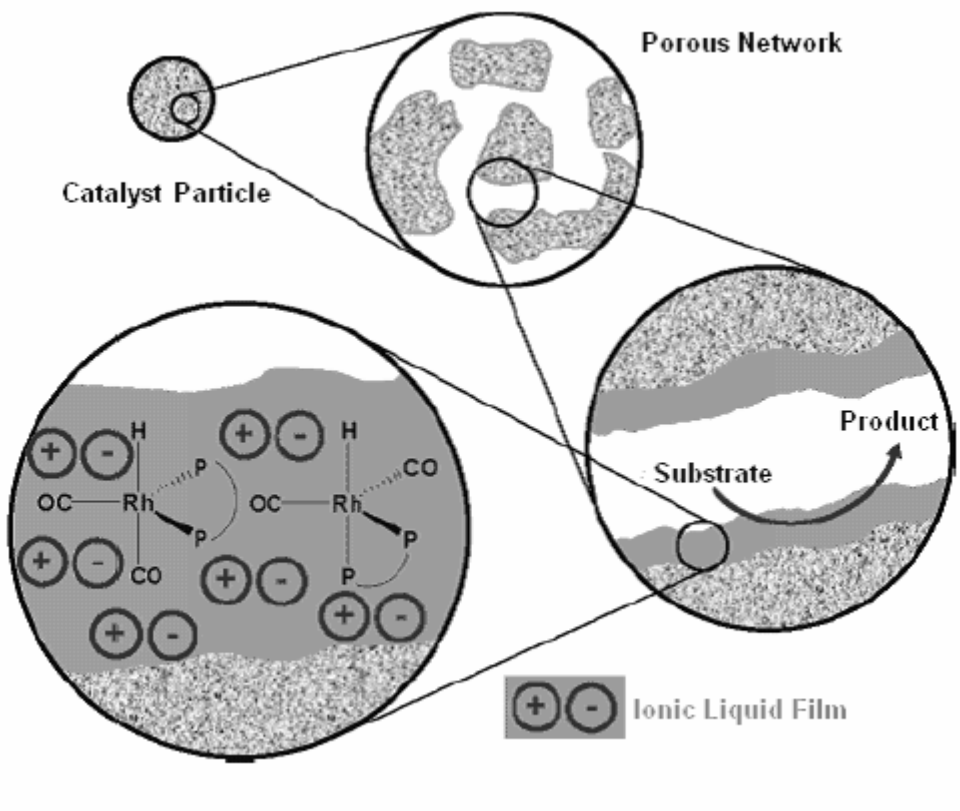


**Figure 2**. Concept for the preparation of heterogeneous catalysts based on immobilized ionic liquids [64]

The use of supported ionic liquids for hydroamination reactions was reported by Suppan and coworkers for the addition of 4-isopropylaniline to phenylacetylene catalyzed by immobilized Rh(I), Pd(II) and Zn(II) complexes in thin films of supported ionic liquid [65]. The intrinsic catalytic activity of the supported complexes was higher than of the corresponding homogeneous catalysts.

It is anticipated that the concept of supported ionic liquids will help bridging the gap between homogeneous and heterogeneous catalysis and will lead to improved catalytic processes in the future.

## 5. Scope of the thesis

The ideal of a heterogeneous catalytic process affording, under mild conditions and in high yield aromatic amines directly from alkenes and aryl-amines, that is, the intermolecular hydroamination of non-activated alkenes, has been the ultimate motivation behind, and the principal theme of this thesis. Despite the various developments achieved over the years, there is still no efficient, generally applicable catalytic system for hydroamination reactions available. We have therefore embarked on the preparation and characterization of a new type of heterogeneous Lewis and Brønsted acidic catalysts in order to provide a substantiated knowledge of the intermolecular hydroamination reactions proceeding on these catalysts and a way of optimizing activity and selectivity.

After an overview of the different catalytic systems used and of some experimental and mechanistic aspects of catalytic hydroamination in Chapter 1, the results have been subdivided into four sections reflecting the main investigation fields of this thesis:

Chapter 2 describes the use of acidic form and zinc ion exchanged zeolites for the intermolecular hydroamination of 1,3-cyclohexadiene with aryl-amines. The mechanism of hydroamination and the influence of the basicity of the arylamine on the reaction rate were studied.

In Chapter 3 the synthesis and characterization of a new type of heterogeneous catalysts for hydroamination reactions is studied. Four different imidazolium based ionic liquids were used to immobilize a palladium complex. BET analysis, IR and solid state NMR spectroscopy were employed as characterization techniques. The

formation of ordered three-dimensional structures in solutions of organometallic complexes in a thin film of supported ionic liquid was the main finding.

In Chapter 4 the catalysts prepared in chapter 3 were tested for the addition of aniline to vinyl-benzene as a test reaction. Formation of both, the Markownikoff product (kinetic regime) and the anti-Markownikoff product (thermodynamic regime) was observed and the mechanism studied.

Chapter 5 deals with the different ionic liquids used for the preparation of the supported catalysts and their influence in the catalytic activity of hydroamination reactions. In particular, the polarity of the ionic liquid strongly influences the catalytic activity. The catalysts were tested for leaching of the palladium complex from the ionic liquid phase to the bulk solvent phase. Tests comparing the catalytic activity of three different systems; homogeneous, two-phase and heterogeneous catalysis were also performed.

Finally, Chapter 6 provides a summary of the results and draws the main conclusions of this thesis.

## 6. References

[1] T. E. Müller, in: I. T. Horváth (Ed), Encyclopedia of Catalysis, Wiley, New York, (2002) 492.

[2] T. E. Müller, M. Beller, Chem. Rev. 98 (1998) 675.

[3] D. M. Roundhill, Catal. Today. 92 (1997) 1.

[4] A.Ricci, Modern Amination Methods, Wiley-VCH, Weinheim, (2000)

[5] B. Cornils, W. A.Herrmann, Applied Homogeneous Catalysis with Organometallic Compounds. Wiley VCH, Weinheim, (2000)

[6] M. Kawatsura, J. F. Hartwig, J. Am. Chem. Soc. 122 (2000) 9546.

[7] A. L. Casalnuovo, J. C. Calabrese, D. Milstein, J. Am. Chem. Soc. 110 (1988) 6738.

[8] J. J. Brunet, D. Neibecker, in: A. Togni, H. J. Grützmacher (Eds), Catalytic Heterofunctionalization, Wiley-VCH, Weinheim, (2001)

[9] M. Nobis, B. Driessen-Holscher, Angew. Chem. Int. Ed. 40 (2001) 3983

[10] L. Ackermann, R. G. Bergman, Org. Lett. 4 (2002) 1475

[11] A. P. Duncan, R. G. Bergman, Chem. Rec. 2 (2002) 431

[12] G. A. Molander, J. A. C. Romero, Chem. Rev. 102 (2002) 2161

[13] T. Straub, A. Haskel, T. G. Neyroud, M. Kapon, M. Botoshansky, M. S. Eisen, Organometallics, 20 (2001) 5017

[14] H. Schaffrath, W. Keim, J. Mol. Catal. A: Chem. 168 (2001) 9

[15] M. Beller, C. Breindl, M. Eichberger, C. G. Hartung, J. Seayad, O. R. Thiel, A. Tillack, H. Trauthwein, Synlett (2002) 1579

[16] D. B. Grotjahn, H. C. Co, Organometallics. 14 (1995) 5463

[17] A. M. Johns, M. Utsunomiya, C. D. Incarvito, J. F. Hartwig, J. Am. Chem. Soc. 128 (2006) 1828.

[18] J. M. Seul, S. Park, J. Chem. Soc. Dalton. Trans. (2002) 1153

[19] J. Penzien, R. Q. Su, T. E. Müller, J. Mol. Catal. A: Chem. 182 (2002) 489.

[20] J. Penzien, T. E. Müller, J. A. Lercher, Micropor. Mesopor. Mater. 48 (2001) 285

[21] A. Ates, C. Quinet, Eur. J. Org. Chem. (2003) 1623

[22] B. M. Trost, W. P. Tang, J. Am. Chem. Soc. 125 (2003) 8744

[23] B. Cornils, W. A. Herrmann, J. Catal. 216 (2003) 23.

[24] M. K. Richmond, S. L. Scott, H. Alper. J. Am. Chem. Soc. 123 (2001) 10521.

[25] M. Utsunomiya, J. F. Hartwig, J. Am. Chem. Soc. 126 (2004) 2702.

[26] J. Pawlas, Y. Nakao, M. Kawatsura, J. F. Hartwig, J. Am. Chem. Soc. 124 (2002) 3669.

[27] O. Lober, M. Kawatsura, J. F. Hartwig, J. Am. Chem. Soc. 123 (2001) 4366.

[28] U. Nettekoven, J. F. Hartwig, J. Am. Chem. Soc. 124 (2002) 1166

[29] K. L. Li, K. K. Hii, Chem. Commun. (2003) 1132.

[30] K. L. Li, P. N. Horton, M. B. Hursthouse, K. K. Hii, Organomet. Chem. 665 (2003) 250.

[31] L. M. Lutete, I. Kadota, Y. Yamamoto, J. Am. Chem. Soc. 126 (2004) 1622

[32] J. Bodis, T. E. Müller, J. A. Lercher, Green Chem. 5 (2003) 227.

[33] J. L. Anthony, E. J. Maginn, J. F. Brennecke, J. Chem. Phys. B. 106 (2002) 7315.

[34] R. Sheldon, Chem. Commun. (2001) 2399.

[35] S. Sugden, H. Wilkins, J. Chem. Soc. (1929) 1291.

[36] Y. Chauvin, B. Gilbert, I. Guibard, J. Chem. Soc. Chem. Commun. (1990) 1715.

[37] J. S. Wilkes, M. J. Zaworotko, J. Chem. Soc. Chem. Commun. (1990) 965.

[38] M. Freemantle, Chem. Eng. News. 76 (1998) 32

[39] R. D. Rogers, K. R. Seddon (Eds) Ionic Liquids as Green Solvents: Progress and prospects, ACS Symp. Ser. Vol. 856. American Chemical Society, Washington D. C. (2003)

[40] M. J. Earle, K. R. Seddon, P. B. McCormac, Green. Chem. 6 (2000) 261.

[41] D. Allen, G. Baston, A. E. Bradley, T. Gorman, A. Haile, I. Hamblett, J. E. Hatter, M. J. F. Healey, B. Hodgson, R. Lewin, K. V. Lovell, B. Newton, W. R. Pitner, D. W. Rooney, D. Sanders, K. R. Seddon, H. E. Sims, R. C. Thied, Green. Chem. 2 (2002) 152.

[42] H. Olivier, J. Mol. Catal. A: Chem. 146 (1999) 285.

[43] D. W Rooney, K. R. Seddon, in: G. Wypych (Ed), Handbook of Solvents, ChemTech Publishing, Toronto, (2001) 1459.

[44] T. A. Rhodes, K. O´Shea, G. Bennett, K. P. Johnston, M. A. Fox, J. Phys. Chem. 99 (1995) 9903.

[45] J. J. Brunet, N. C. Chu, O. Diallo, E. Mothes, J. Mol. Catal. A: Chem. 198 (2003) 107.

[46] V. Neff, T. E. Müller, J. A.Lercher, J. Chem. Soc., Chem. Comm. 8 (2002) 906.

[47] H. M. Senn, P. E. Blöchl, A. Togni, J. Am. Chem. Soc. 122 (2000) 4098.

[48] K. Tanabe, W. F. Hölderich, Appl. Catal. A. 181 (1999) 399.

[49] A. Chauvel, B. Delmon, W. H. Hölderich, Appl. Catal. 115 (1994) 173.

[50] J. Penzien, C. Haeßner, A. Jentys, K. Köhler, T. E. Müller, J. A. Lercher, J. Catal. 221 (2004) 302.

[51] E. M. Flanigen, Stud. Surf. Sci. Catal. 58 (1991) 1.

[52] J. Weitkamp, Solid State Ionics. 131 (2000) 175.

[53] A. Corma, J. Catal. 216 (2003) 298

[54] G. Garralon, A. Corma, V. Fornes, Zeolites. 9 (1989) 84.

[55] I. Kirisci, C. Flego, G. Pazzuconi, W. O. Parker, R. Millini, C. Perego, G. Bellusi, J. Phys. Chem. 98 (1994) 4627.

[56] C. Jia, P. Massiani, D. Barthomeuf, J. Chem. Soc. Faraday Trans. 89 (1993) 3659

[57] J. P. Marques, I. Gener, P. Ayrault, J. C. Bordado, J. M. Lopes, F. R. Ribeiro, M. Guisnet, Micropor. Mesopor. Mater. 60 (2003) 251

[58] M. Guisnet, P. Ayrault, C. Coutanceau, M.F. Alvarez, J. Datka, J. Chem. Soc. Faraday Trans. 93 (1997) 1661.

[59] M. Maache, A. Janin, J.C. Lavalley, J.F. Joly, E. Benazzi, Zeolites 13 (1993) 419.

[60] J. C.Jansen, E. J. Creyghton, S. L. Njo, H. van Koningsveld, H. van Bekkum, Catal. Today. (1997) 205.

[61] J. Sanz, V. Fornes, A. Corma, J. Chem. Soc. Faraday Trans. 84 (1988) 3113.

[62] www.iza-structure.org/databases/ Database of zeolite structures

[63] M. H. Valkenberg, C. de Castro, W.F. Hölderich, Green Chemistry, 4 (2002) 88.

[64] A. Riisager, R. Fehrmann, M. Haumann, B. S. K. Gorle, P. Wasserscheid, Ind. End. Chem. Res. 44 (2005) 9853.

[65] S. Breitenlechner, M. Fleck, T. E. Müller, A. Suppan, Mol. Catal. A: Chem. 214 (2004) 175.

# *Chapter 2*

## *Hydroamination of 1,3-cyclohexadiene with aryl amines catalyzed with acidic form zeolites*

The intermolecular hydroamination of 1,3-cyclohexadiene with aniline using zeolite catalysts was investigated. The reaction mechanism and the influence of amine basicity on the rate of reaction were studied. Zeolite H-BEA was the most active catalyst, while the incorporation of $Zn^{2+}$ (Zn/H-BEA) led to decreasing catalytic activity indicating that the reaction is catalyzed by Brønsted acid sites. Subtle shape selective effects determine reactivity and selectivity of the zeolites.

# 1. Introduction

Catalytic hydroamination is a chemical route with high synthetic potential allowing the formation of a variety of nitrogen containing molecules by direct addition of amines to alkenes and alkynes [1-3]. In comparison to other methods for the synthesis of amines, enamines, and imines [4], hydroamination offers one of the most attractive pathways to such molecules. Conceptionally, the desired higher substituted nitrogen containing products are formed in a single reaction step from inexpensive alkenes and alkynes without the intrinsic formation of side products [5,6]. Various transition metals are known to be suitable as molecular catalysts for both inter and intramolecular hydroamination of alkenes and alkynes [7]. Titanium, ruthenium, palladium, and copper complexes, e.g., have been employed as catalysts for intra- and intermolecular hydroamination of alkynes, allenes, and activated alkenes [8-14].

Intermolecular hydroamination of dienes is more difficult than hydroamination of alkynes and only few catalysts are known. Nucleophilic addition of amines to 1,3-dienes with sodium and alkyllithium salts provides primarily the 1,4-addition products. Other regioisomers are formed as by-products [4]. Lanthanum complexes can efficiently catalyze the intramolecular hydroamination of aminodienes to nitrogen-containing heterocycles [15]. Yoshifuji and co-workers reported the use of palladium complexes to obtain a high product yield for the addition of anilines to 1,3-dienes [16]. A recent study reported on the use of a liquid-liquid two-phase system to catalyze the intermolecular hydroamination of terminal alkynes and dienes with anilines [17]. The use of acids as co-catalyst can enhance the catalytic activity of palladium in the addition of aniline to dienes [18]. A similar influence of Brønsted acids was also observed for the reaction of vinylarenes with arylamines [19]. The role of the acid is still under investigation [20]. In most cases, the addition of acid seems to prevent oligomerization of the dienes as well as telomerisation of two or more olefin molecules with one amine molecule [19,21].

Although various homogeneous catalysts are known for hydroamination reactions, only few examples of heterogeneous catalysts have been reported. The amination of isobutene with ammonia to *tert*-butylamine takes place over Re-Y-zeolite with more than 90% selectivity [22]. However, this catalyst suffers from rapid deactivation. BASF has developed an iron silicate zeolite catalyst of the pentasil type

which shows not only more than 99% selectivity, but also affords commercially acceptable catalyst life [23,24]. Ion exchanged zeolites [25,26] and immobilized zinc salts [27] have been used successfully for the cyclisation of 6-aminohex-1-yne. Immobilized transition metal complexes were used in the addition of 4-isopropylaniline to phenylacetylene [28].

The present work addresses the use of Beta, ZSM-5, Faujasite and Mordenite as catalysts for the intermolecular hydroamination of 1,3-cyclohexadiene with aryl amines. Zeolite H-BEA, in particular, had been shown to be a good solid acid catalyst, especially for reactions involving bulky transition states, such as isobutene/n-butene alkylation [29,30] and is in the focus of this study. Special attention is given to the influence of the amine basicity on the rate of reaction.

## 2. Experimental

### 2.1. General

All reagents were obtained from Aldrich and were used as received. Zinc exchanged zeolites were prepared by repeated ion exchange of the corresponding H-BEA zeolite (Südchemie AG, T-4546, MA039 Hr99) in an aqueous solution of $Zn(CH_3CO_2)_2$ (for details see ref. [26]). The material was dried, calcined and the metal loading was determined by AAS. The Zn/H-BEA zeolites had a loading in the range 0.03 – 0.54 mmol $Zn^{2+} \cdot g^{-1}$ catalyst. The zeolites H-MFI (H-MFI 220, EX 717 H1-C) and H-MOR (H-MOR 90, SN 302 H/01) zeolites were supplied by Südchemie. H-FAU zeolite (CBV 400) was obtained from Zeolyst International. H-BEA zeolites with different crystal sizes were prepared at the Friedrich-Alexander-Universität Erlangen-Nürnberg.

Catalytic experiments were performed under inert nitrogen atmosphere in a Radleys reaction carousel with 12 parallel reactors. The zeolite (0.25 g) was activated overnight at 200°C in vacuum. It was suspended in toluene (15 $cm^3$) and the mixture was heated to reflux at 111°C. Aniline (91 µl, 1 mmol) and 1,3-cyclohexadiene (196 µl, 2 mmol) were added. Samples (50 µl) for gas chromatographic analysis were taken in regular intervals. GC analyses were performed on a Hewlett-Packard HP 5890A gas chromatograph equipped with a cross linked 5% diphenyl- 95% dimethyl-polysiloxane column (30 m, Restek GmbH, Rtx-5 Amine). GC-MS analyses were

performed on a Hewlett-Packard HP 5890 gas chromatograph equipped with an identical column and a mass selective detector HP 5971A. Peak areas were referenced to *n*-dodecane as internal standard. Reactions at temperatures above the boiling point of toluene were performed in a 300 $cm^3$ Parr autoclave. The apparent activation energy was determined in the range 110°C to 200°C, the reaction order in aniline in the concentration range 20 to 140 $mmol \cdot l^{-1}$. To study the influence of the aniline basicity, aniline was replaced with substituted anilines.

2.2. Physical and analytical methods

The Si/Al ratio was determined by AAS using an UNICAM 939 spectrometer. Surface area, pore diameter and pore size distribution of the catalysts were determined by nitrogen adsorption (Sorptomatic 1990 Series instrument) after activation of the samples at 250°C in vacuum.

Temperature programmed desorption profiles were measured in a custom build 6 port parallel set-up. The catalysts were pelletized and a sample (20 mg) placed into each of the quartz tubes. The samples were activated at 450°C in vacuum (at $1 \cdot 10^{-3}$ mbar) for 1 h. The samples were cooled to 150°C and ammonia adsorbed at 3 mbar for 10 min. After saturation, the samples were outgassed for 1 h to remove physisorbed ammonia. Subsequently, the temperature was increased at $10°C \cdot min^{-1}$ and the desorption process monitored with mass spectrometry (Balzers QMS 200).

For infrared (IR) spectroscopic measurements, a self-supporting wafer of the sample was placed into a sorption cell and activated at 450°C in vacuum for 1 h. The sample was cooled to 150°C and pyridine adsorbed at $10^{-1}$ mbar for 1 h. After saturation, the sample was outgassed at 150°C for 1 h. IR spectra of the activated sample were recorded in the region from 4000 to 400 $cm^{-1}$ at 4 $cm^{-1}$ resolution using a Perkin Elmer 2000 spectrometer. The sample was then heated at $10°C \cdot min^{-1}$ to 450°C and outgassed for 1 h. The temperature was subsequently reduced to 150°C and another IR spectrum taken. The concentration of acid sites was estimated from the intensity of the bands at 1544 and 1455 $cm^{-1}$, assigned to pyridinium ions (Brønsted acid sites, $\varepsilon = 1.67$ cm/μmol) and coordinatively bound pyridine (Lewis acid sites, $\varepsilon = 2.22$ cm/μmol), respectively, using molar extinction coefficients reported previously [31].

Scanning electron microscopy images were obtained on a JEOL 500 SEM microscope. Samples were outgassed for 1 day and sputtered with gold. Images were taken by operating the microscope at 23.0 kV.

## 3. Results and Discussion

### 3.1. Catalyst characterization

Three samples of zeolite H-BEA with different particle size, but similar Si/Al ratio (11.6-14.9), as well as the materials H-ZSM-5, H-Mordenite, and H-Y, and a series of zinc exchanged Zn/H-BEA zeolites (Zinc contents 0.03-0.54 $mmol \cdot g^{-1}$) were chosen for this study. To understand the performance of the zeolites in catalysis the H-BEA, H-ZSM-5, H-Mordenite and H-Y samples were fully characterized beforehand (Table 1), while a detailed characterization of the Zn/H-BEA zeolites is given in a recent publication [32].

The particle size was determined from scanning electron microscopy images. The three H-BEA samples, abbreviated BEA1, BEA2 and BEA3, consisted of crystallites with particle size of 0.15-0.20, 0.20-0.25 and 0.60-0.70 μm, respectively (Fig. 1). However, closer inspection showed that each particle was an agglomerate composed of much smaller primary particles with approximately 50-70 nm diameter. The micropore volume slightly decreased with the particle size (0.135, 0.129, 0.112 $ml \cdot g^{-1}$), which reflects that fewer pores can be accessed as the crystallites become larger. H-ZSM-5, H-Mordenite and H-Y had a particle size in a similar range (0.40-0.50, 0.50-0.60, and 0.40-0.50 μm, respectively).

**Table 1.** Physicochemical properties of the H-Zeolites used in this study.

| Catalyst | Structure | Ratio Si/Al | Pore diameter [Å] [1] | Particle size [μm] | Surface area [2] [$m^2 \cdot g^{-1}$] | MSA [3] [$m^2 \cdot g^{-1}$] | Micropore volume [$ml \cdot g^{-1}$] | BAS [4] [$mmol_{Py} \cdot g^{-1}$] | LAS [5] [$mmol_{Py} \cdot g^{-1}$] | TPD [$mmol_{NH_3} \cdot g^{-1}$] |
|---|---|---|---|---|---|---|---|---|---|---|
| H-ZSM-5 | MFI | 45 | 5.1×5.5 [100]<br>5.3×5.6 [010] | 0.40-0.50 | 359 | 191 | 0.084 | 0.21 | 0.09 | 0.35 |
| H-Mordenite | MOR | 45 | 6.5×7.0 [001]<br>2.6×5.7 [001] | 0.50-0.60 | 418 | 284 | 0.138 | 0.14 | 0.02 | 0.33 |
| H-Y | FAU | 2.7 | 7.4 × 7.4 [111] | 0.40-0.50 | 527 | 415 | 0.209 | 0.22 | 0.31 | 0.77 |
| H-BEA1 | BEA | 14.2 | 6.6 × 6.7 [100]<br>5.6 × 5.6 [001] | 0.15-0.20 | 541 | 391 | 0.135 | 0.17 | 0.14 | 0.63 |
| H-BEA2 | BEA | 11.6 | 6.6 × 6.7 [100]<br>5.6 × 5.6 [001] | 0.20-0.25 | 624 | 359 | 0.129 | 0.19 | 0.14 | 0.41 |
| H-BEA3 | BEA | 14.9 | 6.6 × 6.7 [100]<br>5.6 × 5.6 [001] | 0.60-0.70 | 679 | 348 | 0.112 | 0.16 | 0.14 | 0.30 |

[1] The crystallographic direction is given in square brackets.
[2] BET surface area determined by $N_2$ adsorption
[3] micropore surface area (MSA) determined by $N_2$ adsorption
[4] Brønsted acid site (BAS) concentration determined by pyridine (Py) adsorption
[5] Lewis acid site (LAS) concentration determined by pyridine adsorption

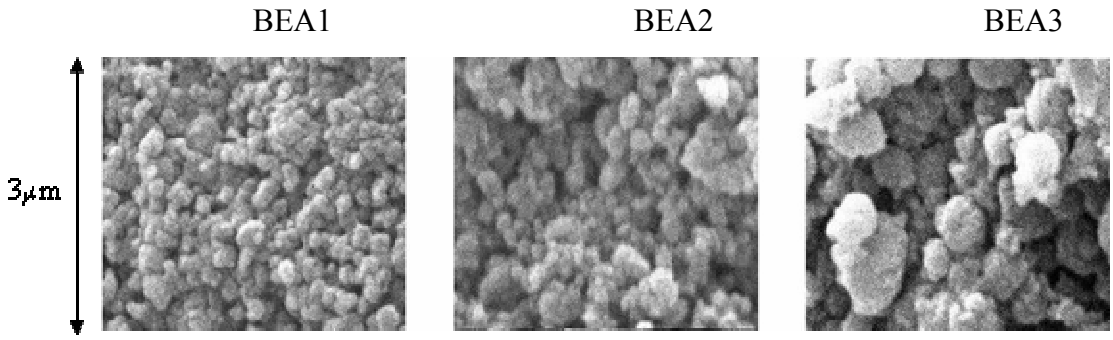


**Figure 1.** SEM Micrographs of the H-BEA zeolites used in this study.

The acidity of the zeolite samples was assessed by temperature programmed desorption (TPD) of ammonia and from infrared spectra after adsorption of pyridine. The TPD traces of ammonia desorbing from the three H-BEA zeolites are presented in Fig. 2. The traces showed two desorption maxima at *ca*. 340°C and 560°C. The low temperature peak is characteristic for desorption of ammonia from weak acid sites while the high temperature peak is related to desorption of ammonia from strong acid sites.

Deconvolution of the two peaks using a linear combination of Gauss functions [33] showed that 0.48, 0.28 and 0.22 $mmol \cdot g^{-1}$ ammonia desorbed from the weak acid sites, while 0.15, 0.13 and 0.08 $mmol \cdot g^{-1}$ ammonia desorbed from the strong acid sites (samples BEA1, BEA2 and BEA3, respectively). From the entire amount of ammonia adsorbed on zeolite BEA1, the overall acid site density was calculated to 0.63 $mmol \cdot g^{-1}$. With increasing particle size, the value decreased to 0.41 and 0.30 $mmol \cdot g^{-1}$ for the zeolite BEA2 and BEA3, respectively.

This strongly suggests that the pore system is less accessible for ammonia molecules the larger the particle size is. However, as ammonia sorbs unspecifically [34] on Brønsted and Lewis acid sites (abbreviated BAS and LAS) the assignment of the low and high temperature peak is somewhat ambiguous. The overall acid site density for H-ZSM-5, H-Mordenite and H-Y was in the same range (0.35, 0.33 and 0.77 $mmol \cdot g^{-1}$, respectively).

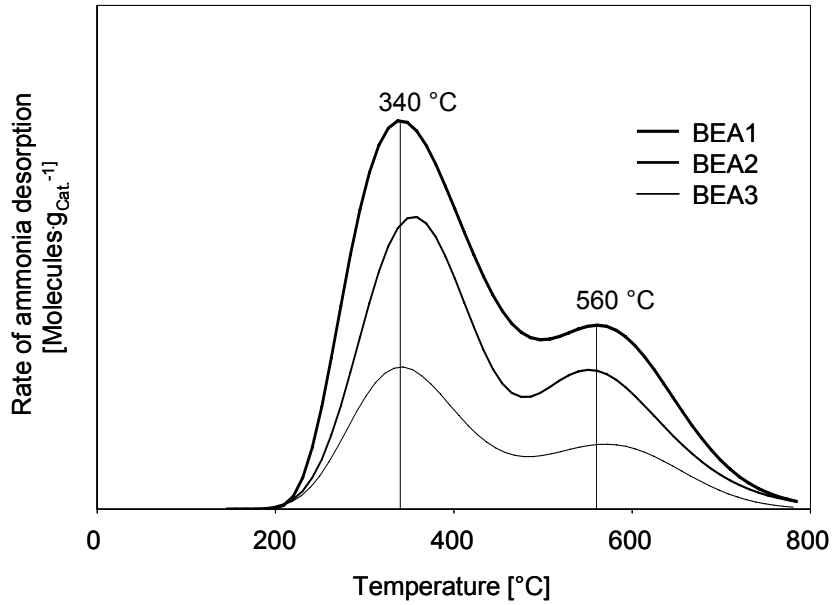


**Figure 2.** TPD profiles for desorption of ammonia from H-BEA zeolites.

The IR spectra of activated zeolites exhibited several bands for isolated and bridging OH groups (Fig. 3). The most intense band was observed at 3739 – 3742 $cm^{-1}$ (attributed to external SiOH groups). While the band is at 3739 $cm^{-1}$ for zeolite BEA1, the band is observed at 3742 $cm^{-1}$ for zeolites BEA2 and BEA3. The inherent high concentration of defect sites in zeolite BEA leads to a high concentration of internal silanol groups, which then become clearly visible in the IR spectrum. These OH groups frequently form hydrogen bonds, which give rise to the band tailing from 3700 $cm^{-1}$ down to 3300 $cm^{-1}$ [35]. The band at 3606 $cm^{-1}$, observed with all samples in nearly the same intensity (0.062, 0.078 and 0.067 normalized absorbance units for BEA1, BEA2, BEA3, respectively), corresponds to bridging hydroxyl groups, which give rise to strong Brønsted acidity of the material [36]. For BEA2, the additional band with low intensity observed at 3780 $cm^{-1}$ is assigned to AlOH groups of extra framework alumina.

After pyridine adsorption at 150°C, the two bands at 3606, and 3780 $cm^{-1}$ vanished completely. This shows that these OH groups are fully accessible to pyridine. In contrast, the peaks in the silanol region remained nearly unchanged after pyridine adsorption. This confirms the weak acidity of the external silanol OH protons [37]. The broad adsorption band between 3700 and 3400 $cm^{-1}$ also appears to be sensitive to pyridine adsorption, however, to a much lesser extent.

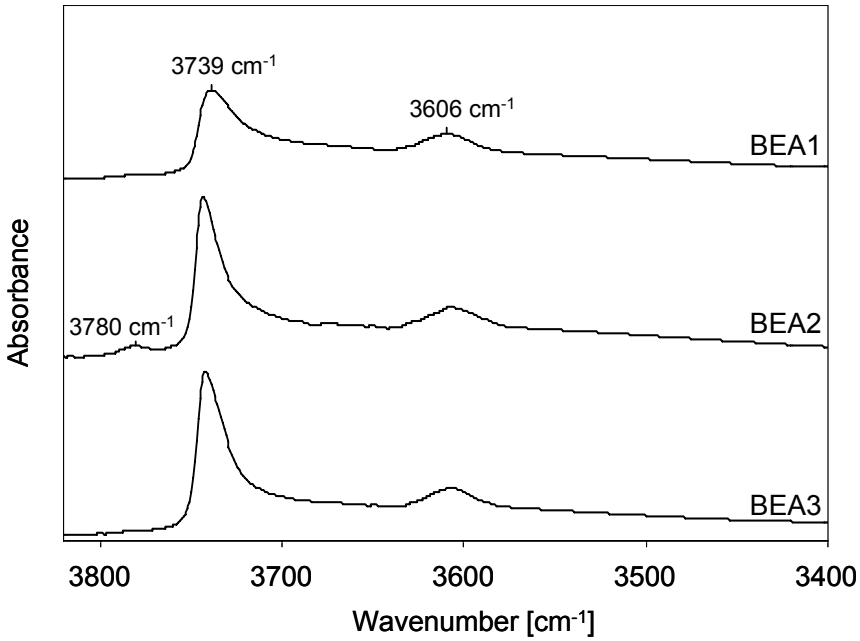


**Figure 3.** Infrared spectra of the hydroxyl region of the H-BEA zeolites.

The ring vibrations of adsorbed pyridine were used to quantify the acid site concentration (Fig. 4). The Brønsted acid sites were identified by the peak at 1544 $cm^{-1}$ (pyridinium ions). Only minor differences in the Brønsted acid site concentration were observed for the three samples (0.16 - 0.19 $mmol \cdot g^{-1}$, see Table 1). Note that the concentration of BAS was independent of the zeolite particle size. After desorption of pyridine by heating to 450°C for 1 h the concentration of pyridinium ions decreased dramatically. In case of zeolite BEA1, all pyridine was removed by this procedure, while for zeolites BEA2 and BEA3, the BAS concentration decreased to 0.04 and 0.03 $mmol \cdot g^{-1}$, respectively. Thus, BEA2 and BEA3 contained a higher proportion of strong BAS than BEA1.

The Lewis acid sites generally associated with accessible $Al^{3+}$ cations gave rise to a peak at 1455 $cm^{-1}$ (coordinatively bound pyridine). However, in the spectra of pyridine adsorbed on BEA1 and BEA3 a further peak at 1443 $cm^{-1}$ was observed. This peak is probably related to sodium cations remaining from the preparation process [38]. Quantitative analysis showed that zeolites BEA1 and BEA3 contained 0.68 and 0.66 wt% sodium, while the sodium concentration in H-BEA2 was 0.01 wt%.

From the combined intensity of the peaks at 1443 and 1455 $cm^{-1}$, the same LAS concentration (0.14 $mmol \cdot g^{-1}$) was measured for all three samples. After outgassing at 450°C, the concentration of pyridine adsorbed on the Lewis acid sites of zeolite BEA2

was reduced by approximately 16% to 0.12 $mmol \cdot g^{-1}$, while for zeolites BEA1 and BEA3, the concentration of adsorbed pyridine molecules decreased by 50% to 0.07 and 0.08 $mmol \cdot g^{-1}$, respectively. Pyridine molecules, which gave rise to the band at 1443 $cm^{-1}$, were completely removed by outgassing at 450°C. This observation is consistent with assignment to weakly acidic sodium cations.

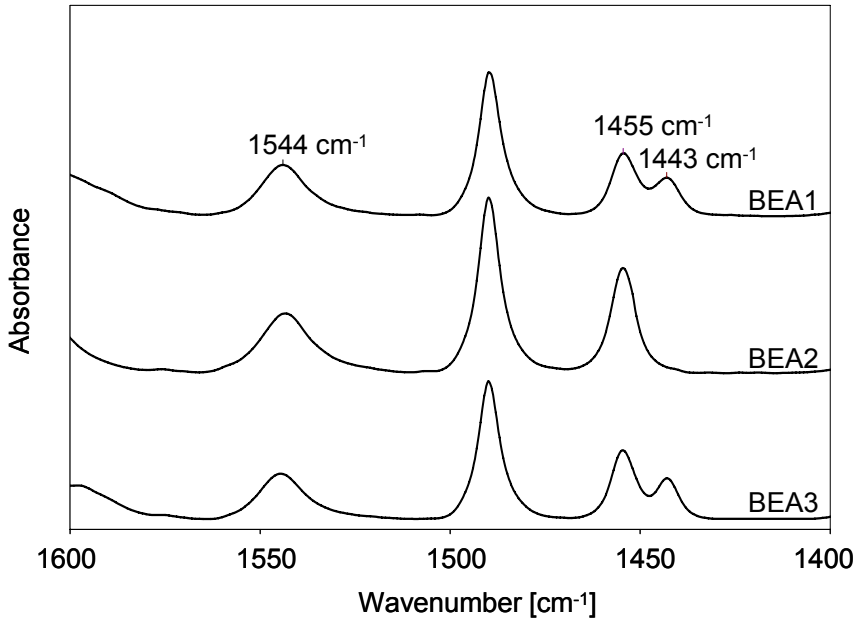


**Figure 4** . Infrared spectra of the H-BEA zeolites after pyridine adsorption.

3.2. Catalytic measurements

The addition of aniline to 1,3-cyclohexadiene was studied as model reaction for hydroamination. The three samples of H-BEA with different particles size, a series of Zn/H-BEA zeolites varying in the zinc content, as well as various H-Zeolites differing in the pore diameter were used as catalysts. All zeolites, except H-ZSM-5, catalyzed the reaction providing cyclohex-2-enyl-phenylamine (**1**) as main product. More detailed analysis of the product mixture indicated that structural isomers differing in the position of the double bond were formed (Fig. 5).

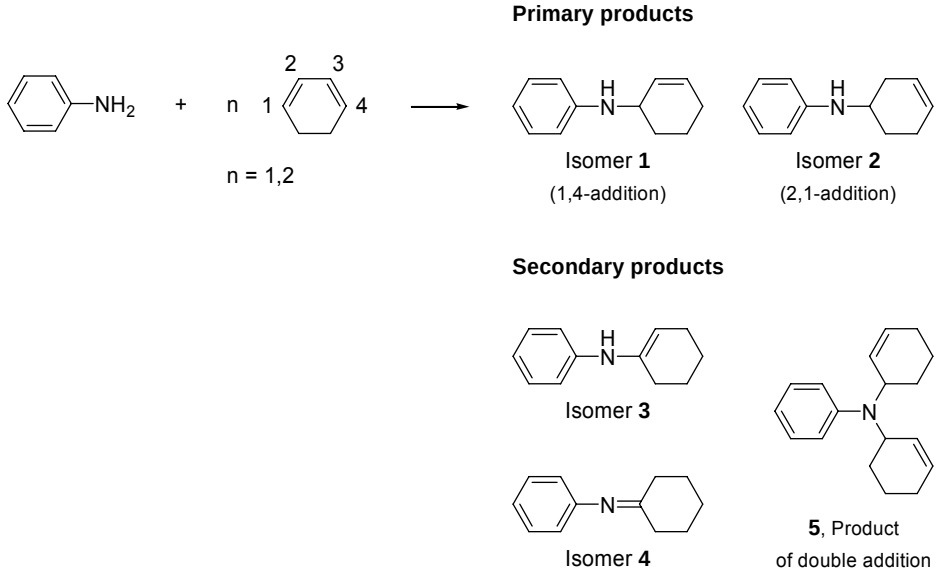


**Figure 5** . Possible reaction products from the addition of aniline to 1,3-cyclohexadiene.

At short reaction times, the formal 1,4- and 2,1-addition products **1** and cyclohex-3-enyl-phenylamine (**2**), respectively, were formed in parallel. Note that the 1,2-addition product is indistinguishable from the 1,4-addition product. At longer reaction times, isomer **1** became the main product, whereas the concentration of isomer **2** decreased (Fig. 6). In parallel, the concentration of cyclohex-1-enyl-phenylamine (**3**) increased. In contrast, the formation of the Schiff-base cyclohexylidene-phenylamine (**4**) was not observed. This can be rationalized by a much lower thermodynamic stability of isomer **4**, probably caused by steric conflict between the β-protons of the phenyl and cyclohexylidene ring which prevents parallel alignment of the phenyl ring and the C=N π-system. At very long reaction times, an increasing amount of di-(cyclohex-2-enyl)-phenylamine (**5**) was observed, which results from addition of two 1,3-cyclohexadiene molecules to one aniline molecule.

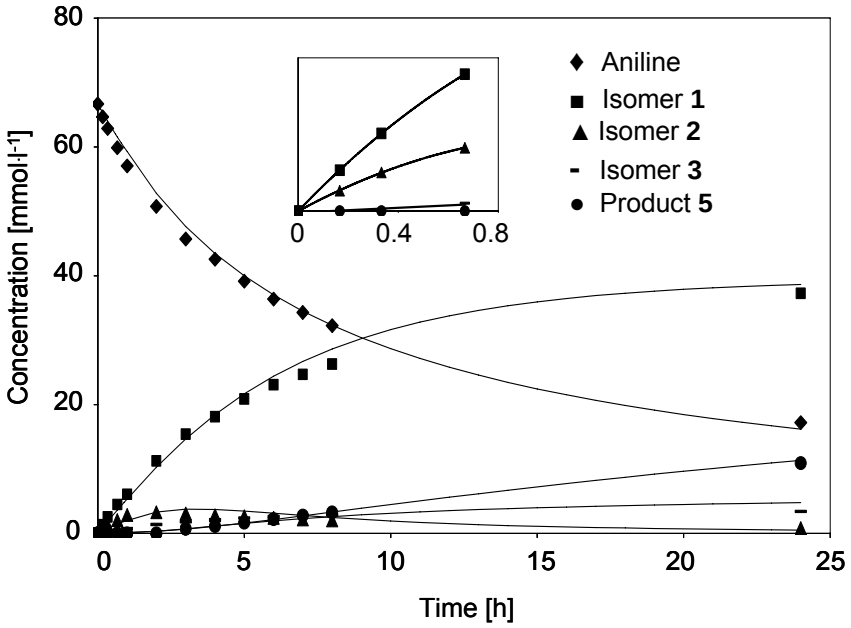


**Figure 6**. Reaction profile of the reaction between 1,3-cyclohexadiene and aniline using H-BEA as catalyst. The continuous lines describe the concentration profile derived from the kinetic model given in Fig. 7.

The reaction profile could be described well on the basis of the model shown in Fig. 7, which enabled deriving the rate constants of the individual reaction steps. For the model, irreversibility of the reactions and first order in all reactants was assumed. In this respect, the reaction order for aniline was determined to 0.93 in the concentration range 20 - 140 mmol·l$^{-1}$. Note that the fitted lines (Fig. 6) appear to be slightly underestimating the overall reactivity with respect to the disappearance of the reactant and the appearance of product **1**, while there is a minor overestimation of their concentration at the end of the reaction. This suggests that the catalysts slightly deactivate with the reaction time. An accurate estimation of the deactivation was, however, beyond the scope of this study.

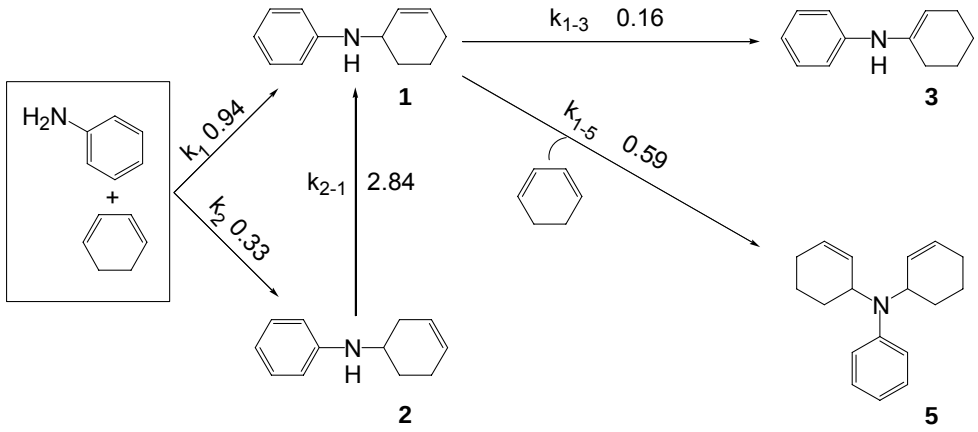


**Figure 7.** Kinetic model for the hydroamination of 1,3-cyclohexadiene with aniline using H-BEA2 as catalyst; units: $k_1$, $k_2$ in $h^{-1}$; $k_{1-3}$, $k_{1-5}$, $k_{2-1}$ in $(mmol/l)^{-1} \cdot h^{-1}$.

For BEA2, the formation of isomer **1** ($k_1$ = 0.94 $h^{-1}$) was three times faster than the formation of isomer **2** ($k_2$ = 0.33 $h^{-1}$). Product **2** isomerised to **1** ($k_{2-1}$ = 2.84 $mmol \cdot l^{-1} \cdot h^{-1}$) almost 10 times faster than it was formed. Isomer **1** isomerised to **3** or reacted to the double addition product **5** with rate constants of $k_{1-3}$ = 0.16 and $k_{1-5}$ = 2.84 $mmol \cdot l^{-1} \cdot h^{-1}$, respectively. All zeolites, except ZSM-5, followed the same reaction sequence where the rate konstant for the reaction **2** → **1** was higher than for the formation of isomer **2**.

The influence of potentially catalytically active Lewis acidic cations such as $Zn^{2+}$ on the rate of the intermolecular hydroamination was explored for a series of ion exchanged zeolites Zn/H-BEA2 with zinc concentrations between 0.03 $mmol \cdot g^{-1}$ and 0.54 $mmol \cdot g^{-1}$. The catalysts were initially selected as they showed excellent catalytic properties for the intramolecular cyclisation of 6-amino-1-hexyne [25]. The experiments were performed using the same ratio in weight between substrate and catalyst. In consequence, the total amount of zinc in the reaction mixture varied.

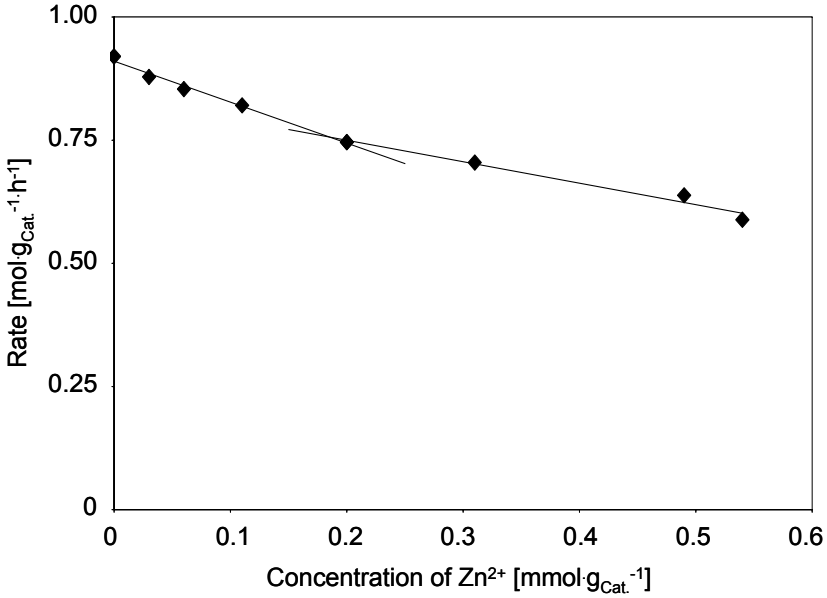


**Figure 8.** Initial rate of formation of isomer **1** with a series of Zn/H-BEA catalyst varying in zinc contents.

In contrast to our expectation, the initial catalytic activity decreased with the zinc loading. The initial rate of hydroamination was 0.92 mmol·$g_{Cat}^{-1}$·$h^{-1}$ for the parent material and decreased to 0.59 mmol·$g_{Cat}^{-1}$·$h^{-1}$ for Zn/H-BEA2 with a zinc concentration of 0.54 mmol·$g^{-1}$. This suggests that the zinc cations incorporated in BEA2 were catalytically not or less active for this reaction. Two regions of $Zn^{2+}$ loading can be distinguished with linear decrease in activity of the material (Fig. 8). For the same series of zeolites two regions of catalytic activity had equally been observed for the addition of aniline to phenylacetylene and the cyclisation of 6-aminohex-1-yne although the rate increased with zinc loading [26].

At low zinc concentrations, the zinc cations are exchanged for protons reducing the concentration of those Brønsted acid sites, which exist so close to each other that the zinc cations can coordinate to both sites [32]. Note the steeper decline of the catalytic activity with increasing zinc concentration for these materials. At higher zinc concentrations (≥ 0.20 mmol·$g^{-1}$) the zinc is present in the zeolite pores mainly as nanosized ZnO clusters, which influence the Brønsted acidity of the zeolite to a lesser degree [32].

The total concentration of Lewis acid sites increased from 0.14 $mmol \cdot g^{-1}$ for the parent H-BEA zeolite (BEA2) to 0.20 $mmol \cdot g^{-1}$ for the catalyst with the highest zinc loading [32]. In contrast, the Brønsted acid site concentration decreased with the zinc exchange degree from 0.19-0.16 $mmol \cdot g^{-1}$. The catalytic activity closely follows the trend in the concentration of BAS. Thus, the Brønsted acid sites seem to be responsible for the catalytic activity, whereas the $Zn^{2+}$ cations in the zeolite are inactive for the reaction. It should be noted, however, that a molecular Brønsted acid (trifluoromethanesulfonic acid) did not catalyze the reaction. These observations indicate that a reaction intermediate is stabilized in the zeolite pores. Also Lewis acid sites resulting from the presence of aluminium in the material might play a role in the catalytic cycle.

In order to explore the potential role of the zeolite structure for the addition of aniline to 1,3-cyclohexadiene, fully ammonia exchanged and activated Brønsted acidic zeolites (without metal cations at exchange positions) with different pore diameters were examined. In particular, the catalytic activity of H-ZSM-5, H-Mordenite, and H-Y was compared with that of H-BEA zeolite. For all zeolites, the rate of reaction was reduced (Fig. 9). No reaction was observed for H-ZSM-5.

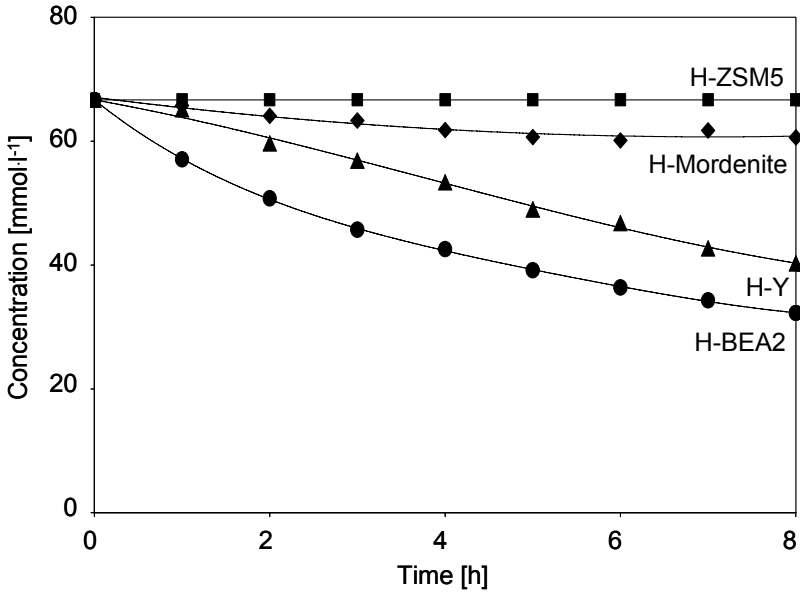


**Figure 9.** Aniline conversion for the reaction between 1,3-cyclohexadiene and aniline catalyzed by different H-zeolites.

The reactants are able to access the acid sites of all zeolites used. It should be noted, however, that the products face strong constraints to diffuse out of the pores. This is especially pronounced for H-ZSM-5 having the smallest channel diameter. The larger, but one-dimensional pores of Mordenite led to low activity with $k_1$ and $k_2$ values of 0.05 and 0.06 $h^{-1}$, respectively (Table 2), while **5**, the product of double addition of 1,3-cyclohexadiene to aniline, was not observed. H-Y zeolite with a three-dimensional large pore system had nearly a six fold higher reaction rate ($k_1$ 0.33 $h^{-1}$ and $k_2$ 0.33 $h^{-1}$) than H-Mordenite. However, the supercage of H-Y is sufficiently large to allow the double addition product **5** to be formed ($k_{1\text{-}5}$ 1.11 $(mmol/l)^{-1} \cdot h^{-1}$; 38% yield after 24h). Zeolite BEA, on the other hand has two interconnecting channel systems forming a smaller space than the faujasite supercage. Consequently, the reactants and the desired products can diffuse in and out the pores and the reaction rate is higher ($k_1$ 0.94 $h^{-1}$ and $k_2$ 0.33 $h^{-1}$). The product of the double addition is formed in lower amounts ($k_{1\text{-}5}$ 0.59 $(mmol/l)^{-1} \cdot h^{-1}$; 17% yield after 24h). The results suggest that the hydroamination reaction can be catalyzed most efficiently in the pores of a zeolite with 12 membered ring openings, such H-BEA zeolite, and that subtle shape selective effects determine reactivity and selectivity.

**Table 2.** Rate constants for single reactions steps and initial reaction rate for the hydroamination of 1,3-cyclohexadiene with aniline calculated on basis of the kinetic model given in Figure 7.

| | Hydroamination | | | Isomerisation | | Initial Rate [1] |
|---|---|---|---|---|---|---|
| Catalyst | $k_1$ $[h^{-1}]$ | $k_2$ $[h^{-1}]$ | $k_{1\text{-}5}$ $[(mmol/l)^{-1} \cdot h^{-1}]$ | $k_{2\text{-}1}$ $[(mmol/l)^{-1} \cdot h^{-1}]$ | $k_{1\text{-}3}$ $[(mmol/l)^{-1} \cdot h^{-1}]$ | $r_{ini}$ $[mmol \cdot g_{Cat}^{-1} \cdot h^{-1}]$ |
| H-ZSM-5 | 0.00 | 0.00 | 0.00 | 0.00 | 0.00 | 0.00 |
| H-Mordenite | 0.05 | 0.06 | 0.00 | 7.06 | 0.04 | 0.20 |
| H-Y | 0.33 | 0.33 | 1.11 | 6.18 | 0.09 | 0.58 |
| H-BEA1 | 2.15 | 1.08 | 1.02 | 3.54 | 0.13 | 1.63 |
| H-BEA2 | 0.94 | 0.33 | 0.59 | 2.84 | 0.16 | 0.92 |
| H-BEA3 | 0.19 | 0.07 | 0.00 | 3.61 | 0.18 | 0.20 |

[1] initial rate of aniline consumption

The influence of the particle size was studied for the series of H-BEA zeolites with increasing particle size and similar Brønsted acid site concentration. The rate of reaction decreased with the particle size (Fig. 10). As the diameter of the micropores strongly influences the activity, we exclude that the reaction takes place exclusively at the pore entrance. The product formation constants for the BEA zeolites employed in this study are reported in Table 2. The rate constants $k_1$ and $k_2$ clearly decreased with the particle size. This is attributed to lower diffusive limitations in BEA1 while significant diffusion constrains appear likely for BEA2 and BEA3. Product **5** having a much larger kinetic diameter is probably formed exclusively at the outer surface. The rate constant $k_{1\text{-}5}$ also decreased with the particle size confirming our conclusions on diffusion limitations. Formation of product **5** was not observed for BEA3. In contrast, isomerization constants $k_{2\text{-}1}$ and $k_{1\text{-}3}$ are apparently not affected by the particle size.

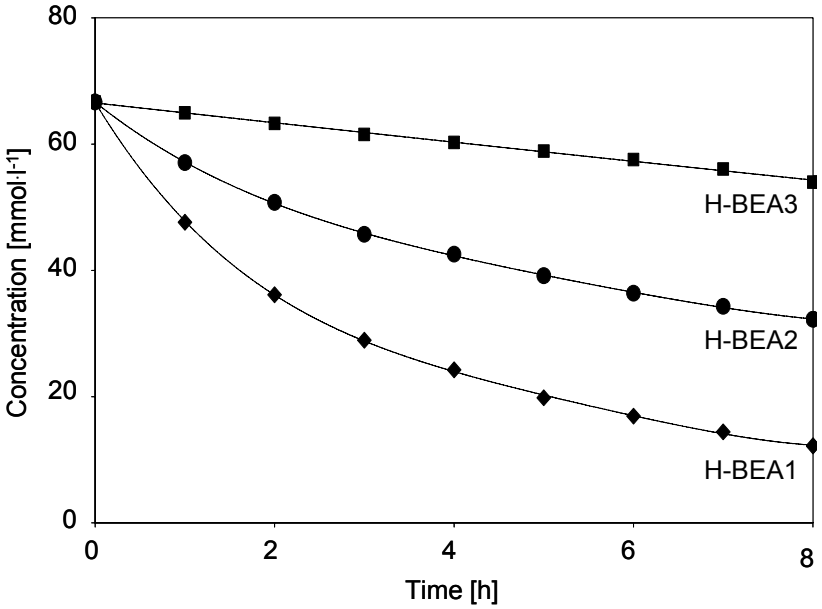


**Figure 10.** Aniline conversion for the reaction between 1,3-cyclohexadiene and aniline catalyzed by H-BEA zeolites with different particle size.

For zeolite BEA2, a low apparent activation energy of 45 $kJ \cdot mol^{-1}$ based on aniline and 38 $kJ \cdot mol^{-1}$ based on the main product of the reaction was determined in the temperature range 110–200°C. The relatively low activation energy would be consistent with pore diffusion limitations.

3.3. Mechanism proposed

The data obtained from the kinetic experiments suggest the mechanism shown in Fig. 11 for the intermolecular hydroamination of 1,3-cyclohexadiene with anilines using zeolite H-BEA as catalyst. The simplest kinetic model would start with a competitive adsorption between aniline and 1,3-cyclohexadiene on the Brønsted acid sites. Aniline being a stronger base than 1,3-cyclohexadiene, preferentially gets adsorbed. However, it is in equilibrium with the free Brønsted acid site and can be displaced by the excess of 1,3-cyclohexadiene in the reaction mixture.

According with Yang and co-workers [41] alkenyl carbenium ions can be formed by direct protonation of dienes on acidic catalysts. The carbenium ions are strongly stabilised in a zeolite by interaction with the BAS and resemble more an alkoxy group. In case of 1,3-cyclohexadiene [42], coordination to one of the BAS provides either a cation with delocalized charge '**a**', or the less stable cation '**b**' [43]. Subsequent nucleophilic attack of the aniline on **a** or **b** leads to the intermediates $\mathbf{a_1}$ and $\mathbf{b_1}$, respectively. Subsequently, one of the ammonium protons is transferred to the BAS and the products **1** and **2** are desorbed.

Two possibilities exist for the nucleophilic attack during reaction pathway **a** providing the 1,2- and 1,4-addition products. These two products are indistinguishable. Only reaction pathway **b** accounts for formation of the 2,1-addition product. After desorption, the primary reaction products **1** and **2** diffuse into the bulk solution and are re-adsorbed prior to isomerisation. The latter is also thought to occur on the Brønsted acid sites. An alternative reaction sequence with hydroamination and isomerisation in succession (without desorption and re-adsorption of the intermediates) can be excluded on basis of the kinetic model.

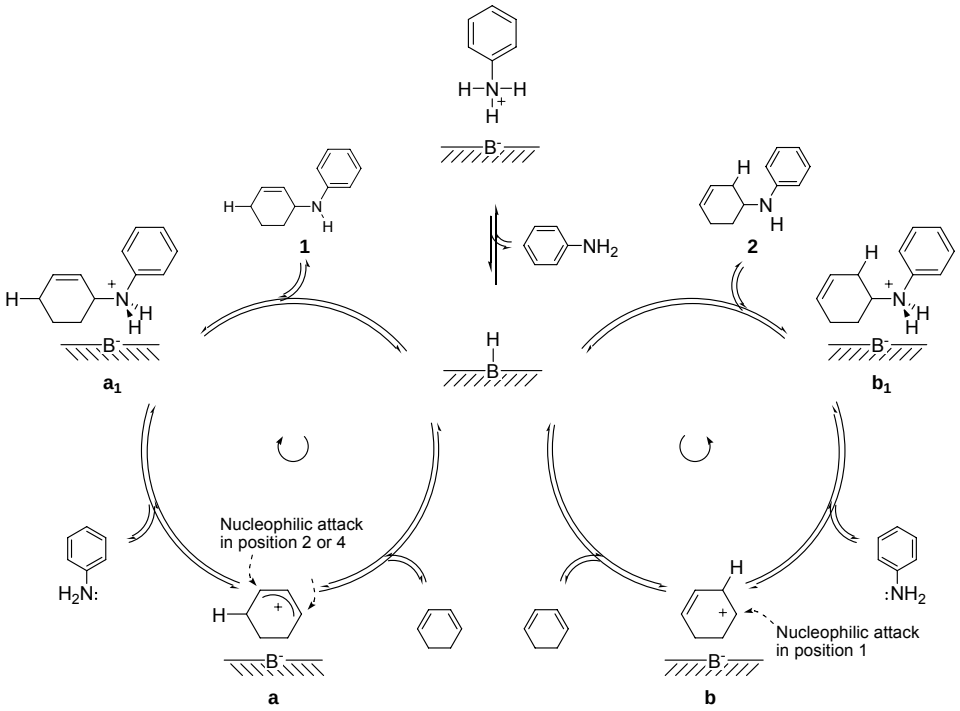


B–H, Brønsted acid site

**Figure 11.** Correlation between the initial rate of the addition of aniline to 1,3-cyclohexadiene and the basicity of the aniline.

## 3.4. Influence of amine basicity

As the reaction is acid catalyzed, the basicity of the reacting amine could drastically change the interaction between reactants and catalyst. Therefore, the influence of aniline basicity on the hydroamination of 1,3-cyclohexadiene was studied. Anilines with a variety of substituents on the aromatic ring were used, in particular, those with substituents in *para*- position to the $NH_2$ group. This allows changing the basicity of the aniline without changing the minimum kinetic diameter of the molecule. It can, thus, be assumed that the *para*-substituted anilines have similar diffusion rates inside the zeolite pores.

**Table 3.** Basicity ($pK_b$) of the arylamines used and rate of reaction in the hydroamination of 1,3-cyclohexadiene.

| Aromatic amine | Substituent | $pK_b$ | Initial rate [1] [$mmol \cdot g_{Cat}^{-1} \cdot h^{-1}$] | Isomer ratio [2] [%] |
|---|---|---|---|---|
| 4-methoxyaniline | *para* -OMe | 8.7 | 0.19 | 90/5/5 |
| 4-ethylaniline | *para* -Et | 8.9 | 0.29 | 94/6/0 |
| 4-fluoroaniline | *para* -F | 9.3 | 0.48 | 97/3/0 |
| aniline | *para* -H | 9.4 | 0.92 | 90/3/7 |
| 2-methoxyaniline | *ortho* -OMe | 9.5 | 0.17 | 93/0/7 |
| 3-methoxyaniline | *meta* -OMe | 9.8 | 0.79 | 94/3/3 |
| 4-chloroaniline | *para* -Cl | 10.0 | 0.82 | 94/0/6 |
| ethyl-4-aminobenzoate | *para* -COOEt | 10.5 | 1.15 | 100/0/0 |
| 4-(trifluoromethyl)aniline | *para* -$CF_3$ | 11.2 | 1.07 | 90/0/10 |
| 4-nitroaniline | *para* -$NO_2$ | 13.0 | 1.80 | 100/0/0 |

[1] initial rate of aniline consumption

[2] after 24 h reaction time; ratio of isomers **1**, **2**, and **3**, respectively

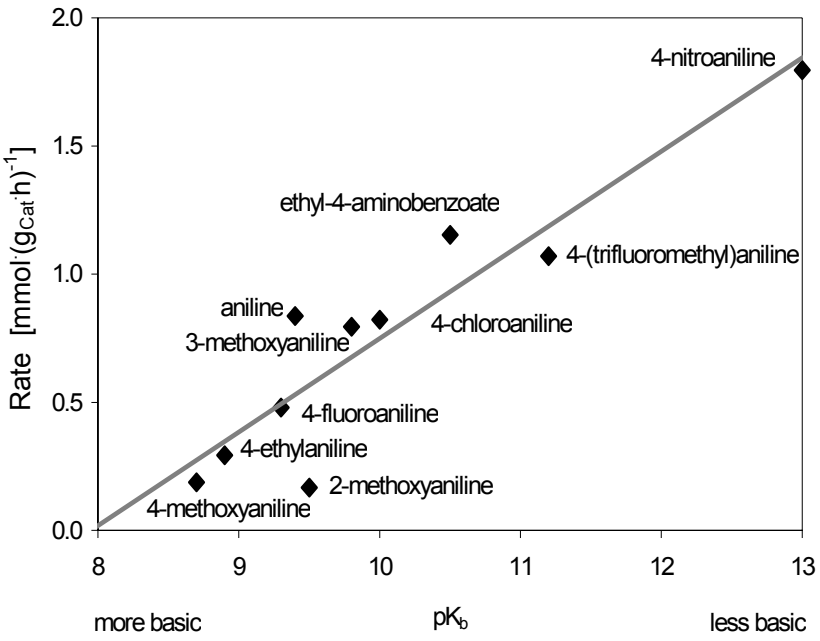


**Figure 12.** Proposed reaction mechanism for the intermolecular hydroamination of 1,3-cyclohexadiene with aniline catalyzed by H-BEA zeolites.

The reaction rate decreased linearly with the basicity ($pK_b$) of the substituted aniline (Table 3, Fig. 12). 2-Methoxyaniline and parent aniline deviated from the correlation to lower / higher rates, respectively. According to the mechanism proposed, aniline and 1,3-cyclohexadiene compete for coordination to the BAS. As the substituted anilines are much more basic than 1,3-cyclohexadiene formation of the anilinium ions is preferred. However, it is assumed that the anilinium ion may be displaced from the Brønsted acid site by excess 1,3-cyclohexadiene.

Less basic amines form less stable anilinium ions and are displaced more easily. Assuming equal diffusion rates, the linear correlation reflects the concentration of sites **a** and **b** in the material. Deviation of 2-methoxyaniline from the above relationship is tentatively explained by the larger minimum kinetic diameter of the N-(cyclohex-2-enyl)-2-methoxyaniline (**6**), which hinders **6** from diffusing out of the pores. In addition, aniline with a methoxy substituent in *ortho*- position may pose a higher constraint for the transition state during the nucleophilic attack (partial shielding of the $-NH_2$ group). In the same way, the relatively high rate observed for the parent aniline might be due to the shorter length of products **1** and **2** relative to the corresponding products of the substituted anilines, thus, providing for a higher diffusion rate.

## 4. Conclusions

Zeolite catalysts with 12 membered ring openings, such as H-BEA, can efficiently catalyze the reaction between aniline and 1,3-cyclohexadiene. Generally, the rate is higher for electron poor (less basic) anilines. Thus it seems apparent that the acid catalysed reaction between 1,3-cyclohexadiene and (the much more basic) aliphatic amines is more difficult to realize. Mechanistically, the key step seems to be the adsorption of 1,3-cyclohexadiene at the Brønsted acid sites and protonation to the corresponding allyl- or enyl- cation. More basic anilines adsorb stronger at the Brønsted acid sites, leading to a lower concentration of protonated 1,3-cyclohexadiene molecules and, in consequence, a lower rate of reaction.

## 5. References

[1] T. E. Müller, M. Beller, Chem. Rev. 98 (1998) 675.

[2] P. W. Roesky, T. E. Müller, Angew. Chem. 115 (2003) 2812.

[3] F. Alonso, I. P. Beletskaya, M. Yus, Chem. Rev. 104 (2004) 3079.

[4] J. Seayad, A. Tillack, C. G. Hartung, M. Beller, Adv. Synth. Catal. 344 (2002) 795.

[5] T. E. Müller, in: I. T. Horváth (Ed), Encyclopedia of Catalysis, Wiley, New York (2002) 492.

[6] R. Taube, in: B. Cornils, W. A. Herrmann (Eds), Applied Homogeneous Catalysis with Organometallic Compounds, Vol 1, VCH, Weinheim, 1996.

[7] For mechanistic background see, e.g., H. M. Senn, P. E. Blöchl, A. Togni, J. Am. Chem. Soc. 122 (2000) 4098.

[8] J. R. Petersen, J. M. Hoover, W. S. Kassel, A. L. Rheingold, A. R. Johnson, Inorg. Chim. Acta. 358. (2005) 687.

[9] L. K. Vo, D. A. Singleton, Org. Lett. 6 (2004) 2469.

[10] B. Kalita, K. M. Nicholas, Tetrahedron. Lett. 46 (2005) 1451.

[11] A. del Zotto, W. Baratta, A. Felluga, P. Rigo, Inorg. Chim. Acta. 358 (2005) 2749.

[12] N. T. Patil, N. K. Pahadi, Y. Yamamoto, Tetrahedron. Lett. 46 (2005) 2101.

[13] D. P. Klein, A. Ellern, R. J. Angelici, Organometallics. 23 (2004) 5662.

[14] L. M. Lutete, I. Kadota, Y. Yamamoto, J. Am. Chem. Soc. 126 (2004) 1622.

[15] S. Hong, T. J. Marks, J. Am. Chem. Soc. 124 (2002) 7886.

[16] T. Minami, H. Okamoto, S. Ikeda, R. Tanaka, F. Ozawa, M. Yoshifuji, Angew. Chem. 113 (2001) 4633.

[17] J. Bodis, T. E. Müller, J. A. Lercher, Green Chem. 5 (2003) 227.

[18] O. Löber, M. Kawatsura, J. F. Hartwig, J. Am. Chem. Soc. 123 (2001) 4366.

[19] M. Kawatsura, J. F. Hartwig, J. Am. Chem. Soc. 122 (2000) 9546.

[20] see e.g. T. E. Müller, J. A. Lercher, V. N. Nguyen, AIChE J. 49 (2003) 214.

[21] M. Utsunomiya, J. F. Hartwig, J. Am. Chem. Soc. 126 (2004) 2702.

[22] K. Tanabe, W. F. Hölderich, Appl. Catal. A. 181 (1999) 399.

[23] A. Chauvel, B. Delmon, W. F. Hölderich, Appl. Catal. 115 (1994) 173.

[24] V. Taglieber, W. F. Hölderich, R. Kummer, W. D. Mross, G. Saladin, US 4929758 (1990), to BASF AG.

[25] J. Penzien, T. E. Müller, J. A. Lercher, Microp. Mesop. Mater. 48 (2001) 285.

[26] J. Penzien, C. Haeßner, A. Jentys, K. Köhler, T. E. Müller, J. A. Lercher, J. Catal. 221 (2004) 302.

[27] V. Neff, T. E. Müller, J. A. Lercher, J. Chem. Soc., Chem. Comm. 8 (2002) 906.

[28] S. Breitenlechner, M. Fleck, T. E. Müller, A. Suppan, J. Mol. Cat. A, 214 (2004) 175.

[29] L. Borreto, M. A. Camblor, A. Corma, J. Perez-Pariente, Appl. Catal. 82 (1992) 37.

[30] K. S. N. Reddy, B. S. Rao, V. P. Shiralkar, Appl. Catal. 95 (1993) 53.

[31] C. A. Emeis, J. Catal. 141 (1993) 347.

[32] J. Penzien, A. Abraham, J. A. van Bokhoven, A. Jentys, T. E. Müller, C. Sievers, J. A. Lercher, J. Phys. Chem. B, 108 (2004) 4116.

[33] D. M. Roberge, H. Hausmann, W. F. Hölderich, Phys. Chem. Chem. Phys. 4 (2002) 3128.

[34] C. Costa, J. M. Lopes, F. Lemos, F. Ramoa Ribeiro, J. Mol. Catal. A, 144 (1999) 221.

[35] J. P. Marques, I. Gener, P. Ayrault, J. C. Bordado, J. M. Lopes, F. Ramoa-Ribeiro, M. Guisnet, Microp. Mesop. Mater. 60 (2003) 251.

[36] J. B. Higgins, R. B. La Pierre. J. L. Schlenker, A. C. Rohrman, J. D. Wood, G. T. Kerr, W. J. Rohrbaugh, Zeolites, 8 (1988) 446.

[37] R. J. Gorte, Catal. Lett. 62 (1999) 1.

[38] J.A. Lercher, G. Ritter, H. Vinek, J. Colloid Interface Sci. 106 (1985) 215.

[39] J. Penzien, T. E. Müller, J. A. Lercher, J. Chem. Soc., Chem. Commun. 18 (2000) 1753.

[40] A. E. W. Beers, J. A. Van Bokhoven, K. M. de Lathouder, F. Kapteijn, J. A. Moulijn, J. Catal. 218 (2003) 239.

[41] S. Yang, J. N. Kondo, K. Domen, Catal. Today, 73 (2002) 113.

[42] S. Spange, S. Adolph, R. Walther, Y. Zimmermann, J. Phys. Chem. B. 107 (2003) 298.

[43] J. Pawlas, Y. Nakao, M. Kawatsura, J. F. Hartwig, J. Am. Chem. Soc. 124 (2002) 3669.

# *Chapter 3*

## *Formation of solvent cages around organometallic complexes in thin films of supported ionic liquid*

The first experimental evidence for the formation of ordered three-dimensional structures in solution of organometallic complexes in a thin film of supported ionic liquids was obtained. The ordering effect leads to drastically reduced mobility of ionic liquid and complex molecules.

## 1. Introduction

Dissolving organometallic complexes in supported films of ionic liquids has recently been introduced as strategy to immobilize molecular catalysts. This allows fixing molecular catalysts in a widely tailorable environment without the drawbacks of complex grafting chemistry. The first examples appear to be highly promising [1-5]. However, the influence of an environment with high dielectric constant on structure and reactivity of the complexes remained unknown. Therefore, the detailed characterization of supported films by solid state NMR spectroscopy [6] was explored for a fully functional catalytic system.

As case study, we focused on a bi-functional catalyst of [Pd(DPPF)($CF_3CO_2$)$_2$] (Lewis acid function) and $CF_3SO_3H$ (Brønsted acid function) immobilized in a thin film of imidazolium salts (Fig. 1), which showed exceptional activity in the addition of aniline to styrene providing the Markownikoff product N-(1-phenylethyl)aniline under kinetic control and the anti-Markownikoff product N-(2-phenylethyl)aniline under thermodynamic control [7].

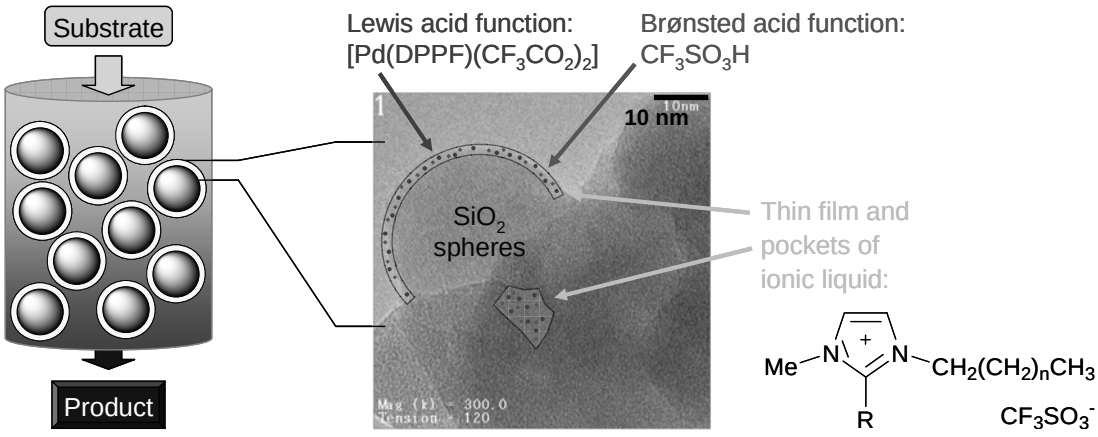


**Figure 1.** Concept of immobilizing organometallic complexes in supported films of ionic liquid (R = H, Me; Alkyl = $C_2H_5$, $C_4H_9$, $C_6H_{13}$) and transmission electron micrograph of the catalyst Pd/EMIm/$SiO_2$.

## 2. Experimental

2.1. Catalysts preparation

The palladium complex was prepared *in situ* following a published procedure [8]. For catalysts Pd/IL/$SiO_2$, $CF_3SO_3H$ (for quantities see Table 1) was dissolved in 1-alkyl-3-methyl-imidazolium trifluoromethane sulphonate with alkyl = ethyl (EMIm), butyl (BMIm), hexyl (HMIm) or molten 1-hexyl-2,3-dimethyl-imidazolium trifluoro-methane sulphonate ($HM_2Im$). A solution of $Pd(CF_3CO_2)_2$ and 1,1'-*bis*(diphenyl-phosphino)ferrocene (DPPF) in $CH_2Cl_2$ was added and the mixture stirred for 10 min. Silica (Aerosil 355 by Degussa, 150 $m^2/g$) was ground to particle size 60-200 μm and added to the mixture. The suspension was stirred for 10 min, then frozen rapidly and the volatiles were removed in a partial vacuum, while the sample was warming slowly to RT. A free flowing powder was obtained. For reference, a series of catalysts IL/$SiO_2$ was prepared without palladium complex.

**Table 1.** Amounts used in the preparation of the supported material Pd/IL/$SiO_2$.

| Ionic liquid | Ionic liquid (ml) | $Pd(CF_3CO_2)_2$ (mg) | DPPF (mg) | $CF_3SO_3H$ (mg) | Silica (g) |
|---|---|---|---|---|---|
| EMIm | 2.5 | – | – | 150 | 5.0 |
| | 2.5 | 133 | 333 | 150 | 5.0 |
| BMIm | 2.5 | – | – | 150 | 5.0 |
| | 2.5 | 133 | 333 | 150 | 5.0 |
| HMIm | 2.5 | – | – | 150 | 5.0 |
| | 2.5 | 133 | 333 | 150 | 5.0 |
| $HM_2Im$ | 2.5 [1] | – | – | 150 | 5.0 |
| | 2.5 [1] | 133 | 333 | 150 | 5.0 |

1 $HM_2Im$ is solid at RT, a molten sample was used.

2.1. Catalysts chracterization

The pore structure was analyzed by nitrogen adsorption at 77 K on a PMI Automated BET Sorptometer. The palladium content in the supported catalysts was determined by neutron activation. For TEM of Pd/EMIm/$SiO_2$, the sample was

ground, suspended in hexane and dispersed using an ultrasonic bath. Drops of the dispersion were applied to a copper grid-supported carbon film. A JEM-2010 Jeol transmission electron microscope operating at 120 kV was used.

For the NMR measurements, the samples were pressed into $ZrO_2$ rotors and spun at 10 kHz (except where noted otherwise). The $^1H$ MAS NMR measurements were performed on a Bruker AV600 spectrometer ($B_0$ = 14.1 T). For cooling the bearing and drive gas stream were sent through a heat exchanger in liquid nitrogen. The spectra were recorded as the sum of 16 scans using single pulse excitation with a pulse length of 2.6 μs and recycle time of 3 s. The spectra were referenced to an external adamantane standard ($\delta_H$ = 1.78 ppm).

The $^{31}P$ MAS NMR measurements were performed on a Bruker AV500 spectrometer ($B_0$ = 11.7 T). The spectra were recorded as the sum of 5000 scans using a proton decoupling pulse sequence with a pulse length of 2.5 μs and recycle time of 5 s. The spectra were referenced to an external $(NH_4)H_2PO_4$ standard ($\delta_P$ = 1.11 ppm).

Reference samples for NMR spectroscopy were prepared by dissolving $CF_3SO_3H$ in EMIm, BMIm or HMIm (amounts 1/10 of those in Table 1). A solution of $Pd(CF_3CO_2)_2$ and (DPPF) in 10 ml $CH_2Cl_2$ was added and the solution stirred for 10 min. The volatiles were removed in a partial vacuum. One drop of the viscous liquid was dissolved in $CD_2Cl_2$. $^{31}P\{^1H\}$ NMR spectra were recorded on a Bruker AV250 spectrometer ($B_0$ = 5.8 T) as the sum of 32 scans using a single pulse excitation sequence with a pulse length of 2.5 μs and recycle time of 2 s. For all samples, a single NMR signal was observed at 47.1 ppm with 2.5 Hz line width.

## 3. Results and Discussion

### 3.1. Catalyst characterization

Catalysts were prepared by immobilization of $[Pd(DPPF)(CF_3CO_2)_2]$ and $CF_3SO_3H$ in imidazolium salts $(C_3N_2H_2MeRAlkyl)^+$ $CF_3SO_3^-$ supported on silica. Four different ionic liquids were used, which provide a series of catalysts $Pd/IL/SiO_2$ with decreasing polarity of the ionic liquid (IL) in the sequence EMIm > BMIm > HMIm > $HM_2Im$. For comparison, a series of reference samples ($IL/SiO_2$) was prepared, for which only the Brønsted acid $CF_3SO_3H$ was supported in the thin film of the ionic liquid. Analysis of the porosity by nitrogen adsorption showed that the

mesopore volume decreased from 0.76 $cm^{3}\cdot g^{-1}$ (parent catalyst) to ca. 0.13 $cm^{3}\cdot g^{-1}$ for the supported catalysts. Closer inspection of the isotherm showed that the ionic liquid entirely filled pores with less than 9 nm radius, whereas larger pores remained unaffected.

**Table 2.** Data of catalyst characterization.

| Sample | BET surface area ($m^{2}\cdot g^{-1}$) | Pore volume ($cm^{3}\cdot g^{-1}$) | Pd contents ($mmol\cdot g^{-1}$) |
|---|---|---|---|
| $SiO_2$ | 142 | 0.76 | – |
| EMIm/$SiO_2$ | 22 | 0.15 | – |
| BMIm/ $SiO_2$ | 20 | 0.13 | – |
| HMIm/ $SiO_2$ | 23 | 0.18 | – |
| $HM_2Im$/ $SiO_2$ | 22 | 0.15 | – |
| Pd/EMIm/$SiO_2$ | 13 | 0.10 | 0.037 |
| Pd/BMIm/$SiO_2$ | 12 | 0.09 | 0.038 |
| Pd/HMIm/$SiO_2$ | 20 | 0.15 | 0.040 |
| Pd/$HM_2Im$/$SiO_2$ | 15 | 0.10 | 0.039 |

Transmission electron micrographs showed the spherical beads of the fumed silica support (Fig. 1). However, the ionic liquid film was much thinner than expected (calculated to 3 nm thickness). Thus, the majority of the ionic liquid molecules were not part of an even, physisorbed film on the silica surface, but rather resided in the mesopores. However, in the IR spectra the SiOH band of the parent silica (3741 $cm^{-1}$) was broadened and shifted to ca. 3320 $cm^{-1}$ for the supported catalysts indicating that all SiOH groups were involved in hydrogen bonding. This proves that the entire silica surface has been covered by ionic liquid. Note that the fact that all SiOH groups are interacting, does not allow us to conclude, how thick the film is.

The $^{1}H$ MAS NMR spectra of the materials were surprisingly well resolved and the signal for each proton of the imidazolium cation was identified (Fig. 2). The additional broad signal is assigned to the acidic proton of $CF_3SO_3H$. A comparison of the room temperature NMR spectra of pure EMIm (where the NMR tube contained a capillary filled with $CD_2Cl_2$ as reference), EMIm/$SiO_2$ and Pd/EMIm/$SiO_2$ is provided in Figure 3.

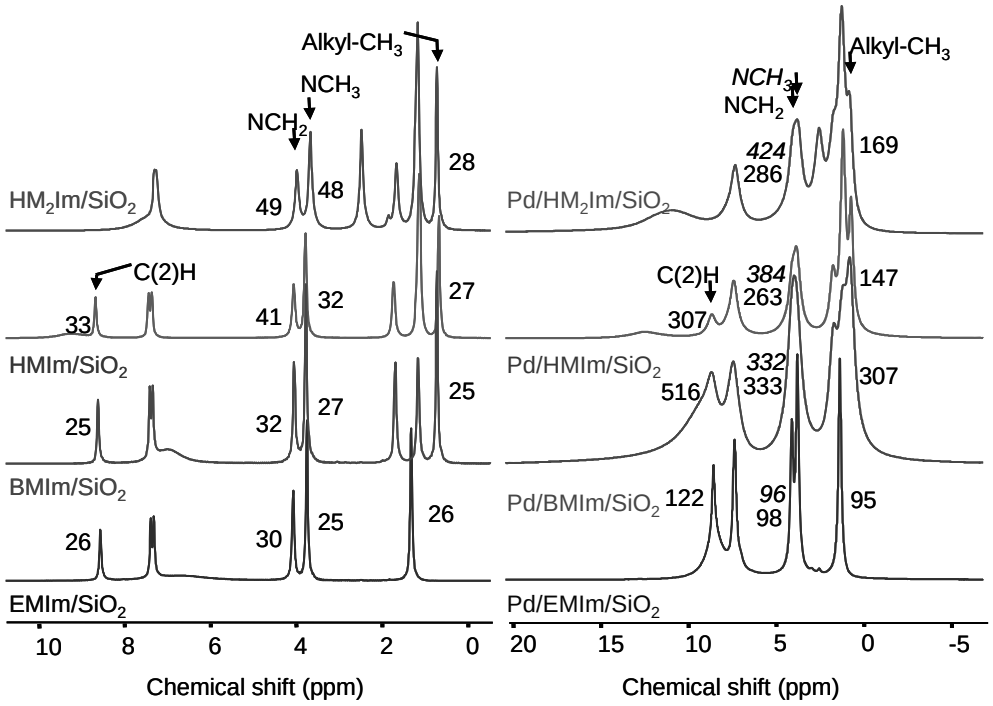


**Figure 2.** $^{1}$H MAS NMR spectra (298 K) of series IL/$SiO_2$ (left) and Pd/IL/$SIO_2$ (right) and line-widths (Hz) of selected signals

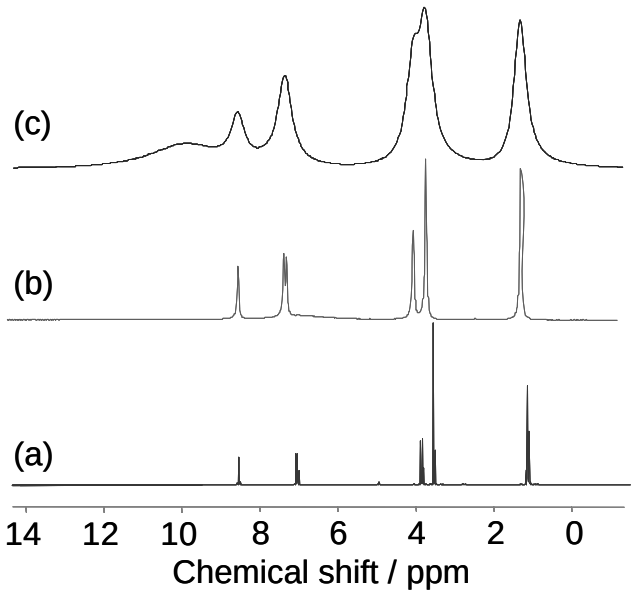


**Figure 3.** Comparison of the room temperature NMR spectra of (a) EMIm dissolved in $CD_2Cl_2$, (b) EMIm/$SiO_2$ and (c) Pd/EMIm/$SiO_2$

A large increase of the line-width was observed when [Pd(DPPF)($CF_3CO_2$)$_2$] and $CF_3SO_3H$ were immobilized in the supported ionic liquids (Fig. 2). This suggests a substantial decrease in the mobility of the imidazolium cations. Reference samples prepared by dissolution of [Pd(DPPF)($CF_3CO_2$)$_2$] and $CF_3SO_3H$ in the parent ionic liquids showed a large increase in viscosity compared to the parent ionic liquid [9] confirming that the mobility of the molecules was considerably lowered.

The position of the NMR signals was equal in the two series IL/$SiO_2$ and Pd/IL/$SiO_2$ (within ±0.1 ppm). Note that the molar ratio of $Pd^{2+}$, DPPF, $CF_3SO_3H$ and ionic liquid in the catalysts was 1 : 1.5 : 2.5 : 25-33. A single peak with Lorentzian shape was observed for each proton of the imidazolium cations in the series Pd/IL/$SiO_2$. This indicates that the ionic liquid did not coordinate directly to the palladium centre in [Pd(DPPF)($CF_3CO_2$)$_2$] and that all ionic liquid molecules in the supported film were equally affected by the presence of the palladium complex. Rapid exchange of coordinated and free imidazolium cations could be excluded by variable temperature NMR spectra (*vide infra*).

The line-width of the nitrogen bound methyl and methylene groups increased with increasing size of the imidazolium cation in the order EMIm/$H^+$ < BMIm/$H^+$ < HMIm/$SiO_2$ < Pd/$HM_2Im/SiO_2$ (Fig. 2). In NMR spectra of solids, the chemical shift anisotropy is not averaged out by the motion of the molecules, but can be reduced by magic angle spinning (MAS) [10]. The influence of the spinning rate is demonstrated in Figure 4. At frequencies above 5000 Hz, the spectra were independent of rotation speed indicating that coupling constants to other nuclei in the sample were well below 5000 Hz. Quadrupolar interactions were also insignificant ($I_H$ = ½). Differences in T2, which is not influenced by MAS, thus, were responsible for the changes in line-width and can be taken as a measure for the mobility of a particular atomic group [11-13]. The increase in line-width, therefore, shows that the mobility of the aromatic ring decreased with increasing size of the imidazolium cation. On the other hand, the line-width of the terminal methyl group in the alkyl side chain was equal (25-28 Hz) showing that the flexibility of the alkyl group was not influenced by the size of the cation.

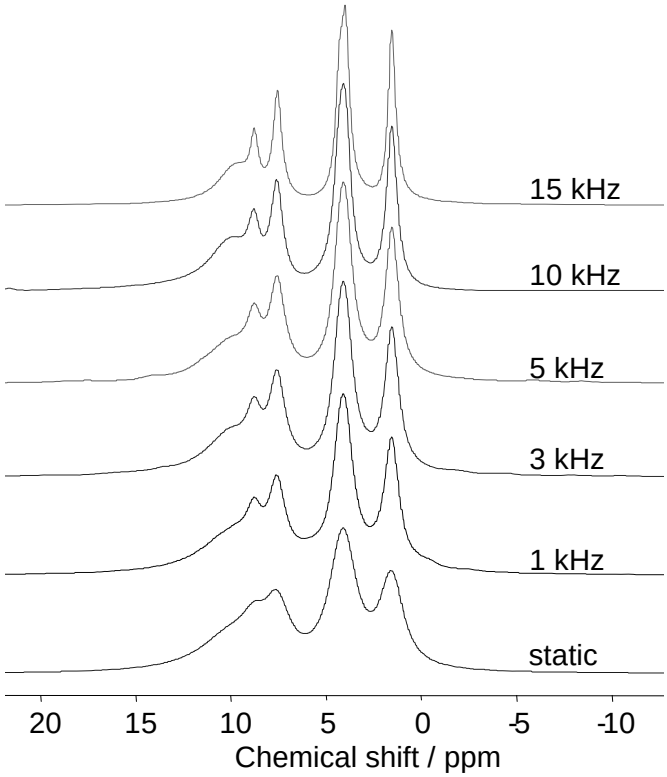


**Figure 4.** Influence of the spinning rate on the $^{1}H$ NMR spectrum of Pd/EMIm/$SiO_2$.

In $^{31}P$ MAS NMR spectroscopy, the signal due to the phosphine ligand of the palladium complex was observed at 47.3 ppm with a relatively large line-width of 440-1360 Hz. In comparison, the $^{31}P\{^{1}H\}$ NMR signal for a solution of [Pd(DPPF)-$(CF_3CO_2)_2$], $CF_3SO_3H$ and IL in $CD_2Cl_2$, was observed at 47.1 ppm with a much smaller line width of 2.5 Hz. This suggests that the mobility of the palladium complexes in the supported ionic liquid was also restricted. To explain these observations we propose that the imidazolium cations form a solvent cage around the palladium complexes, thereby establishing a long range ordered system [14, 15], which in turn is responsible for the reduced mobility.

Similar to the IL/$SiO_2$ series, the line-width of the nitrogen bound methyl and methylene group in the $^{1}H$ MAS NMR spectra was significantly higher than of the terminal methyl group of the alkyl chain (Fig. 2). A maximum in the line-width of the N-$CH_2$ and the alkyl-$CH_3$ groups was observed for Pd/BMIm/$SiO_2$. In particular, the line-width of the methyl group in the hexyl chain was much lower than that in the butyl chain. This suggests that the first four carbon atoms of the alkyl chains contribute most to the intermolecular interactions between IL and palladium complexes. Probably, hydrophobic interactions between alkyl chain and the aromatic

rings of the phosphine ligand lead to domain formation [16]. Thus, the line-width in NMR spectra provides a ‘molecular ruler’ for where these interactions are most significant.

The dynamic interaction of ionic liquid and Pd complex was investigated in further detail by temperature resolved MAS NMR experiments (Fig. 5). For all samples, the line-width of all peaks decreased exponentially with temperature. A change of slope in the logarithmic plot shows that a phase transition from a frozen glass to liquid occurred at *ca*. 348 K for Pd/EMIm/$SiO_2$ and Pd/BMIm/$SiO_2$ (Fig. 6). For Pd/HMIm/$SiO_2$, the phase transition occurred above 373 K. After the phase transition the line-width in the spectra of the Pd/IL/$SiO_2$ samples was similar to that of the IL/$SiO_2$ series at 298 K.

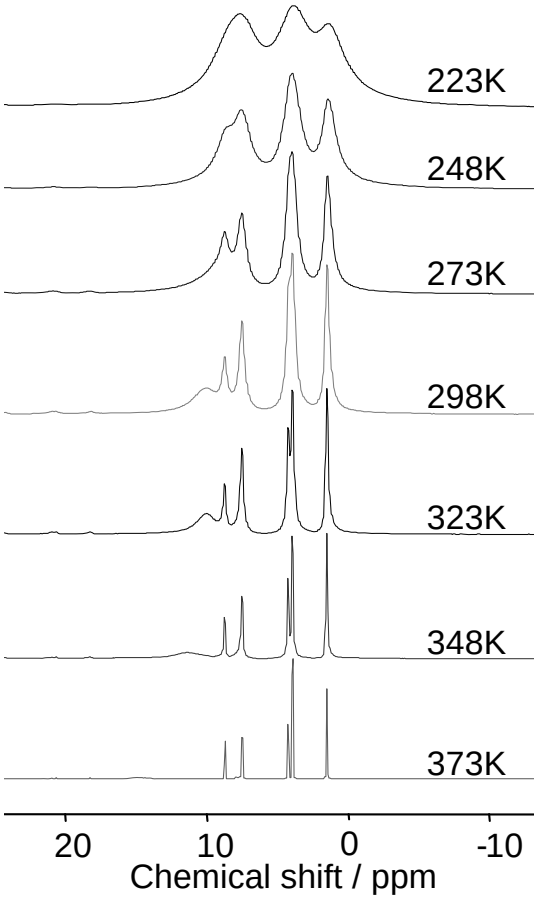


**Figure 5.** Variable temperature $^1$H MAS NMR spectra of the catalyst Pd/EMIm/$SiO_2$

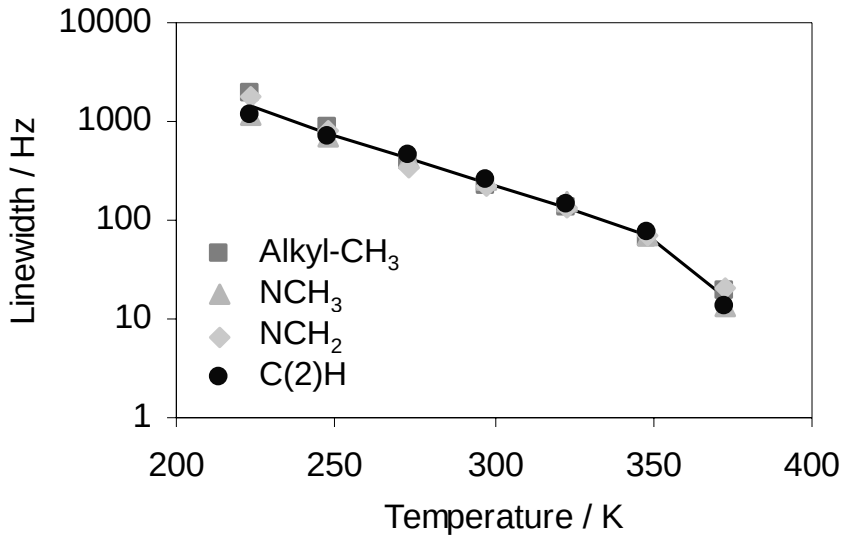


**Figure 5.** Temperature dependence of the line-width of selected protons in the $^{1}H$ MAS NMR spectra of Pd/EMIm/$SiO_2$

We suggest that the solvent cages are formed by disruption of inter-ionic interactions between the ionic liquid molecules during dissolution of the palladium complexes. This, in turn, causes the local structure of the ionic liquid to break down [17]. In an attempt to minimize the potential energy, the spheres of ionic liquid molecules around the complexes assume a minimum size. It is estimated, based on the molar ratio of complex to ionic liquid and the fact that only one set of signals was observed in NMR spectroscopy, that the supramolecular aggregates consist of one complex molecule and up to 25-33 cations and anions of the ionic liquid. The aggregates arrange to a regular packing with glass-like structure. At the phase transition the solvent cages break down and the molecules acquire similar mobility to the parent supported liquid, which does not contain the dissolved complex.

## 4. Conclusions

The present report is the first experimental evidence for the formation of ordered three-dimensional structures in solutions of organometallic complexes in a thin film of supported ionic liquid. The ordering effect leads to a drastically reduced mobility of ionic liquid and complex molecules, and could be used to induce unusual properties in the supported complexes. Possible applications include the enhancement of metal-substrate interactions, the re-orientation of substrate molecules within in the solvent

cage during a two-step catalytic process, and the possibility of directing the approach of molecules to catalytically active centers.

## 5. References

[1] T. Welton, Coord. Chem. Rev. 248 (2004) 2459

[2] S. Breitenlechner, M. Fleck, T. E.Müller, A. Suppan, J. Mol. Cat. A. 214 (2004) 175.

[3] A. Riisager, P. Wasserscheid, R. Hal, R. Fehrmann, J. Catal. 219 (2003) 452.

[4] C. P. Mehnert, R. A. Cook, N. C. Dispenziere, M. Afeworki, J. Am. Chem. Soc. 124 (2002) 12932.

[5] H. Hagiwara, Y. Sugawara, K. Isobe, T. Hoshi, T. Suzuki, Org. Lett. 6 (2004) 2325.

[6] T. Tao, V. H. Pan, J.-W. Zhou, G. E. Maciel, Solid State Nucl. Magn. Res. 17 (2000) 52.

[7] O. Jimenez, T. E. Müller, C. Sievers, A. Spirkl, J. A. Lercher, Chem. Comm. (2006) 2974.

[8] M. Kawatsura, J. F. Hartwig, J. Am. Chem. Soc. 122 (2000) 9546.

[9] P. Bonhote, A. P. Dias, N. Papageorgiou, K. Kalyanasundaram, M. Gratzel, Inorg. Chem. 35 (1996) 1168.

[10] D. D. Laws, H.-M. L. Bitter, A. Jerschow, Angew. Chem. Int. Ed. 41 (2002) 3096 and references cited therein.

[11] A. Lauenstein, J. Tegenfeldt, J. Phys. Chem. B 101 (1997) 3311.

[12] A. Johansson, J. Tegenfeldt, J. Chem. Phys. 104 (1996) 5317.

[13] R. Spindler, D. F. Shriver, J. Am. Chem. Soc. 110 (1988) 3036.

[14] R. Atkin, G. G. Warr, J. Am. Chem. Soc. 127 (2005) 11940.

[15] R. A. Mantz, P. C. Trulove, R. T. Carlin, R. A. Osteryoung, Inorg. Chem. 34 (1995) 3846.

[16] Y. T. Wang, G. A. Voth, J. Am. Chem. Soc. 127 (2005) 12192.

[17] L. Crowhurst, N. L. Lancaster, J. M. P. Arlandis, T. Welton, J. Am. Chem. Soc. 126 (2004) 11549.

# *Chapter 4*

## *Markownikoff and anti-Markownikoff hydroamination with palladium catalysts immobilized in thin films of silica supported ionic liquids*

Novel bi-functional catalysts combining soft Lewis acidic and strong Brønsted acidic functions provided exceptional catalytic activity for the addition of aniline to vinyl-benzene

## 1. Introduction

The concept of immobilising organometallic complexes in a thin film of supported ionic liquids was utilised to synthesise novel bi-functional catalysts combining soft Lewis acidic and strong Brønsted acidic functions. The materials showed exceptional catalytic activity for the addition of aniline to styrene providing the Markownikoff product under kinetically controlled conditions and mainly the *anti*-Markownikoff product in the thermodynamic regime.

The direct addition of amines to weakly or non-activated alkenes (hydro-amination) is an important target reaction. For industrial applications, however, the known catalysts provide insufficient activity and long-term stability. Thus, a new generation of - preferentially solid - catalysts is required. Bi-functional catalysts combining soft Lewis acidic function (activation of alkene) and strong Brønsted acidic function (acceleration of rate determining step (r.d.s.)) were reported to provide high catalytic activities [1-4]. A new concept, immobilisation of homogeneous catalysts in a supported film of ionic liquid [5-9], allows joining both functions in one material and tailoring systematically its performance in catalysis.

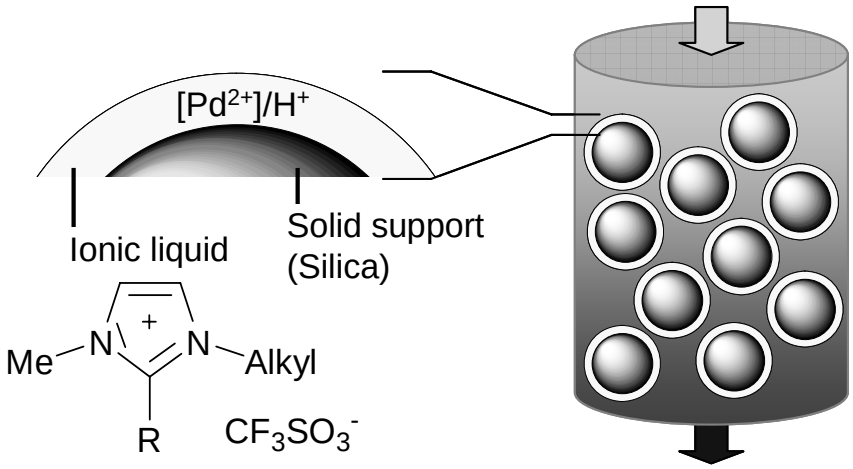


**Figure 1.** Concept of immobilizing of homogeneous catalysts for application in fixed reactors, R = H, Me; Alkyl = $C_2H_5$, $C_4H_9$, $C_6H_{13}$.

## 2. Experimental

2.1. Catalysts preparation

Catalysts were prepared (see Table 1) by dissolving an *in situ* mixture of $Pd(CF_3CO_2)_2$, 1,1'-bis(diphenylphosphino)ferrocene (DPPF) and $CF_3SO_3H$ (TfH) in 1-ethyl-3-methyl-imidazolium trifluoromethane sulphonate (EMIm), 1-butyl-3-methyl-imidazolium trifluoromethane sulphonate (BMIm) or 1-hexyl-2,3-dimethyl-imidazolium trifluoromethane sulphonate ($HM_2Im$). Silica (aerosil 355 by Degussa, 150 $m^2/g$) was ground to particle size 60-200 μm and impregnated with the solution to obtain a free flowing powder.

| Ionic liquid | Ionic liquid (ml) | $Pd(CF_3CO_2)_2$ (mg) | DPPF (mg) | $CF_3SO_3H$ (mg) | Silica (g) |
|---|---|---|---|---|---|
| EMIm | 2.5 | – | – | 150 | 5.0 |
| | 2.5 | 33 | 83 | 150 | 5.0 |
| | 2.5 | 66 | 166 | 150 | 5.0 |
| | 2.5 | 133 | 333 | 150 | 5.0 |
| BMIm | 2.5 | – | – | 150 | 5.0 |
| | 2.5 | 33 | 83 | 150 | 5.0 |
| | 2.5 | 66 | 166 | 150 | 5.0 |
| | 2.5 | 133 | 333 | 150 | 5.0 |
| HMIm | 2.5 | – | – | 150 | 5.0 |
| | 2.5 | 33 | 83 | 150 | 5.0 |
| | 2.5 | 66 | 166 | 150 | 5.0 |
| | 2.5 | 133 | 333 | 150 | 5.0 |
| $HM_2Im$ | 2.5 [1] | – | – | 150 | 5.0 |
| | 2.5 [1] | 33 | 83 | 150 | 5.0 |
| | 2.5 [1] | 66 | 166 | 150 | 5.0 |
| | 2.5 [1] | 133 | 333 | 150 | 5.0 |

1 $HM_2Im$ is solid at RT, a molten sample was used.

**Table 1.** Amounts used in the preparation of the supported catalysts

2.2. Determination of the absortion constant of aniline and vinyl-benzene

A fixed bed reactor was filled with 50 mg catalyst and glass beads (remaining volume). A constant flow of heptane (1 $ml \cdot min^{-1}$) was passed over the catalyst bed and the temperature of the reactor and feed increased to 120 °C. The concentration of aniline was then increased stepwise to $1.85 \cdot 10^{-4}$, $2.27 \cdot 10^{-4}$ and $2.70 \cdot 10^{-4}$ $mol \cdot l^{-1}$. The concentration of aniline at the exit was followed with UV spectroscopy. The uptake was calculated from the time-concentration diagram by comparison with an experiment, where the reactor had been filled only with glass beads. Aniline absorption was only observed in the first step. The experiment was repeated with styrene, but no absorption was observed.

2.3. Catalytic testing in batch mode

Catalytic experiments were performed in an inert atmosphere of nitrogen using a 12-batch reactor (Radleys). The catalyst (0.25 g) was suspended in octane (15 $cm^3$) and heated to reflux at 125 °C. Aniline (1 mmol), styrene (1.5 mmol) and undecane (internal GC standard) were added. Samples (50 μl) were taken periodically and analyzed by gas chromatography.

2.4. Catalytic testing in fixed bed reactor

A fixed bed reactor was filled with catalyst (50 mg) and glass beads (remaining volume) and a solution of aniline (0.10 $mol \cdot l^{-1}$) and styrene (0.15 $mol \cdot l^{-1}$) in heptane passed over the catalyst (flow 0.2 $ml \cdot min^{-1}$). The temperature was increased stepwise from 150 °C to 300 °C. After steady state was obtained, samples of the product mixture were collected for gas chromatography. The temperature was then reduced to 150 °C and confirmed that the initial activity was obtained.

## 3. Results and Discussion

As Lewis acid function, the palladium complex $[Pd(DPPF)(CF_3CO_2)_2]$, prepared *in-situ* from $Pd(CF_3CO_2)_2$ and 1,1'-bis(diphenylphosphino)ferrocene (DPPF) was chosen. Trifluoromethane sulphonic acid (TfOH) provided the Brønsted acid function. Complex and acid ($Pd^{2+}/H^+$ = 1/10) were immobilised in a thin film of imidazolium based ionic liquids on a silica support (Fig. 1). Systematic increase in the length of the

alkyl chain provided a series of catalysts with decreasing polarity of the ionic liquid phase.

As test reaction, the addition of aniline to styrene was investigated (Eq. 1). The reaction can, in principle, provide the Markownikoff product *N*-(1-phenylethyl)aniline (1) and the *anti*-Markownikoff product *N*-(2-phenylethyl)aniline (2). In batch experiments performed at low temperatures (125°C), the Markownikoff addition product 1 was the only product apart from some oligomerization products of styrene. The initial catalytic activity increased linearly with the Pd loading (Fig. 2) corresponding to first order in Pd complex. However, a minimum loading of 0.011 $mmol_{Pd}^{2+} \cdot g_{Cat}^{-1}$ seemed necessary and no conversion was observed at lower loadings or without palladium. Samples were taken during the experiments performed in the batch mode and analysed for palladium contents. The amount of palladium leached into the reaction solution was below the detection limit of AAS. No further reaction was observed, when the filtered reaction mixture was maintained at 125 °C. This suggests that, in each case, an equal amount of the Pd complex was irreversibly adsorbed on the silica surface and did not contribute to the catalytic activity.

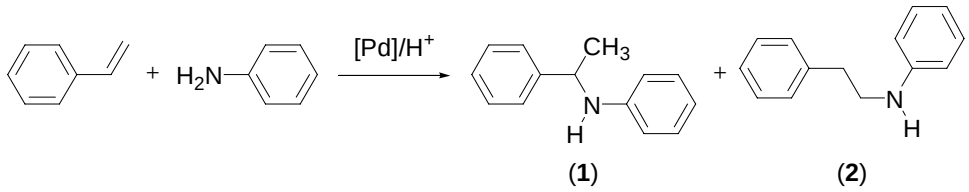


(**1**) (**2**) (1)

Particularly noteworthy is that the initial catalytic activity was strongly dependent on the choice of the ionic liquid. The highest catalytic activity was observed for the EMIm based catalyst (1.47 $mmol \cdot (g_{Cat} \cdot h)^{-1}$ at a Pd loading of 0.044 $mmol_{Pd}^{2+} \cdot g_{Cat}^{-1}$, corresponding to a turnover frequency of 24 $mol \cdot (mol_{Pd}^{2+} \cdot h)^{-1}$), whereas BMIm and $HM_2Im$ provided lower catalytic activities (0.89 and 0.43 $mmol \cdot (g_{Cat} \cdot h)^{-1}$, respectively).

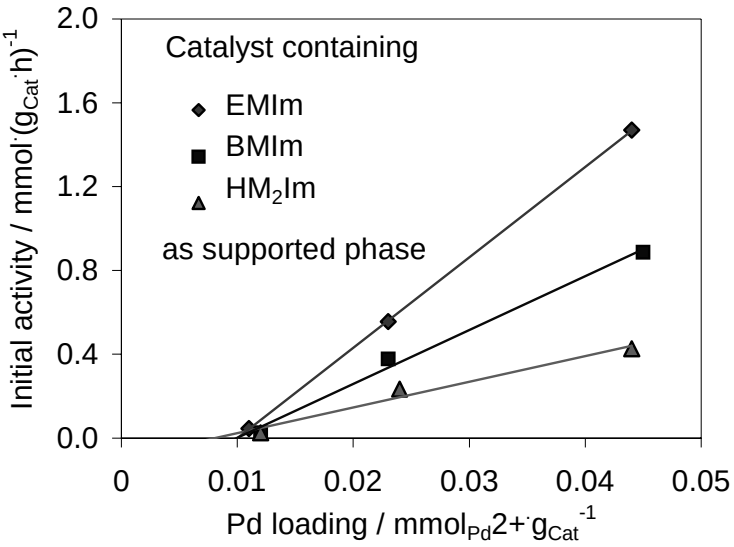


**Figure 2.** Catalytic activity of the Lewis/Brønsted bi-functional catalysts in the addition of aniline to styrene (slurry phase, 125 °C)

Thus, the highly polar environment of the EMIm containing catalyst is concluded to be particularly favourable. This is attributed to the higher solubility of the reactants in EMIm as the catalyst phase, or to an intrinsically higher rate of reaction in the more polar ionic liquid.

The absorption constant of aniline from heptane into the supported ionic liquid phase decreased slightly in the sequence EMIm > BMIm > HM2Im (0.235, 0.221 and 0.204 mmol.$g^{-1}$, respectively). Only part of the absorbed aniline was physically dissolved in the supported ionic liquid (0.037, 0.018 and 0 mmol.g-1, respectively), while the remainder was either protonated, or bound to the Pd centre (aniline/Pd = 2/1). In contrast, no significant absorption of styrene was measured. However, it was reported that co-absorption of aniline and styrene leads to enhanced styrene uptake [10].

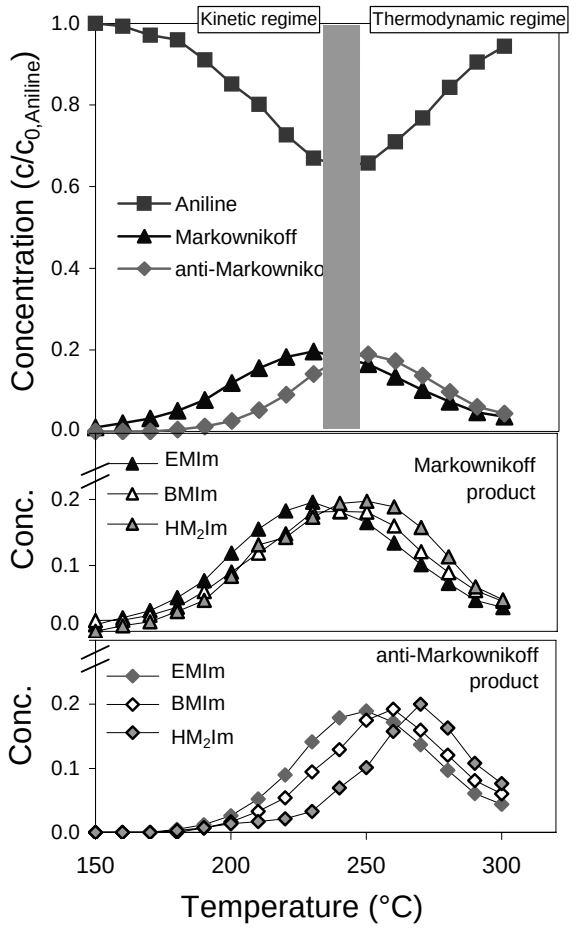


**Figure 3.** Temperature dependence with EMIm based catalyst (fixed bed reactor, 0.044 $mmol_{Pd}^{2+} \cdot g_{Cat}^{-1}$, top) and comparison of the yield in **1** (middle) and **2** (bottom) with catalysts differing in the supported ionic liquid.

The temperature dependence of the catalytic activity was explored in a fixed bed reactor. Above 150 °C, the conversion increased exponentially with temperature attaining a maximum of 35 % (EMIm based catalyst, 0.044 $mmol_{Pd}^{2+} \cdot g_{Cat}^{-1}$) at approximately 240 °C (kinetic regime). At temperatures higher than 240 °C, the conversion decreased as the thermodynamic limit of the (slightly exothermic) reaction was encountered. In the kinetic regime, the main product was **1**, while significant amounts of **2** were formed under thermodynamic control. In the thermodynamic regime, the ratio of products **1** to **2** was approximately equal for all catalysts (0.77(3):1, 0.75(1):1 and 0.65(4):1 for the EMIm, BMIm and $HM_2Im$ based catalysts, respectively) and nearly independent of the temperature. Assuming activity coefficients close to one, the difference in thermodynamic stability of the two products was calculated to $\Delta_r G° \approx 1.4(4)$ $kJ \cdot mol^{-1}$ (**2** being the more stable product).

In the kinetic regime, the selectivity to **1** was 100 % at ≤ 170 °C for all catalysts and decreased steadily with temperature. Interestingly, the relative product concentration was strongly dependent on the choice of the ionic liquid. At 220 °C, e.g., the selectivity to **1** was 67, 73 and 87 % for the EMIm, BMIm and $HM_2Im$ based catalysts, respectively.

The activity of the three catalyst series for formation of **1** was similar in the kinetic regime, decreasing slightly in the sequence EMIm > BMIm > $HM_2Im$. In contrast, for formation of **2** the EMIm based catalyst was 1.7 (4.3) times more active than the BMIm ($HM_2Im$) based catalyst (220 °C). Steady state conversion of 65 % (EMIm based catalyst, 0.044 $mmol_{Pd}^{2+} \cdot g_{Cat}^{-1}$, 240 °C) corresponds to an integral reaction rate of 8.4 $mmol \cdot (g_{Cat} \cdot h)^{-1}$ and a turnover frequency of 199 $mol \cdot (mol_{Pd}^{2+} \cdot h)^{-1}$.

## 4. Conclusions

Based on the observations given above, and considering the current literature on hydroamination [11, 12], we conclude that two different mechanisms are operative (Figure 4). The Markownikoff product **1** is probably formed *via* coordination of the olefinic π-system of styrene to the palladium centre, which renders it susceptible to a nucleophilic attack of the lone electron pair of the aniline nitrogen atom [11]. Subsequent protolytic cleavage of the metal-carbon bond is rate determining. The formation of the *anti*-Markownikoff product **2** occurs *via* intermediate formation of a palladium hydride, insertion of the olefinic double bond of styrene and nucleophilic attack (r.d.s.) of the lone electron pair of the aniline nitrogen atom at the α-carbon atom [12].

In case of the Markownikoff product, the more polar ionic liquid is concluded to provide intrinsically higher rate of reaction, which is related to stabilisation of a polar transition state associated with the rate determining step [13]. In case of the *anti*-Markownikoff product, the higher aniline concentration in the ionic liquid phase with higher polarity is speculated to lead to higher turnover frequencies in the rate determining step.

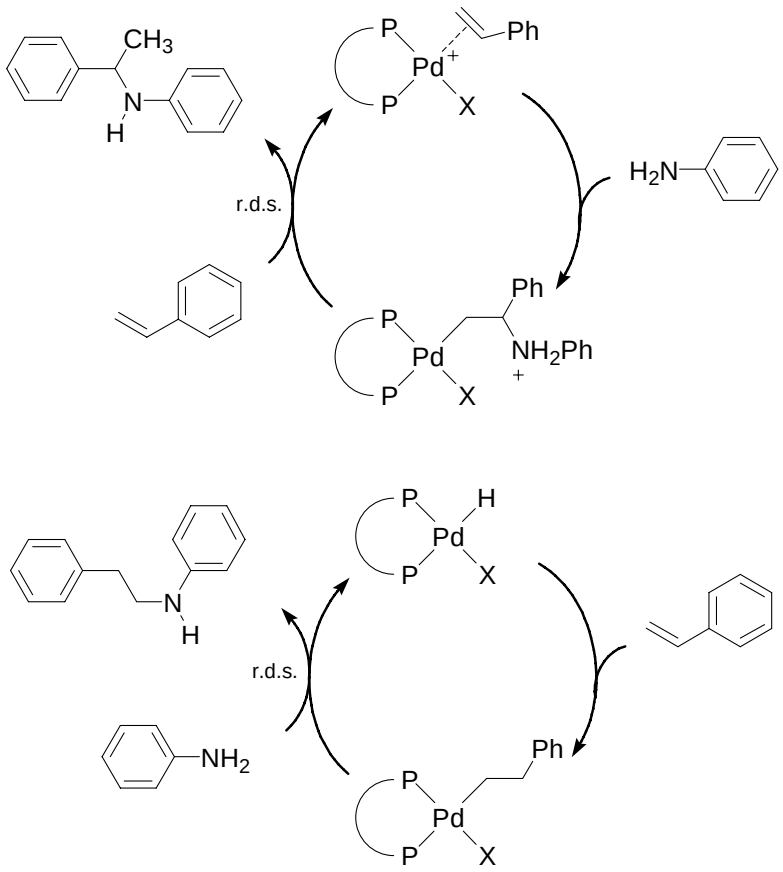


**Figure 4.** Mechanisms proposed for the formation of **1** (top) and **2** (bottom), X = $CF_3SO_3^-$, $CF_3CO_2^-$.

## 5. References

[1] M. Kawatsura, J. F. Hartwig, J. Am. Chem. Soc. 122 (2000) 9546.

[2] I. Kadota, A. Shibuya, L. M. Lutete, Y. Yamamoto, J. Org. Chem. 64 (1999) 4570.

[3] R. Q. Su, T. E. Müller, Tetrahedron, 57 (2001) 6027.

[4] J. Penzien, C. Haeßner, A. Jentys, K. Köhler, T. E. Müller, J. A. Lercher, J. Catal. 221 (2004) 302.

[5] T. Welton, Coord. Chem. Rev. 248 (2004) 2459.

[6] S. Breitenlechner, M. Fleck, T. E. Müller, A. Suppan, J. Mol. Cat. A. 214 (2004) 175.

[7] A. Riisager, P. Wasserscheid, R. Hal, R. Fehrmann, J. Catal. 219 (2003) 452.

[8] C. P. Mehnert, R. A. Cook, N. C. Dispenziere, M. Afeworki, J. Am. Chem. Soc. 124 (2002) 12932.

[9] H. Hagiwara, Y. Sugawara, K. Isobe, T. Hoshi, T. Suzuki, Org. Lett. 6 (2004) 2325.

[10] J. Bodis, T. E. Müller, J. A. Lercher, Green Chem. 5 (2003) 227.

[11] H. M. Senn, P. E. Blöchl, A. Togni, J. Am. Chem. Soc. 122 (2000) 4098.

[12] U. Nettekoven, J. F. Hartwig, J. Am. Chem. Soc. 124 (2002) 1166.

[13] L. Crowhurst, N. L. Lancaster, J. M. P. Arlandis, T. Welton, J. Am. Chem. Soc. 126 (2004) 11549.

# *Chapter 5*

## *Palladium complexes immobilized in thin films of supported ionic liquids for the direct addition of aniline to vinyl-benzene*

The concept of immobilising organometallic complexes in thin films of supported ionic liquid enables fine-tuning the approach of reactants to the catalytically active metal centres. The restricted space in the thin film leads to strong co-operative effects between neighbouring complexes. These effects dramatically change the outcome of catalytic reactions, as was demonstrated for the addition of aniline to vinyl-benzene (hydroamination). In particular, the catalytic activity is strongly influenced by the polarity of the ionic liquid. Catalyst stability with no leaching of the metal complex into the bulk organic phase was also demonstrated.

## 1. Introduction

Higher substituted amines are important intermediates to nitrogen containing molecules, including many pharmaceuticals and agrochemicals. Hydroamination offers one of the most attractive pathways to such kind of products as new CN bonds are formed in a single reaction step from easily accessible alkenes and alkynes [1, 2]. However, the direct addition of an amine to an olefin has a high activation barrier due to the repulsive electrostatic interaction between the lone pair of the amine and the π system of the olefin. The entropy of reaction being negative, performing the reaction at elevated temperature to overcome this barrier is precluded as the equilibrium is shifted to the reactants with increasing temperature. Therefore, catalysis is obligatory for this conversion [2].

For the addition of aromatic amines to alkenes, highly active and selective homogeneous catalysts are known. Titanium, rhodium, palladium and ruthenium complexes were employed to catalyze the intermolecular hydroamination of alkynes and dienes with anilines [3-9]. Intermolecular amination of alkenes are nevertheless much more difficult, and only few catalysts are well known. Beller and co-workers recently reported the addition of morpholine to vinyl-benzene with anti-Markovnikov regiochemistry in the presence of a rhodium catalyst [10]. The Beller group also reported the rhodium-catalyzed amination of vinyl-benzenes with anilines that gives direct access to substituted quinolines in a new domino reaction [11]. As side reaction the anti-Markovnikov hydroamination of vinyl-benzene was observed.

Kawatsura and Hartwig reported the palladium-catalyzed hydroamination of vinyl-arenes with anilines to give the Markovnikov product [12]. A variety of substituted vinyl-benzenes and anilines could be used, although electron rich anilines reacted more efficiently. It was noted that the presence of acid accelerates the reaction. The influence of the acid was also observed for the addition of aryl-amines to 1,3-cyclohexadiene catalyzed by acidic form zeolites [13].

In spite of the fact that different homogeneous catalysts are known for hydroamination reactions, only few examples of heterogeneous catalysts have been reported [14]. The BASF process for *tert*-butylamine production from isobutene and ammonia takes place with more than 90 % selectivity over a modified beta zeolite [15, 16]. Recently, a method to support palladium complexes on $SiO_2$, $Al_2O_3$ and $TiO_2$,

was reported for the cyclization of 3-aminopropyl-vinylether [17]. Significant support effects on the catalytic activity were observed in the sequence $SiO_2 > TiO_2 > Al_2O_3$. Characterization of the material revealed the existence of a Pd-O bond between the palladium complex and the support (Eq. 1), which seems to be the responsible for the differences in activity. The most ionic Pd-OSi bond is favourable for the cyclization of amino alkenes, while the Pd-OAl bond with a more covalent character does not promote the reaction efficiently.

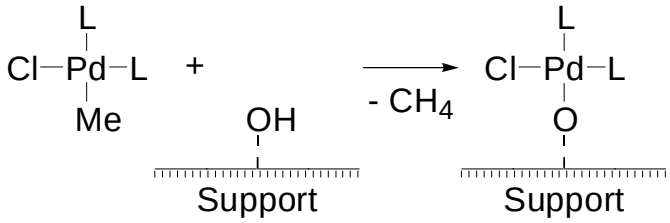


(2)

Catalytically active metal cations (such as $Rh^+$, $Pd^{2+}$, $Cu^+$, $Zn^{2+}$) were incorporated in zeolites and displayed a high activity for inter and intra molecular hydroamination of alkynes due to the simultaneous presence of Brønsted acidic hydroxyl groups and Lewis acidic metal cations [18]. Surprisingly high catalytic activities were also observed for molecular catalysts in two-phase systems where the catalyst was dissolved in an ionic liquid [19, 20]. This was explained by the highly polar environment, which stabilises polar transition states in the catalytic cycle. However, most importantly, the concentration of reactants and products in the ionic liquid phase is different from those in the bulk organic phase. Thus, it seemed highly promising to support a bifunctional catalytic system in an ionic liquid as an ideal approach to combine the advantages of both homogeneous and heterogeneous catalysis.

Catalytic properties of homogeneous catalysts can be transferred onto solid supports using supported ionic liquids [21]. Preparation of solid acids using immobilizing techniques is advantageous because of the easily tuneable acidity. This tuning of acidity also depends on the appropriate choice of support. Changing the length of side chains of the inorganic cation can enhance hydrophilicity or hydrophobicity of the liquid film. Immobilization of ionic liquids facilitates the use of fixed bed reactors and recovery of the catalyst [22]. The concept of supported ionic liquid has been used successfully in several reactions [23, 24]. Hölderich and co-

workers reported two different methods for the preparation of immobilized ionic liquids and their application in Friedel-Crafts acylation of aromatics [25,26]. Mehnert et al reported the use of rhodium supported ionic liquids for hydroformylation catalysis [27].

The present work reports on the preparation of well-tailored catalysts combining both approaches, i.e., the presence of localized Brønsted and transition metal Lewis acid sites. To obtain a heterogeneous catalyst a solution of immobilized palladium complex in ionic liquid was supported on silica. The catalyst was tested for the intermolecular hydroamination of vinyl-benzene with aniline.

## 2. Experimental

### 2.1. General

The ionic liquids 1-alkyl-3-methyl-1-H-imidazolium trifluoromethane sulfonate, alkyl = ethyl (EMIm), butyl (BMIm) and hexyl (HMIm) with a maximum water and halide content of 32 and 322 ppm, respectively, were obtained from Merck. Palladium (II) trifluoroacetate [$Pd(CF_3CO_2)_2$], 1,1'-bis(diphenylphosphino)ferrocene (DPPF) (97 %), trifluoromethane sulfonic acid (TfOH) (98 %), dichloromethane (>99.5 %), undecane (+99 %), and aniline (99.5%) were obtained from Aldrich; octane (>99 %) and vinyl-benzene (99.5 %) were purchased from Fluka and used as received. The silica support Aerosil 355 was kindly provided by Degussa AG.

### 2.2. Physical and analytical methods.

The silicon content of the supported catalysts was determined by AAS using a UNICAM 939 spectrometer. The palladium content was measured by neutron activation. For liquid phase $^{1}H$ and $^{13}C$ NMR, 1 drop of each ionic liquid was diluted in $CD_2Cl_2$. Reference samples for liquid phase $^{1}H$, $^{13}C$, $^{19}F$ and $^{31}P$ NMR were prepared in the same way as the supported catalysts without addition of silica. The solution was transferred to an NMR tube and measured on a Bruker AM 400 instrument using the solvent signal of $CD_2Cl_2$ as reference. For solid state NMR, the samples were packed in 4 mm $ZrO_2$ rotors and spun at 14 kHz. $^{1}H$, $^{13}C$, $^{19}F$ and $^{31}P$ NMR spectra were recorded on a Bruker 500 TM Ultrashield with a magnetic field strength 11.75 T. Surface area and pore structure were analyzed by nitrogen adsorption at 77 K on a PMI Automated BET Sorptometer. For IR characterization,

the sample was pressed into a self-supporting wafer, which was placed into a sorption cell, where it was activated in vacuum for 4 h at 150 °C. Spectra of the sample were taken using a Perkin Elmer 2000 spectrometer. The spectra were recorded in the region from 4000 to 400 $cm^{-1}$ at a resolution of 4 cm-1. Scanning electron microscope images were obtained on a JEOL 500 SEM. Images were taken by operating the microscope at 23.0 kV. For transmission electron microscope images, the samples were grinded, suspended in hexane and ultrasonically dispersed. Drops of the dispersions were applied on a copper grid-supported carbon film. Micrographs were recorded on a JEM-2010 Jeol transmission electron microscope operating at 120 kV.

Gas chromatography (GC) analysis were performed on a Hewlett-Packard HP 5890A gas chromatograph equipped with a cross linked 5 % diphenyl-95 % dimethyl-polysiloxane column (30 m, Restek GmbH, Rtx-5 Amine) and a flame ionization detector (Temperature program: 5 min at 120 °C, 10 °C/min to 290 °C, 1 min at 290 °C). GC-MS analyses were performed on a Hewlett-Packard HP 5890 gas chromatograph equipped with an identical column and a mass selective detector HP 5971A.

2.3. Preparation of the supported catalysts

$[Pd(CF_3CO_2)_2]$ and DPPF in molar ratio 2 to 3 (amounts see Table 1) were suspended in 50 ml dichloromethane under inert conditions and stirred for 0.5 h (Solution 1). $CF_3SO_3H$ (150 mg, 0.1 mmol) was dissolved in 2.5 ml of the ionic liquid (Solution 2). Solution 1 was added to Solution 2 and stirred for 10 min. Silica (Degussa, Aerosil 355, 5 g) was ground to a powder and a sieve fraction with a particle size in the range 60-200 μm activated overnight at 200 °C in vacuum. The silica powder was then added to the mixture and the suspension stirred for 1 hour. Finally, the suspension was rapidly frozen and the volatiles removed while the sample was warming slowly (freeze-dried) to give a well flowing orange powder. For comparison reasons, a further series of samples was prepared in the same way, but without addition of $[Pd(CF_3CO_2)_2]$ and DPPF.

**Table 1.** Amounts used in the preparation of the supported catalysts.

| Catalyst | Silica (g) | Ionic Liquid (ml) | $Pd(CF_3CO_2)_2$ (mg) | DPPF (mg) | $CF_3SO_3H$ (mg) |
|---|---|---|---|---|---|
| $EMIm/SiO_2$ | 5.0 | 2.5 | 0 | 0 | 150 |
| $Pd1/EMIm/SiO_2$ | 5.0 | 2.5 | 33 | 83 | 150 |
| $Pd2/EMIm/SiO_2$ | 5.0 | 2.5 | 66 | 166 | 150 |
| $Pd3/EMIm/SiO_2$ | 5.0 | 2.5 | 132 | 332 | 150 |
| $BMIm/SiO_2$ | 5.0 | 2.5 | 0 | 0 | 150 |
| $Pd1/BMIm/SiO_2$ | 5.0 | 2.5 | 33 | 83 | 150 |
| $Pd2/BMIm/SiO_2$ | 5.0 | 2.5 | 66 | 166 | 150 |
| $Pd3/BMIm/SiO_2$ | 5.0 | 2.5 | 132 | 332 | 150 |
| $HMIm/SiO_2$ | 5.0 | 2.5 | 0 | 0 | 150 |
| $Pd1/HMIm/SiO_2$ | 5.0 | 2.5 | 33 | 83 | 150 |
| $Pd2/HMIm/SiO_2$ | 5.0 | 2.5 | 66 | 166 | 150 |
| $Pd3/HMIm/SiO_2$ | 5.0 | 2.5 | 132 | 332 | 150 |
| $HM_2Im/SiO_2$ | 5.0 | 2.5[1] | 0 | 0 | 150 |
| $Pd1/HM_2Im/SiO_2$ | 5.0 | 2.5[1] | 33 | 83 | 150 |
| $Pd2/HM_2Im/SiO_2$ | 5.0 | 2.5[1] | 66 | 166 | 150 |
| $Pd3/HM_2Im/SiO_2$ | 5.0 | 2.5[1] | 132 | 332 | 150 |

[1] As $HM_2Im$ is solid at room temperature a molten sample was used.

## 2.4. Catalysis

### 2.4.1. Testing in batch mode

Experiments were performed under inert nitrogen atmosphere in a Radleys reaction carousel with 12 parallel reactors. The catalyst (0.25 g) was suspended in octane (15 ml) and heated to reflux at 125 °C. Aniline (1.82 ml, 20 mmol), vinyl-benzene (3.44 ml, 30 mmol) and undecane (1 ml, internal GC standard) were added to each of the reactors. Samples (50 μl) were taken periodically and analyzed by GC to quantify conversion and selectivity of the reaction. The activation energy was determined in the range 150 °C to 180 °C using a Slurry phase reactor SPR16 (Amtec) equipped with 16 independent stirred – tank reactors (pressure autoclaves). The catalyst (0.1 g) was suspended in octane (4 ml) and heated to the desired temperature and a pressure of 10 bar. Subsequently, 4 ml of an octane solution containing aniline (8 mmol), vinyl-benzene (12 mmol) and undecane (0.4 ml) were

pumped to the reactor and the reaction started. Samples were taken automatically by the reactor every 10 minutes and analyzed by GC.

2.4.2. Tests on leaching of palladium complex

Reaction mixtures prepared in same way as described above were filtered hot after either 4 or 12 h reaction time. The filtrates were kept at reflux and further samples were taken after 24 h total reaction time.

2.4.3. Catalytic testing in fixed bed reactor

A fixed bed reactor was filled with catalyst (50 mg) and glass beads (remaining volume). A solution of aniline (0.10 $mol \cdot l^{-1}$), vinyl-benzene (0.15 $mol \cdot l^{-1}$) and un-decane (internal standard) in octane was passed over the catalyst (flow 0.2 $ml \cdot min^{-1}$). The temperature was increased from 150 °C to 300 °C in steps of 10 °C (intervals 20 min). After steady state was obtained, samples of the product mixture were collected at the end of the reactor for gas chromatography. The temperature was then reduced to 150 °C and confirmed that the initial activity was obtained.

2.4.4. Determination of the absorption constants for aniline and styrene

A fixed bed reactor was filled with catalyst (50 mg) and glass beads (remaining volume). A constant flow of octane (1 $ml \cdot min^{-1}$) was passed over the catalyst bed and the temperature of the reactor and feed increased to 120 °C. The concentration of aniline was then increased stepwise to $1.85 \cdot 10^{-4}$, $2.27 \cdot 10^{-4}$ and $2.70 \cdot 10^{-4}$ $mol \cdot l^{-1}$. The concentration of aniline at the exit was followed with UV spectroscopy at 298 nm. The uptake was calculated from the time-concentration diagram by comparison with an experiment, where the reactor had been filled only with glass beads. The experiment was repeated with vinyl-benzene.

## 3. Results and Discussion

3.1. Preparation of the supported catalysts

To systematically study the effect of the ionic liquid, sixteen different supported catalysts were prepared varying in palladium concentration (0, 0.011, 0.022 and 0.042 $mmol \cdot g^{-1}$) and choice of the 1-alkyl-3-methylimidazolium salt (Figure 1, Table 2). By changing the substituent from alkyl = ethyl to butyl and hexyl, the polarity of the ionic

liquid was systematically changed from relatively polar to quite non-polar. As inert support flame dried silica with a surface area of 150 $m^2/g$ was ground and separated with sieves with 60 and 200 μm mesh size. To show the viability of the concept, the material was then tested as catalyst for the intermolecular hydroamination of vinyl-benzene with aniline.

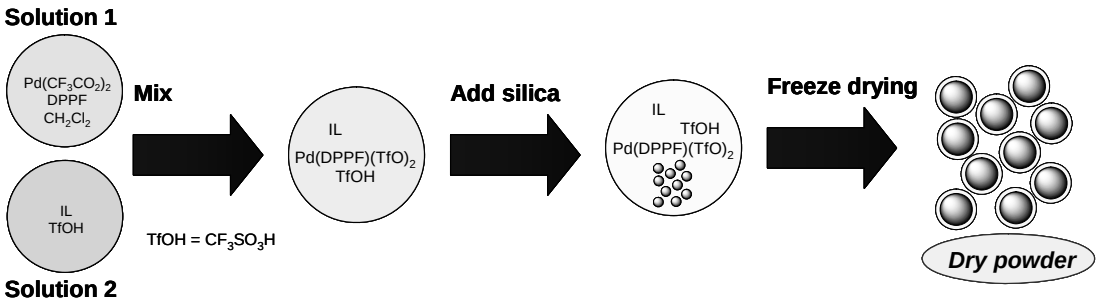


**Figure 1.** Experimental procedure for the preparation of supported catalysts

**Table 2.** Elementary composition and physicochemical properties of the supported catalysts used in this study

| Catalyst | Si (calc.) [wt. %][1] | C (calc.) [wt. %][2] | H (calc.) [wt. %][2] | N (calc.) [wt. %][2] | Pd (calc.) [wt. %][3] | Surface area [4] $[m^2 \cdot g^{-1}]$ | Pore volume $[ml \cdot g^{-1}]$ |
|---|---|---|---|---|---|---|---|
| $SiO_2$ | - | - | - | - | - | 150 | 0.84 |
| EMIm/$SiO_2$ | 23.7 (28.8) | 12.70 (13.33) | 1.85 (1.70) | 3.98 (4.31) | - | 38 | 0.25 |
| Pd1/EMIm/$SiO_2$ | 24.0 (28.4) | 13.23 (13.58) | 2.01 (1.72) | 4.21 (4.23) | 0.11 (0.12) | - | - |
| Pd2/EMIm/$SiO_2$ | 22.7 (27.6) | 15.73 (14.04) | 2.50 (1.73) | 4.04 (4.10) | 0.22 (0.23) | - | - |
| Pd3/EMIm/$SiO_2$ | 21.0 (26.0) | 14.22 (14.88) | 2.20 (1.74) | 3.72 (3.88) | 0.40 (0.44) | - | - |
| BMIm/$SiO_2$ | 25.3 (29.5) | 14.16 (14.85) | 2.32 (2.03) | 3.52 (3.74) | - | 39 | 0.24 |
| Pd1/BMIm/$SiO_2$ | 24.2 (29.1) | 14.49 (15.09) | 2.27 (2.03) | 3.42 (3.68) | 0.11 (0.12) | - | - |
| Pd2/BMIm/$SiO_2$ | 23.6 (28.2) | 14.92 (15.52) | 2.35 (2.02) | 3.35 (3.57) | 0.21 (0.24) | - | - |
| Pd3/BMIm/$SiO_2$ | 27.3 (26.6) | 15.63 (16.30) | 2.44 (2.02) | 3.14 (3.36) | 0.41 (0.45) | - | - |
| HMIm/$SiO_2$ | 27.2 (30.1) | 15.17 (15.89) | 2.26 (2.26) | 3.46 (3.28) | - | 42 | 0.23 |
| Pd1/HMIm/$SiO_2$ | 25.7 (29.8) | 15.77 (16.12) | 2.44 (2.25) | 3.11 (3.22) | 0.14 (0.13) | - | - |
| Pd2/HMIm/$SiO_2$ | 25.0 (28.8) | 17.13 (16.53) | 2.63 (2.24) | 2.89 (3.12) | 0.23 (0.24) | - | - |
| Pd3/HMIm/$SiO_2$ | 25.7 (27.2) | 16.39 (17.26) | 2.51 (2.22) | 3.12 (2.94) | 0.43 (0.46) | - | - |
| $HM_2Im/SiO_2$ | 26.4 (30.2) | 15.38 (16.58) | 2.53 (2.40) | 2.82 (3.13) | - | 45 | 0.25 |
| Pd1/$HM_2$Im/$SiO_2$ | 25.5 (29.8) | 15.76 (16.79) | 2.37 (2.38) | 2.61 (3.08) | 0.12 (0.13) | - | - |
| Pd2/$HM_2$Im/$SiO_2$ | 26.0 (28.9) | 16.52 (17.17) | 2.51 (2.36) | 2.85 (2.99) | 0.24 (0.24) | - | - |
| Pd3/$HM_2$Im/$SiO_2$ | 24.1 (27.2) | 16.75 (17.87) | 2.62 (2.34) | 2.47 (2.82) | 0.41 (0.46) | - | - |

(Calc.) Values in brackets correspond to the calculated value

[1] Silicon content determined by atomic absorption spectroscopy

[2] CHN analysis

[3] Palladium content determined by neutron activation

[4] BET surface area determined by $N_2$ adsorption

3.2. Characterization of the supported catalysts

Scanning electron micrographs of the supported catalysts are shown in Figure 2a. Silica particles of 150 – 300 µm diameter can be distinguished, which consist of spherical primary particles of approximately 10 nm radius. An expected thin film of the ionic liquid (calculated to 3 nm thickness) on the surface of the primary silica particles was not observed even with high magnification transmission electron microscopy (Figure 2b).

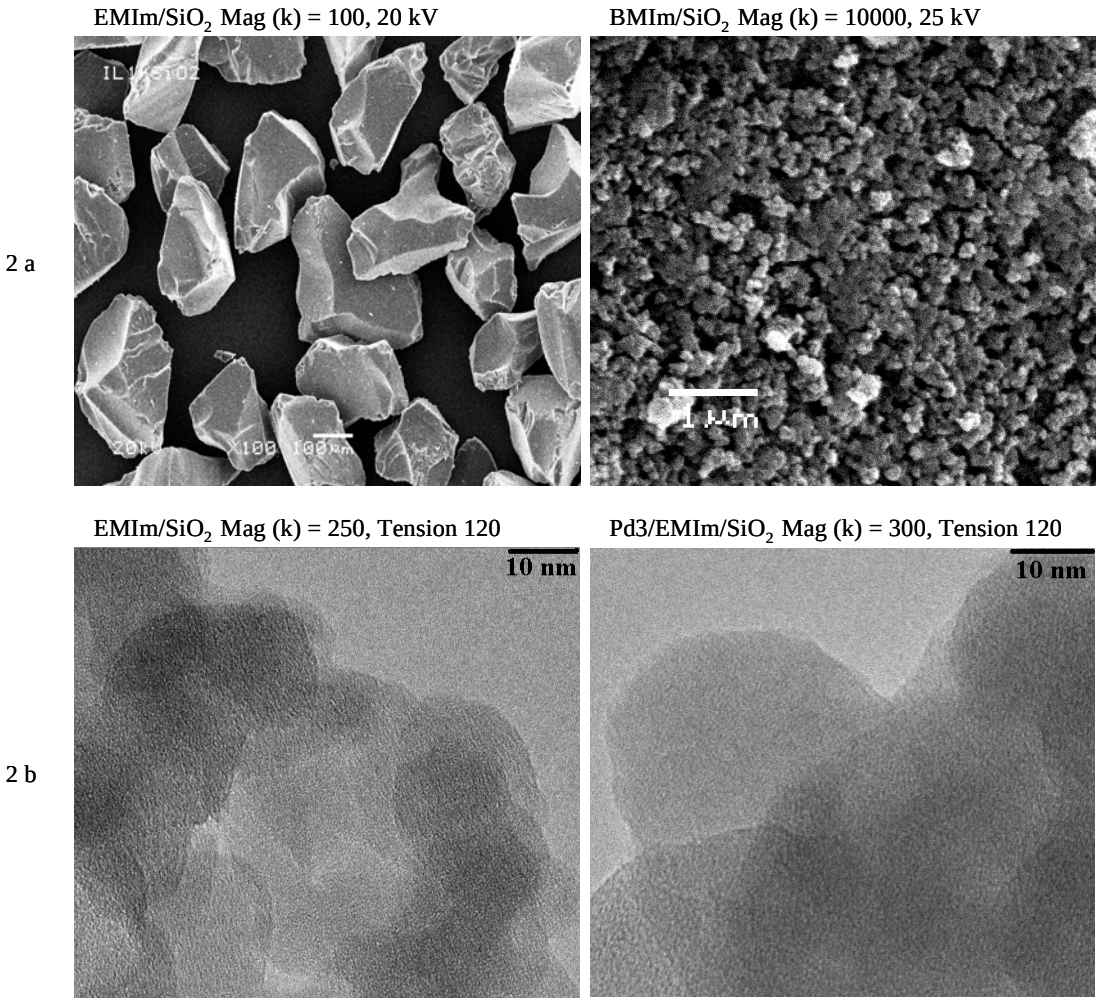


2 a

2 b

**Figure 2.** Scanning electron micrographs (2a) and transmission electron micrographs (2b) of supported ionic liquids

The distribution of the ionic liquid in the particles was then indirectly observed by BET analysis, which showed that impregnation led to a decrease in the surface area from (155 $m^{2}{\cdot}g^{-1}$) for the parent material to (37 - 45 $m^{2}{\cdot}g^{-1}$) for the supported catalysts. Detailed analysis of the BET isotherms showed that the pore volume associated with

small pores had decreased dramatically (Fig. 3) from 0.84 $cm^{3}\cdot g^{-1}$ in the parent material to circa 0.20 $cm^{3}\cdot g^{-1}$ in the supported catalysts. Mesopores with up to 18 nm diameter were entirely filled, whereas large pores remained nearly unchanged. In consequence, the mean pore radius was shifted slightly from 9.3 nm to higher values (9.6 – 11.8 nm).

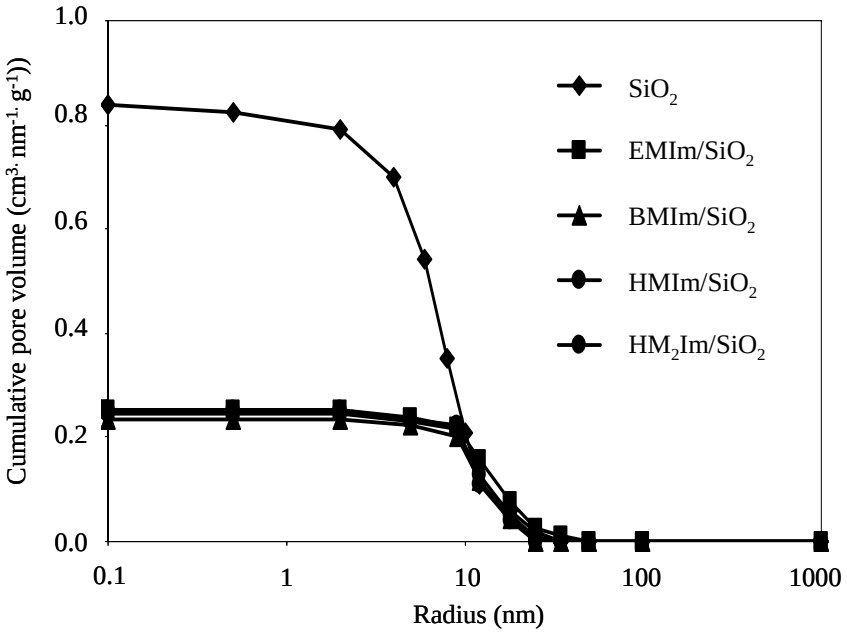


**Figure 3.** BET analysis of the supported catalysts in comparison to silica

In the region of hydroxyl stretching bands, the IR spectra of the silica support showed two bands corresponding to silanol groups (3745 $cm^{-1}$) and bridging hydroxyl groups (broad band centred at 3594 $cm^{-1}$). Infrared spectra of the supported catalysts showed that the signal due to the silanol groups of the parent silica disappeared upon treatment with the ionic liquid solution indicating that all silanol groups (SiOH) were involved in hydrogen bonding interactions with the thin film of ionic liquid (Figure 4). This conclusion is also supported by the presence of an intense very broad band in the spectra of supported catalysts, which is centred at 3340 $cm^{-1}$. For the supported catalysts, several bands are presented in the ranges 2700 -3300 $cm^{-1}$, which were assigned to the asymmetric and symmetric stretching vibrations of the $CH_3$, $CH_2$ groups ($\nu CH_3$, $\nu CH_2$) of the ionic liquids. The bands between1700 and 1600 $cm^{-1}$ correspond to the C=C stretching vibration ($\nu$C=C). Finally, in the range 1500-1300 $cm^{-1}$ the CH bending modes of the ionic liquids ($\delta$CH) were observed.

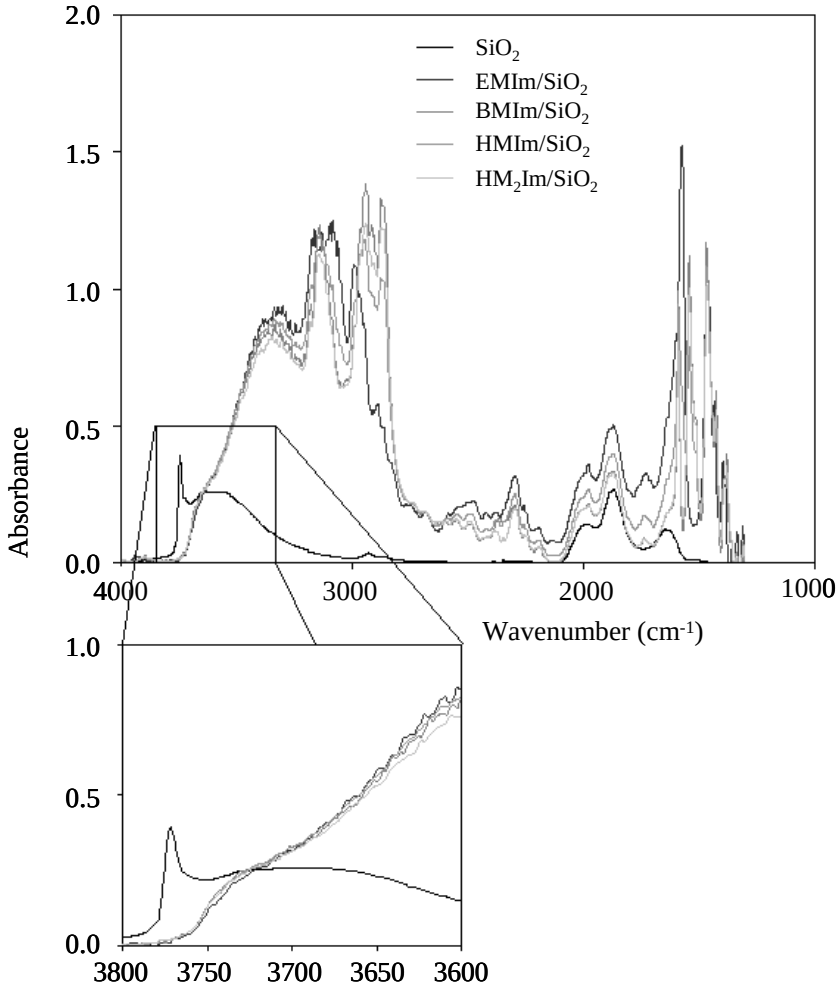


**Figure 4.** Infrared spectra of the supported ionic liquids in comparison with the parent silica

Detailed NMR analysis on the supported catalysts showed that the ionic liquid did not coordinate directly to the palladium centre in $[Pd(DPPF)(CF_3CO_2)_2]$. In $^{19}F$ MAS NMR spectroscopy showed a relative asymmetric signal due to the fluor present in the ($CF_3SO_3$) was observed at -78.73 ppm. The asymmetry of the signal is assigned to the presence of the ($CF_3CO_2$) anions from the $[Pd(CF_3CO_2)_2]$. $^{31}P$ MAS NMR spectroscopy, showed a signal at 47.3 ppm due to the phosphine ligand of the palladium complex, with a relatively large line-width of 440-1360 Hz. In comparison, the $^{31}P\{^1H\}$ NMR signal for a solution of $[Pd(DPPF)(CF_3CO_2)_2]$, $CF_3SO_3H$ and IL in $CD_2Cl_2$, was observed at 47.1 ppm with a much smaller line-width of 2.5 Hz [29].

The mobility of the ionic liquid was reduced as was concluded from broadening of the $^1H$ signals with increasing the size of imidazolium cation in the order EMIm < BMIm < HMIm < $HM_2Im$ (Table 3). A dramatic increase of the line-width of the $^1H$

NMR signals of the imidazolium cation was also observed when the palladium complex was immobilized in the supported ionic liquids. Temperature controlled $^{1}H$ MAS NMR spectra of the supported catalysts were taken to follow the mobility of the imidazolium ring. A decrease of the line width of the $^{1}H$ NMR signals was observed with increasing temperature (Figure 5). The addition of the palladium complex is equivalent to a temperature decrease of circa 60 – 70 K. With these observations, we conclude that the mobility of both, the imidazolium ring of the ionic liquid and the palladium complex is decreased in the supported catalysts [29].

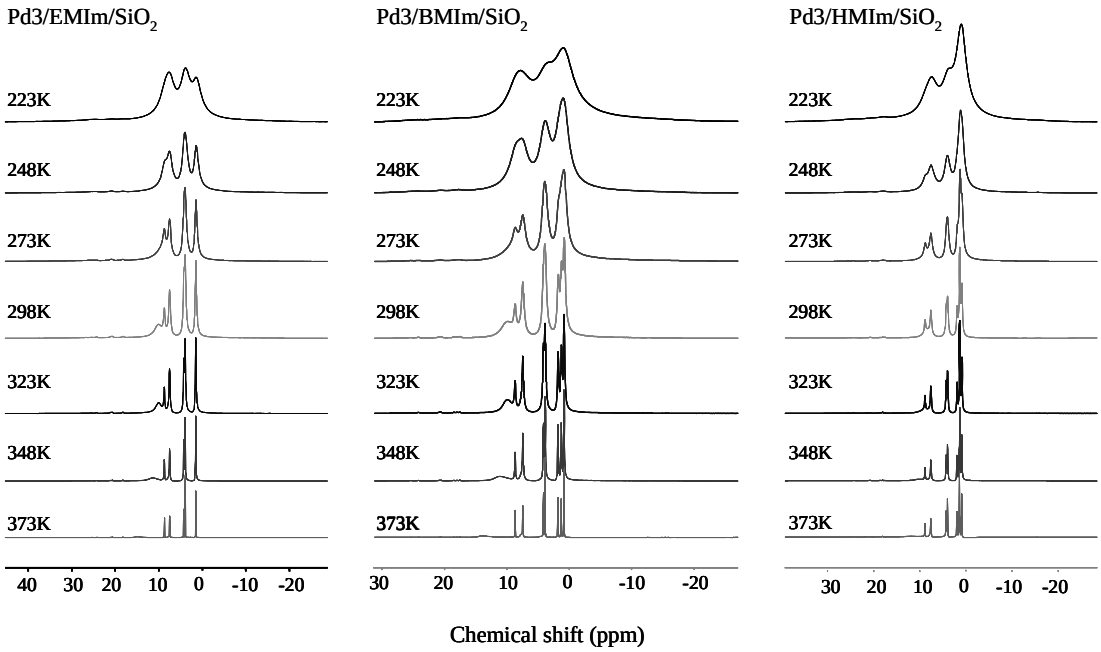


**Figure 5.** Temperature controlled $^{1}H$ MAS NMR spectra of the supported catalysts: Pd3/EMIm/$SiO_2$ (left), Pd3/BMIm/$SiO_2$ (centre), Pd3/HMIm/$SiO_2$ (right),

Similar results were obtained with $^{13}C$ MAS NMR spectroscopy. The line width of the imidazolium signals in the supported catalysts was increased when compared with these of the neat ionic liquids (Table 4). A slight low to high field shift of the $CH_2$-N signal was observed when increasing the length of the ionic liquid in the order EMIm < BMIm < HMIm < $HM_2$Im (Figure 6). In addition, for $HM_2$IM the N-C(H)=N signal was moved to higher field due to the influence of the additional C-C bond in N-C(C)-N with signal at 13.96 ppm. The presence of small signals at 75, 78, 130 and 134 ppm was observed. These signals correspond to the phenyl (Ph) and ferrocene (Cp) rings of the phosphine ligand in [Pd(dppf)($CF_3SO_3$)$_2$].

**Table 3.** $^{1}H$ NMR position and line-width of the imidazolium cations in the supported catalysts

| Catalyst | C(2)H | | $N-CH_2$ | | $N-CH_3$ | | Alkyl-$CH_3$ | |
|---|---|---|---|---|---|---|---|---|
| | Position (ppm) | Linewidth (Hz) | Position (ppm) | Linewidth (Hz) | Position (ppm) | Linewidth (Hz) | Position (ppm) | Linewidth (Hz) |
| EMIm/SiO2 | 8.59 | 26 | 4.10 | 30 | 3.77 | 25 | 1.35 | 26 |
| BMIm/SiO2 | 8.64 | 25 | 4.07 | 32 | 3.80 | 27 | 0.75 | 25 |
| HMIm/SiO2 | 8.70 | 33 | 4.08 | 41 | 3.81 | 32 | 0.71 | 27 |
| $HM_2Im$/SiO2 | - | - | 4.01 | 49 | 3.70 | 48 | 0.75 | 28 |
| Pd/EMIm/SiO2 | 8.54 | 122 | 4.08 | 98 | 3.76 | 96 | 1.34 | 95 |
| Pd/BMIm/SiO2 | 8.65 | 516 | 4.08 | 333 | 3.79 | 332 | 0.79 | 307 |
| Pd/HMIm/SiO2 | 8.64 | 307 | 4.07 | 263 | 3.77 | 384 | 0.70 | 147 |
| Pd/$HM_2Im$/SiO2 | - | - | 4.03 | 286 | 3.70 | 424 | 0.81 | 169 |

**Table 4.** $^{13C}$ NMR position and line-width of the supported ionic liquids

| Catalyst | C=C | | N=C | | $N-CH_2$ | | $N-CH_3$ | | Alkyl-$CH_3$ | |
|---|---|---|---|---|---|---|---|---|---|---|
| | Position (ppm) | Linewidth (Hz) | Position (ppm) | Linewidth (Hz) | Position (ppm) | Linewidth (Hz) | Position (ppm) | Linewidth (Hz) | Position (ppm) | Linewidth (Hz) |
| EMIm/SiO2 | 122.53 | 30.14 | 136.63 | 30.62 | 45.45 | 26.25 | 36.33 | 27.44 | 14.95 | 25.67 |
| | 124.21 | 30.54 | | | | | | | | |
| BMIm/SiO2 | 123.06 | 61.64 | 136.86 | 53.88 | 50.08 | 51.39 | 36.57 | 63.56 | 13.23 | 52.39 |
| | 124.31 | 60.06 | | | | | | | | |
| HMIm/SiO2 | 122.34 | 48.47 | 136.34 | 57.65 | 49.64 | 55.06 | 35.66 | 53.27 | 13.13 | 51.97 |
| | 123.56 | 57.80 | | | | | | | | |
| $HM_2Im$/SiO2 | 121.52 | 39.56 | 144.86 | 32.99 | 49.01 | 35.77 | 35.41 | 33.22 | 9.58 | 32.33 |
| | 123.02 | 32.99 | | | | | | | | |

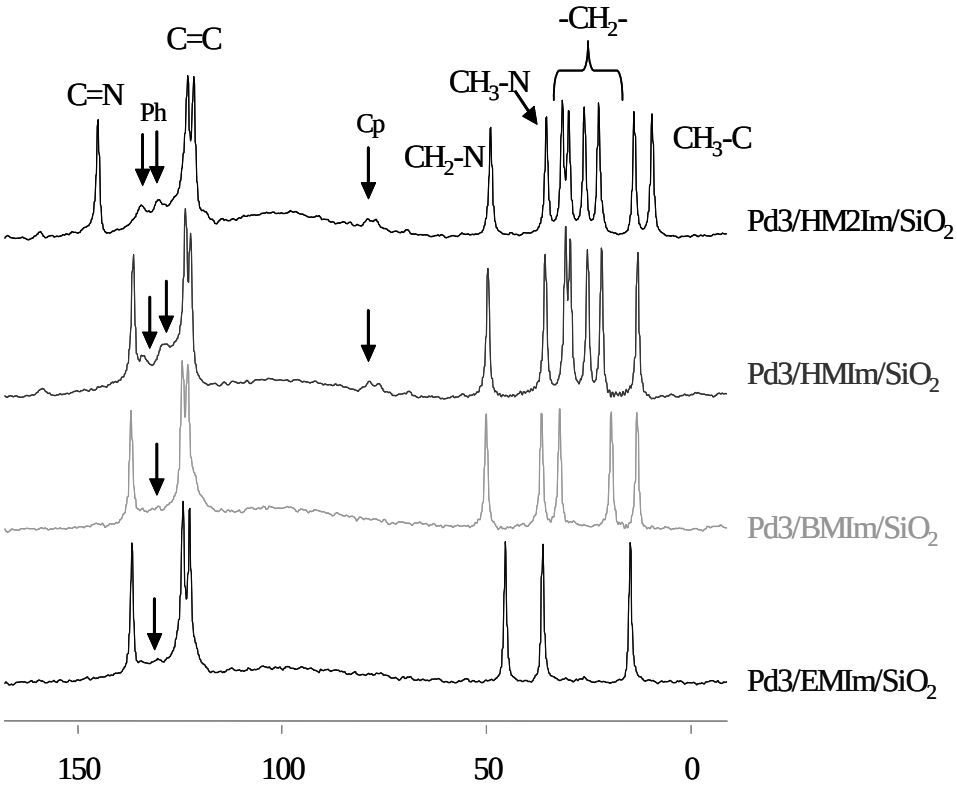


**Figure 6.** $^{13}C$ MAS NMR spectra of the supported catalysts.

These observations are explained by formation of a solvent cage around the palladium complex which is causedby disruption of the inter-ionic interactions during dissolution of the palladium complex in the ionic liquid. The reduced mobility provides experimental evidence for the formation of ordered three dimensional structures in solutions of organometallic complexes in thin films of supported ionic liquids (Figure 7). In this respect, the supported complexes are very different from complexes dissolved in classic solvents [29].

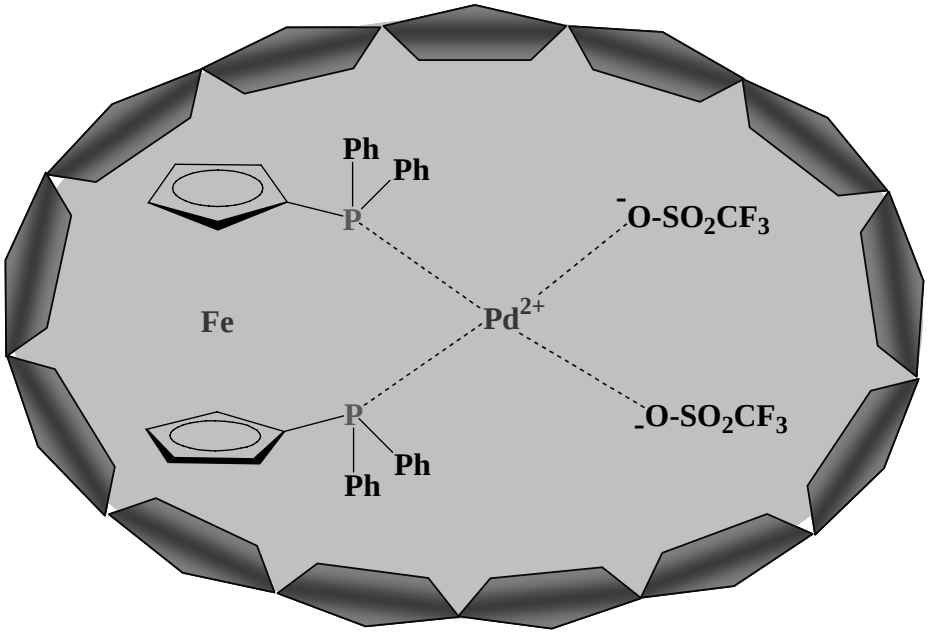


**Figure 7.** Artist's impression of the solvent cage of ionic liquid molecules around the organometallic palladium complex

3.3. Catalytic activity of the supported catalysts

Cationic metal complexes are known to catalyse the direct addition of amines to alkenes and alkynes (hydroamination). The highest activities were reported for bifunctional systems of Lewis acidic metal complexes of, e.g., Pd and a strong Brønsted acid. Here, the palladium complex $[Pd(DPPF)(CF_3SO_3)_2]$ and trifluoromethane sulfonic acid as co-catalyst were chosen and supported in a thin film of 1-alkyl-3-methyl-imidazolium trifluoromethane sulfonate on silica.

The material was then tested for catalytic activity in the addition of aniline to vinyl-benzene (Eq. 2).

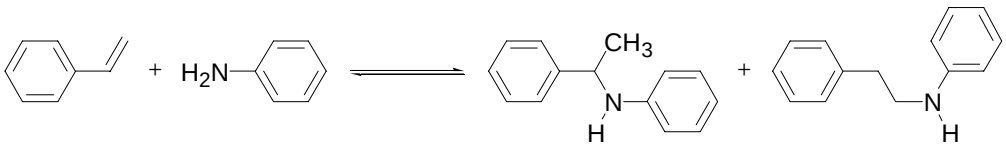


(2)

The main product was phenyl-(1-phenyl-ethyl)-amine, when the experiment was performed at 125 °C (*vide infra*). The catalytic activity increased in the sequence $HM_2Im$ < HMIm < BMIm < EMIm (Fig. 8). Thus, the IL with higher polarity provided a higher activity. This suggests that a polar transition state, which had been

identified previously as the limiting factor for catalysis of hydroamination reactions [30], is lowered in energy in the presence of the ionic liquid. The initial catalytic activity increased linearly with the Pd loading, corresponding to first order in palladium. However for the catalyst with 0.011 mmol $Pd^{2+}$.$g_{Cat}^{-1}$, the activity was much lower than anticipated. Apparently there is a lower limit for the palladium concentration, which is consistent with strong adsorption of the palladium complexes on surface OH groups of the silica. This interaction would render part of the palladium complexes catalytically inactive. The reference samples, which did not contain a palladium complex, but only $CF_3SO_3H$ displayed no activity.

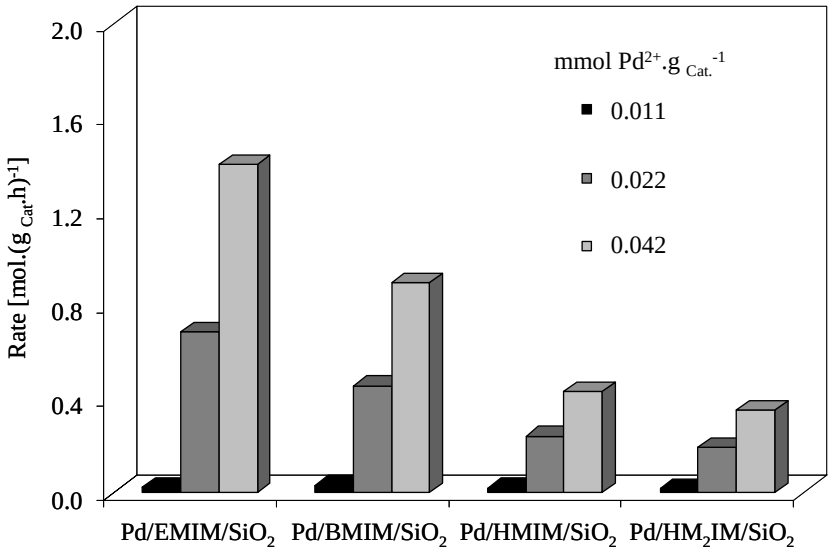


**Figure 8.** Catalytic activity of the supported catalysts in the addition of aniline to vinyl-benzene

With a molar ratio aniline / $Pd^{2+}$ = 1904 for the catalyst Pd3/EMIm/$SiO_2$ with 0.042 (mmol $Pd^{2+}$.g $Cat^{-1}$) an average turnover frequency of TOF 24 $h^{-1}$ and TON 580 is calculated for a period of 24 h. In comparison, for the homogeneous catalyst 99 % yield were reported after 7h reaction time, which is equivalent to TOF 7 $h^{-1}$ and TON 50 [12]. When compared under equal reaction conditions, the catalytic activity of the supported catalysts slightly exceeded the activity of the corresponding homogeneous and two-phase catalyst (Table 5). For all catalysts, the selectivity was 100 % on the basis of aniline and between 50 and 95 % based on vinyl-benzene, mainly due to oligomerisation as side reaction.

**Table 5.** Comparison of the catalytic activity of the supported catalyst with the corresponding homogeneous and two phase catalysis

| Catalyst | Rate $[mol \cdot (mol_{Pd^{2+}} \cdot h)^{-1}]$ |
|---|---|
| Homogeneous [1] | 23.2 |
| Two-Phase [2] | 32.2 |
| Supported ($Pd3/EMIm/SiO_2$) | 33.3 |

[1] Catalyst preparation according to reference [12]

[2] Preparation followed the same procedure as for the supported catalysts except that the addition of silica was omitted

The activation energy was measured for the supported catalysts in the range 150 – 180 °C based on the consumption of aniline. The activation energy decreased in the sequence EMIm > BMIm> HMIM> $HM_2Im$ and thus, with decreasing polarity of the ionic liquid. Note that this is in contrast to expectation, as the lowest activation energy would be expected for the most active catalyst.

**Table 6.** Apparent activation energy for the addition of aniline to vinyl-benzene catalyzed by palladium complexes immobilized in a thin film of supported ionic liquid

| Catalyst | Activation Energy $[kJ.mol^{-1}]$ |
|---|---|
| $Pd3/EMIm/SiO_2$ | 89.69 |
| $Pd3/BMIm/SiO_2$ | 74.49 |
| $Pd3/HMIm/SiO_2$ | 55.47 |
| $Pd3/HM_2Im/SiO_2$ | 46.42 |

To better understand the influence of the ionic liquid an the catalytic activity, the solubility of the reactants in the ionic liquid was measured. Significant differences in the absorption of reactants and products in the ionic liquid film exist. The reactants, in particular aniline, are highly soluble in the ionic liquid phase, while the products are hardly soluble (Table 7). Slight differences in the sequence $HM_2Im$ < BMIm < EMIm were observed for aniline absorption. On the other hand, vinyl-benzene was not

absorbed in the ionic liquid. Nevertheless, a co-absorption effect in presence of aniline enhances the probability for vinyl-benzene to cross the phase boundary.

**Table 7.** Aniline absorption on supported ionic liquids on silica

| Catalyst | Absorbed Aniline [1] [mmol.g $_{Cat.}^{-1}$] |
|---|---|
| EMIm/$SiO_2$ | 0.23 |
| BMIm/$SiO_2$ | 0.22 |
| $HM_2Im/SiO_2$ | 0.20 |

[1] Determined by UV Spectroscopy

If solubility of the reactants is a key factor, the amount of supported ionic liquid will strongly influence the catalytic activity. Therefore, a series of catalysts varying the amount of the ionic liquid but with the same palladium content was prepared and tested for the addition of aniline to vinyl-benzene (Fig. 9). The catalytic activity increased exponentially with increasing the amount of the ionic liquid. As expected, the ionic liquid free catalyst displayed the lowest activity. These results support the conclusion that the catalysts were operating without mass transport limitations.

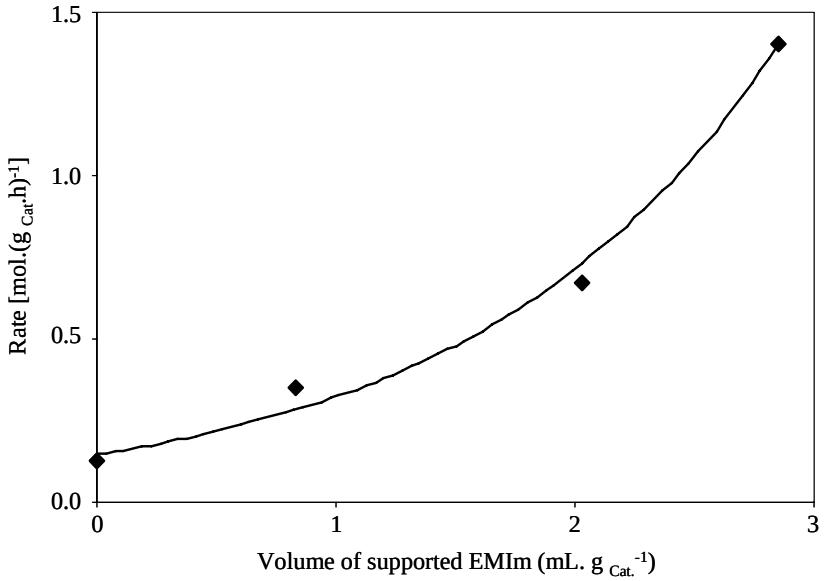


**Figure 9.** Dependence between the amount of ionic liquid and the catalytic activity of supported catalysts

The reaction was followed in a fixed bed reactor and the temperature increased stepwise to 300 °C. A typical temperature – concentration profile is shown in Fig. 10. The activity of the catalysts increased exponentially at temperatures above 150 °C to reach a maximum at approximately 250 °C. Whereas only the Markownikoff isomer phenyl-(1-phenyl-ethyl)-amine was formed at lower temperatures, the corresponding anti-Markownikoff isomer phenethyl-2-phenyl-amine was also observed at higher temperatures.

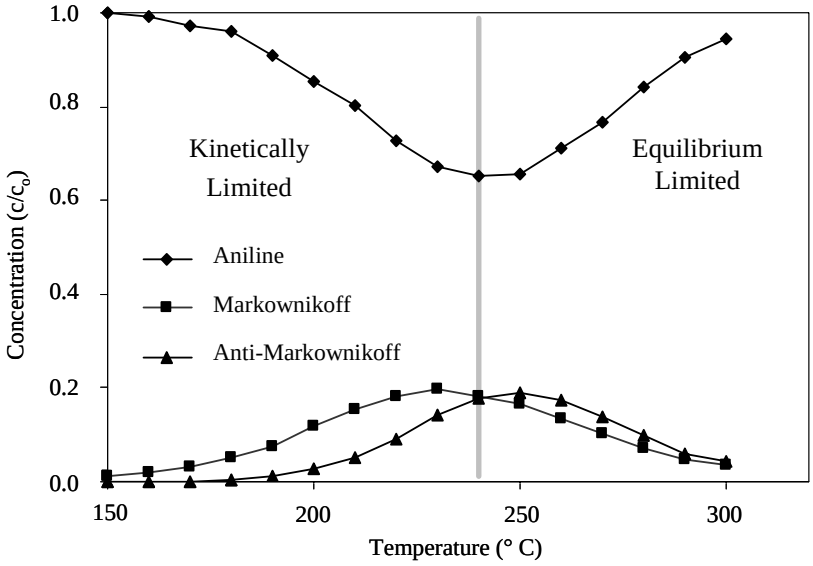


**Figure 10.** Temperature concentration profile from a fixed bed reactor for the addition of aniline to vinyl-benzene catalyzed by immobilized palladium in supported ionic liquids

In the thermodynamic region, the decrease in conversion occurred at lower temperatures for the EMIm than for BMIm and $HM_2Im$ based catalysts. Thus, in the less polar ionic liquid the reaction equilibrium is shifted towards the product. At temperatures above 250 °C, the conversion decreased as the thermodynamic limit of the (exothermic) reaction was encountered. It is particularly noteworthy that the rate of reaction in the kinetic regime (i.e. the activation energy) and the conversion in the thermodynamic regime (i.e. the reaction enthalpy) depended on the choice of the ionic liquid (Fig. 11). This clearly proves the concept that the thermodynamics can be modified by combining catalytic reaction and phase equilibria between two liquid phases (i.e. octane – IL)

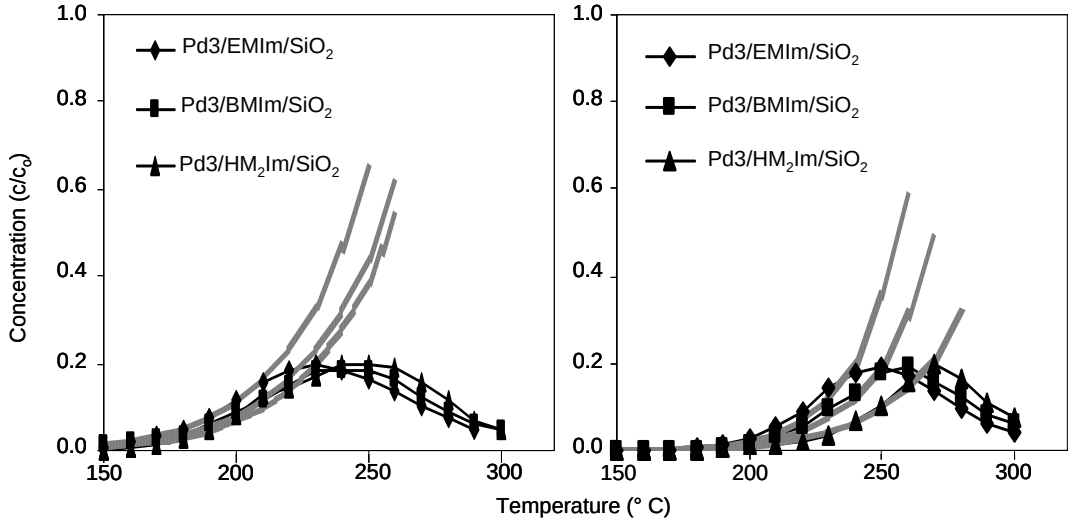


**Figure 11.** Formation of the Markownikoff (right) and the anti-Markownikoff (left) products from the addition of aniline to vinyl-benzene

Last, but not least, the supported catalyst was tested for stability with respect to leaching of the active palladium complex. The catalyst suspension was filtered hot and the heterogeneous catalyst removed from the reaction mixture after either 4 or 12 h, respectively. The reaction was then carried on, but no further conversion was observed. Thus, leaching of the palladium catalyst into the bulk organic phase did not seem to occur. AAS analysis confirmed the absence of palladium in the filtrate (Table 8).

**Table 8.** Test for catalyst leaching

| Catalyst | Palladium contents [1] [mmol·$g_{Cat.}^{-1}$] |
|---|---|
| Pd2/EMIm/$SiO_2$ | 0.22 |
| Used Pd2/EMIm/$SiO_2$ | 0.22 |
| Filtered reaction mixture | $<10^6$ |

[1] Determined by AAS

Several mechanisms have been suggested for hydroamination [12]. For Lewis acidic late transition metal complexes in the presence of a Bronsted acid, two mechanisms appear most likely including a nucleophilic attack on a coordinated vinyl-benzene or insertion of vinyl-benzene into a palladium – hydride bond as key

step [31]. Based on the observations given above, we conclude that for the addition of aniline to vinyl-benzene catalyzed with palladium immobilized in supported ionic liquids, the formation of the Markownikoff product probably follows the first mechanism path with coordination of the olefinic π-system of vinyl-benzene to the palladium centre, which renders it susceptible to a nucleophilic attack of the lone electron pair of the aniline nitrogen atom [32]. The *anti*-Markownikoff product is formed via intermediate formation of a palladium hydride, insertion of the olefinic double bond of vinyl-benzene and nucleophilic attack (r.d.s.) of the lone electron pair of the aniline nitrogen atom at the α-carbon atom [33]. The proposed mechanism for the formation of the two products in the addition of aniline to vinyl-benzene is shown in Fig. 12.

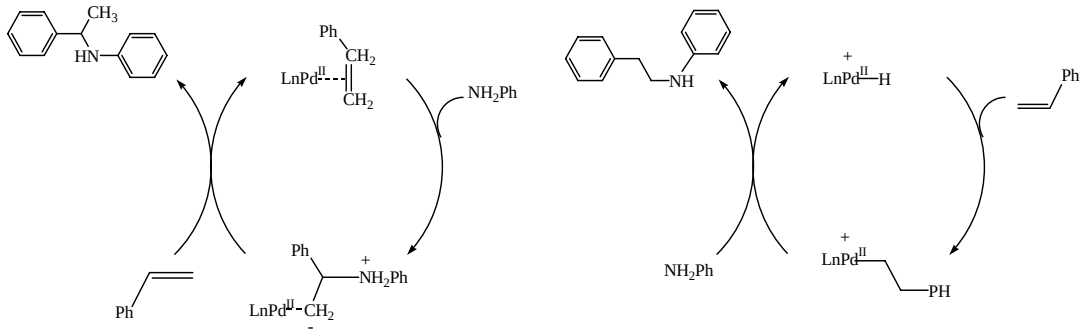


**Figure 12.** Reaction mechanism proposed for the addition of aniline to vinyl-benzene and formation of anti-Markownikoff (left) and Markownikoff (right) products

## 4. Conclusions

The concept of immobilizing organometallic complexes in a thin film of supported ionic liquid combines advantages of homogeneous catalysis (optimum utilisation of metal centres, high selectivity) with those of heterogeneous catalysis (facile recovery of catalyst, application in continuous processes). We have shown the practicability of the concept for the addition of aniline to vinylbenzene, where Lewis acidic metal complexes (based on metal cations such as $Pd^{2+}$) are excellent catalysts. Generally, the reaction rate increased with (i) increasing palladium loading and (ii) decreasing polarity of the ionic liquid. The complexes can very efficiently be immobilised in the ionic liquid and no leaching was observed.

Detailed characterisation of the supported catalysts showed that a thin film of ionic liquid covers the entire silica surface. However, most of the ionic liquid resides in the mesopores forming pockets of ionic liquid. In NMR, the signals of ionic liquid and complex molecules were considerably broadened, which shows that the mobility of the imidazolium cations and the complex molecules was dramatically reduced. We propose the formation of solvent cages of ionic liquid around the palladium complexes.

In summary, the concept of immobilizing homogeneous catalysts in a thin film of ionic liquid has been proven as functional. As designer solvents ionic liquids provide a means to locally change concentrations in the vicinity of the catalytically active metals centres. It is especially noteworthy that the concentration of reactants and products in the ionic liquid phase was different from those in the bulk organic phase. Due to their tuneable acidity and polarity, ionic liquids are particularly favourable for this application. Their appropriate selection allows to influence adsorption properties and, in consequence, catalytic activity, and selectivity.

## 5. References

[1] T. E. Müller, in: I. T. Horváth (Ed), Encyclopedia of Catalysis, Wiley, New York, (2002) 492.

[2] R. Taube, in: B. Cornils, W. A. Herrmann (Eds), Applied Homogeneous Catalysis with Organometallic Compounds, Vol 1, VCH, Weinheim, 1996.

[3] I. Bytschkov, S. Doye, Eur. J. Org. Chem. (2001) 4411.

[4] L. Ackermann, R. G. Bergman, Org. Lett. 4 (2002) 1475.

[5] E. Haak, I. Bytschkov, S. Doye, Angew. Chem. Int. Ed. 38 (1999) 3389.

[6] M. Nobis, B. Drießen-Hölscher, Angew. Chem. Int. Ed. 40 (2001) 3983.

[7] M. Tokunaga, M. Ota, M. Haga, Y. Wakatsuki, Tetrahedron. Lett. 42 (2001) 3865.

[8] C. G. Hartung, A. Tillack, H. Trauthwein, M. Beller, J. Org. Chem. 66 (2001) 6339.

[9] T. Shimada, Y. Yamamoto, J. Am. Chem. Soc. 124 (2002) 12670.

[10] M. Beller, H. Trauthwein, M. Eichberger, C. Breindl, J. Herwig, T. E. Müller, O. R. Thiel, Chem. Eur. J. 5 (1999) 1306.

[11] M. Beller, O. R. Thiel, H. Trauthwein, C. Hartung, Chem. Eur. J. 6 (2000) 2513.

[12] M. Kawatsura, J. F. Hartwig, J. Am. Chem. Soc. 122 (2000) 9546.

[13] O. Jimenez, T. E. Müller, W. Schwieger, J. A. Lercher, J. Catal. 239 (2006) 42

[14] H. M. Senn, P. E. Blöchl, A. Togni, J. Am. Chem. Soc. 122 (2000) 4098.

[15] K. Tanabe, W. F. Hölderich, Appl. Catal. A. 181 (1999) 399.

[16] A. Chauvel, B. Delmon, W. H. Hölderich, Appl. Catal. 115 (1994) 173.

[17] M. Tada, M. Shimamoto, T. Sasaki, Y. Iwasawa, Chem. Commun. (2004) 2562.

[18] J. Penzien, C. Haeßner, A. Jentys, K. Köhler, T. E. Müller, J. A. Lercher, J. Catal. 221 (2004) 302.

[19] J. Bodis, T. E. Müller, J. A. Lercher, Green Chem. 5 (2003) 227.

[20] V. Neff, T. E. Müller, J. A.Lercher, J. Chem. Soc., Chem. Comm. 8 (2002) 906.

[21] A. Corma, H. Garcia, Chem. Rev. 103 (2003) 4307

[22] M. H. Valkenberg, C. de Castro, W.F. Hölderich, Green Chemistry, 4 (2002) 88.

[23] E. Benazzi, H. Olivier, Y. Chauvin, J. F. Joly, A. Hirschauer, Abstr. Pap. Am. Chem. Soc. 212 (1996) 45.

[24] J. Huang, T. Jiang, H. Gao, B. Han, Z. Liu, W. Wu, Y. Chang, G. Zhao, Angew. Chem. 116 (2004) 1421.

[25] M. H. Valkenberg, C. de Castro, W. F. Hölderich, Appl. Catal. A: General. 215 (2001) 185.

[26] M. H. Valkenberg, C. de Castro, W. F. Hölderich, Top. Catal. 14 (2001) 139.

[27] C. P. Mehnert, R. A. Cook, N. C. Dispenziere, M. Afeworki, J. Am. Chem. Soc. 124 (2002) 12932.

[28] S. Breitenlechner, M. Fleck, T. E. Müller, A. Suppan, Mol. Catal. A: Chem. 214 (2004) 175.

[29] C. Sievers, O. Jimenez, T. E. Müller, S. Steuernagel, J. A. Lercher. *Formation of solvent cages around organometallic complexes in thin films of supported ionic liquid.* Submitted

[30] T. E. Müller, M. Berger, M. Grosche, E. Herdtweck, F. P. Schmidtchen, Organometallics, 20 (2001) 4384.

[31] O. Jimenez, T. E. Müller, C. Sievers, A. Spirkl, J. A. Lercher, Chem. Comm. (2006) 2974.

[32] H. M. Senn, P. E. Blöchl, A. Togni, J. Am. Chem. Soc. 122 (2000) 4098.

[33] U. Nettekoven, J. F. Hartwig, J. Am. Chem. Soc. 124 (2002) 1166.

# *Chapter 6*

***General conclusions***

Main conclusions of the thesis

# 1. General conclusions

Countless examples of nitrogen-containing organic molecules can be found in pharmaceutical, agricultural, and industrial applications. The synthesis of carbon-nitrogen bonds is therefore of fundamental interest in organic chemistry. Amongst the numerous methods developed for the synthesis of nitrogen-containing building blocks, such as amines, imines, and enamines, the most efficient and atom-economical method is the direct addition of amines to carbon-carbon double and triple bonds, the so called hydroamination.

Although a general hydroamination procedure applicable to a wide variety of substrates remains elusive, tremendous strides have been made towards the achievement of this challenging goal. Increasing interest in hydroamination has been sparked over the last years by the discovery of several new catalytic systems for the hydroamination of alkenes and alkynes. We have studied a fairly undeveloped but very important catalytic transformation, where heterogeneous acid i. e. materials can catalyze the intermolecular hydroamination of amines and alkenes. As test reactions, the addition of aryl-amines to 1,3-cyclohexadiene catalyzed with acidic and metal exchanged zeolites, and the addition of aniline to vinyl-benzene catalyzed with palladium complexes immobilized in supported ionic liquids, were studied.

In the first part of the thesis we have shown that a solid acid catalyst with 12 membered ring openings, such as H-Beta, can efficiently catalyze the reaction between aniline and 1,3-cyclohexadiene. In the other hand, a negative influence on the catalytic activity was observed for zinc ion exchanged zeolites. The catalytic activity decreased with increasing zinc loading indicating that the reaction is catalyzed by the Brønsted acid sites in the zeolite.

Acidic form zeolites are able to catalyse the addition of aniline to 1,3-cyclohexadiene, however the products face strong constrains to diffuse out of the pores, in particular for zeolites with smaller channel diameter like H-ZSM5. H-Y zeolite with a three-dimensional large pore system provides very high reaction rates. However, the supercage of H-Y is sufficiently large to allow the product of double addition of 1,3-cyclohexadiene to aniline to be also formed. Beta zeolite has two interconnecting channel systems with intermediate pore diameters and consequently the reactants and the desired product can diffuse comfortably and the reaction rate is

higher. It is concluded that shape selective effects determine reactivity and selectivity. In the reaction between aniline and 1,3-cyclohexadiene the rate is higher for electron poor (less basic) anilines. Therefore, it seems apparent that the corresponding reaction between 1,3-cyclohexadiene and (the even more basic) aliphatic amines is more difficult to realize. Furthermore, *para*- substituents in the aromatic ring with high values of $pK_b$ increase the rate of reaction. For anilines where the substituent is in *orto*- position the structure of the aniline prevails on the $pK_b$ and the reaction rate goes down.

In the second part of the thesis, palladium complexes were immobilized in thin films of silica supported ionic liquids and tested for the addition of aniline to vinyl-benzene. By varying the substituent (alkyl = ethyl, butyl, hexyl), the polarity of the ionic liquid was systematically changed from relatively polar to quite non-polar. The catalysts were characterized using different techniques, as e. g., BET, NMR, IR, TEM and Neutron activation. An expected thin film of ionic liquid with approx. 3 nm thickness was not observed in the supported catalysts. However, the BET surface area was reduced from 150 $m^2/g$ of the parent silica to between 37 and 45 $m^2/g$ for the supported catalysts, indicating that the ionic liquid resides in the pores of silica. Strong hydrogen bonding interactions between support and thin film of ionic liquid were founded; nevertheless, interactions between the palladium complex and silica were not observed. Restrictions in the mobility of the palladium complexes and the imidazolium cation of the ionic liquids were observed, when the catalysts are supported on silica. These observations lead us to conclude that the ionic liquid form solvent cages around the palladium complex. This thesis reports an experimental evidence for the formation of such ordered three-dimensional structures. The ordering effect leads to a drastically reduced mobility of ionic liquid and complex molecules, and could be used to induce unusual properties in the supported complexes.

The catalysts were tested for the intermolecular hydroamination of vinyl-benzene with aniline. The catalytic activity increases with (i) the palladium loading and (ii) the polarity of the ionic liquid. For all catalysts, the selectivity was 100 % based on aniline and between 50 and 95 % based on vinyl-benzene, mainly due to oligomerisation as side reaction. When compared under equal conditions, the catalytic activity of the supported catalysts slightly exceeds the activity of the corresponding homogeneous catalysts. These observations are explained by a concentration effect in

the the palladium complex. The reactants are highly soluble in the ionic liquid phase, while the products are hardly soluble. Thereby, the reaction is accelerated. Further, the reaction rate is enhanced in the presence of protons, which act as co-catalysts.

In summary, the concept of immobilizing homogeneous catalysts in a thin film of ionic liquid has been proven as functional. The complexes can be immobilised very efficiently in the ionic liquid and no leaching was observed. Due to their tuneable acidity and polarity, ionic liquids are particularly favourable for this application. Their appropriate selection allows to influence adsorption properties and, in consequence, catalytic activity, selectivity and chemical equilibrium.